PRESTRESSED CONCRETE INSTITUTE

Vol. 3, June, 1958 No. 1

JOURNAL

OF THE PRESTRESSED CONCRETE INSTITUTE

IN THIS ISSUE

Shear Failure of Two-Span Continuous Concrete Beam Without Web Reinforcement ..... Issac Zekaria

Post Tensioning Operations ..... E. M. Smith

Prestressed Concrete Units of the Petaluma Creek Bridge at Black Point, California ..... Herbert Brauner

Field Studies of Prestress Loss Due to Shrinkage and Creep ..... Ralph W. Kluge

Tests of a Prestressed Concrete Hyperbolic Paraboloid Shell ..... T. Y. Lin & R. Itaya

Fatigue Tests of Prestressed Concrete Beams Pretensioned with ½ Inch Strands ..... A. M. Ozell & J. F. Diniz

WATCO Forms Permit Stripping A Complete Beam In One Operation To Reduce Handling, Labor Costs

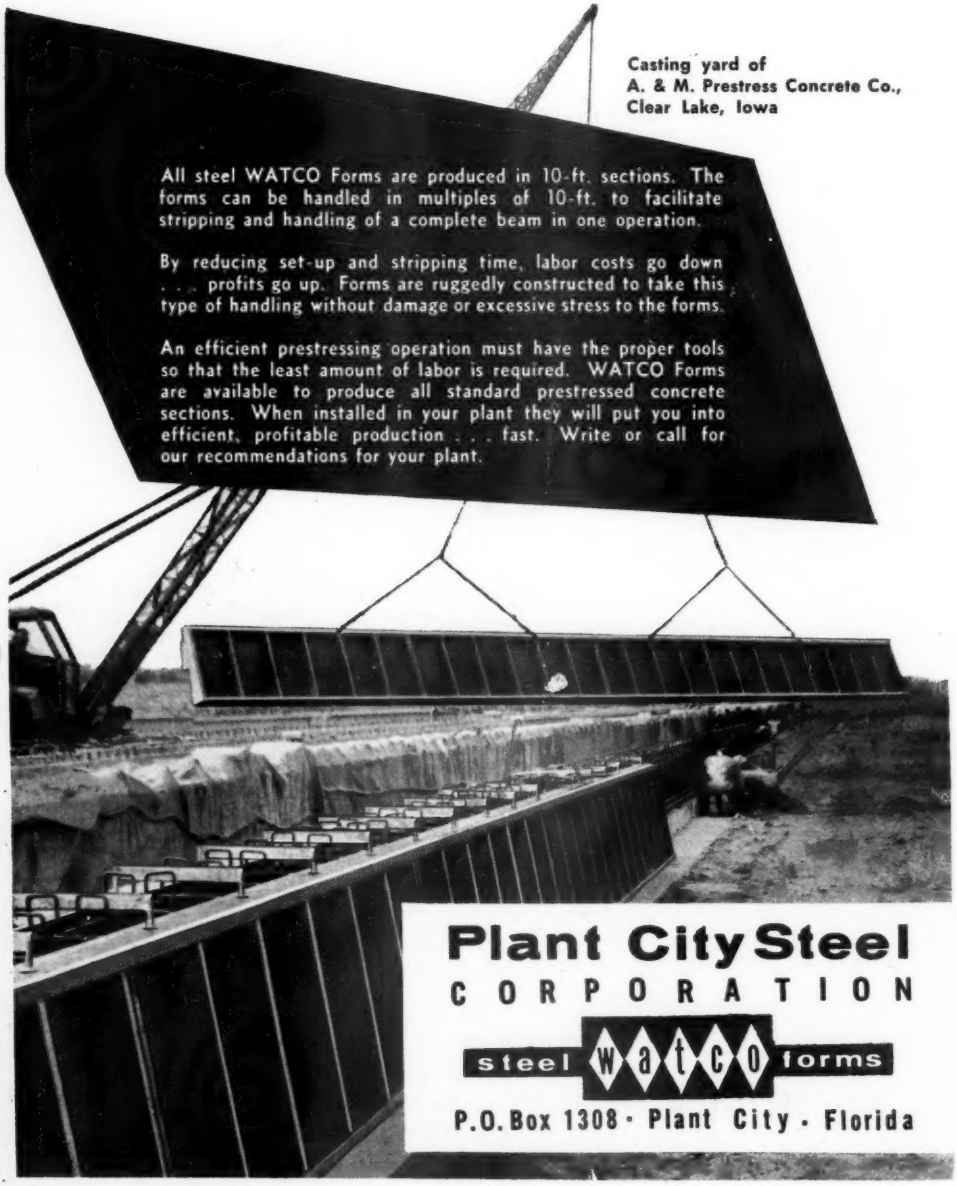

Casting yard of
A. & M. Prestress Concrete Co.,
Clear Lake, Iowa

All steel WATCO Forms are produced in 10-ft. sections. The forms can be handled in multiples of 10-ft. to facilitate stripping and handling of a complete beam in one operation.

By reducing set-up and stripping time, labor costs go down . . . profits go up. Forms are ruggedly constructed to take this type of handling without damage or excessive stress to the forms.

An efficient prestressing operation must have the proper tools so that the least amount of labor is required. WATCO Forms are available to produce all standard prestressed concrete sections. When installed in your plant they will put you into efficient, profitable production . . . fast. Write or call for our recommendations for your plant.

Plant City Steel
CORPORATION

steel watco forms

P.O. Box 1308 · Plant City · Florida

Plastiment Concrete Densifier

Cuts Construction Time

ON HARTFORD'S WINDSOR BRIDGE

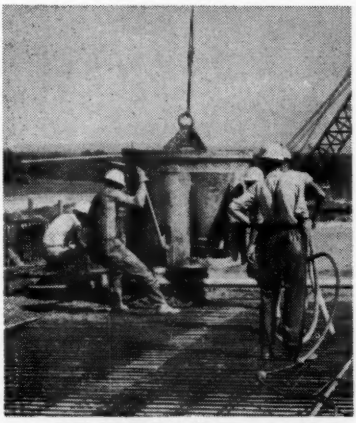

▲ DECK CONCRETE IS PLACED AND VIBRATED INTO A MONOLITHIC MASS WITH BEAMS.

14 PAIRS OF 120 FOOT SPANS WERE CONCRETED IN 99 DAYS. ▼

Rapid construction of concrete spans on this 1677 foot bridge across the Connecticut River came as no surprise to the contractor and consulting engineers. . . . Using this new procedure, these monolithic cast-in-place prestressed concrete spans were completed in a record 99 days. . . . This new monolithic beam and slab construction procedure was made possible by controlling the set of concrete with Plastiment Concrete Densifier.

The contractor increased the Plastiment proportion for the 7 foot deep beams which were placed in the morning. . . . After lunch this concrete was further consolidated by revibration. . . . Then the deck slab concrete containing a normal Plastiment proportion was placed and carefully vibrated into a monolithic mass with the beams. . . . Although initial set was retarded, strength developed very rapidly to 3000 psi within four days. . . . Prestressing operations were begun, forms removed, and in less than 10 days 20-ton truck mixers were moving across the span to place other spans.

The Plastiment characteristics of set control and rapid development of high strength make possible considerable savings in construction time. . . . It also provides an additional bonus of structural benefits including reduced cracking, increased density and higher bond to steel. . . . Let Plastiment save time and dollars for you. . . . For complete information write for Bulletin PCD.

Greater Hartford Bridge Authority—Owner
The Preload Company, Inc., N. Y. C.—Consulting Engineers for Prestressed Design and Construction
Merritt-Chapman & Scott, N. Y. C.—Contractor
DeLeuw Cather & Brill, N. Y. C.—Consulting Engineers for Owner
Thomas Worcester, Boston Mass.—Design Consultants

Ad 26-10

SIKA CHEMICAL CORPORATION
PASSAIC, NEW JERSEY
DISTRICT OFFICES: ATLANTA • BOSTON • CHICAGO • DALLAS • PHILADELPHIA • PITTSBURGH • NEW ORLEANS • SALT LAKE CITY • WASHINGTON • DEALERS IN PRINCIPAL CITIES — AFFILIATES AROUND THE WORLD
Sika

Why Frontier Dolomite Concrete Products Corp. manufacturers of prestressed concrete, specifies Meridian Steel Jacking Rods

Eager to produce top-quality prestressing jobs, yet keep costs down and production on schedule, Frontier Dolomite Concrete Products Corp. specifies Meridian Steel Jacking Rods. Here is why:

Meridian Jacking Rods are fabricated exclusively of our own MERICO steel. This insures a consistently uniform product.

Balanced tool steel analysis and cold melt electric furnace manufacture give MERICO steel an extremely high tensile strength—165,000 lbs. PSI; its yield point is 140,000 lbs. PSI.

MERICO steel is normalized, heat-treated and stress-relieved. Crystallization is eliminated. As a result, Meridian Jacking Rods give many years of satisfactory service. They resist vast temperature changes and maintain their shape even on constant, extra-long pulls.

Meridian Jacking Rods' great tensile strength and extra high yield point allow you to consider reduced diameters in your operations. With reduced diameter jacking rods, you benefit through elimination of unnecessary extra weight and associated problems. The result is greater economy for you!

Meridian Steel bars are perfectly machined. So are Meridian Steel split nuts, collars, hexagon nuts and washers. All components are matched for perfect fit before shipment. Meridian products are furnished threaded in either National Course or Acme. Bars are available up to 4½″ round and up to 22′ in length. For complete information on Meridian prestressing products, write for free folder. *Act now.*

Meridian steels have been successfully serving American industry for over 30 years.

Aware of the need for a steel that safely meets the growing demands of the prestressed concrete industry, LEAP *tested and approved Meridian Steels!*

MERIDIAN STEEL COMPANY, INC.

1776 BROADWAY, NEW YORK 19, N. Y.

Meridian Steel Company, Inc.
1776 Broadway, New York 19, N. Y.
Please send me your free folder containing complete data on Meridian prestressing products.
JP-68
My name_____
Title_____
Company_____
City_____ Zone____ State____

CF&I PRESTRESSED

CONCRETE STRAND

With the rapid acceptance and increased use of prestressed concrete structures, more and more quality-conscious prestressing plants are discovering the advantages of CF&I Prestressed Concrete Strand.

As a leading producer of wire and wire products, CF&I maintains quality controls which enable them to make Prestressed Concrete Strand to exacting specifications. This 7-wire, uncoated strand is stress-relieved *after stranding* which improves its elastic properties, flexibility, ease of handling and guarantees more uniform physical properties. It has excellent bonding characteristics which make it ideal for pretensioned applications.

Other CF&I Products for THE PRESTRESSED CONCRETE INDUSTRY

Clinton Welded Wire Fabric
CF&I Concrete Reinforcing Bars
Cal-Tie Wire
CF&I Wire (High and Low Carbon)
Wickwire Rope and Slings
Prestressed Concrete Wire

CF&I PRESTRESSED CONCRETE STRAND
THE COLORADO FUEL AND IRON CORPORATION

In the East: **WICKWIRE SPENCER STEEL DIVISION**—Atlanta • Boston • Buffalo • Chicago Detroit • New Orleans • New York • Philadelphia

In the West: **THE COLORADO FUEL AND IRON CORPORATION**—Albuquerque Amarillo • Billings • Boise • Butte • Denver • El Paso • Ft. Worth • Houston • Lincoln (Neb.) • Los Angeles • Oakland • Oklahoma City • Phoenix • Portland • Pueblo • Salt Lake City • San Antonio • San Francisco • San Leandro • Seattle • Spokane • Wichita

CF&I OFFICES IN CANADA: Montreal • Toronto
CANADIAN REPRESENTATIVES AT: Calgary • Edmonton • Vancouver • Winnipeg

5673A

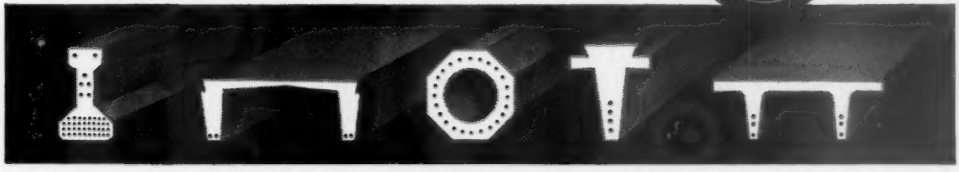

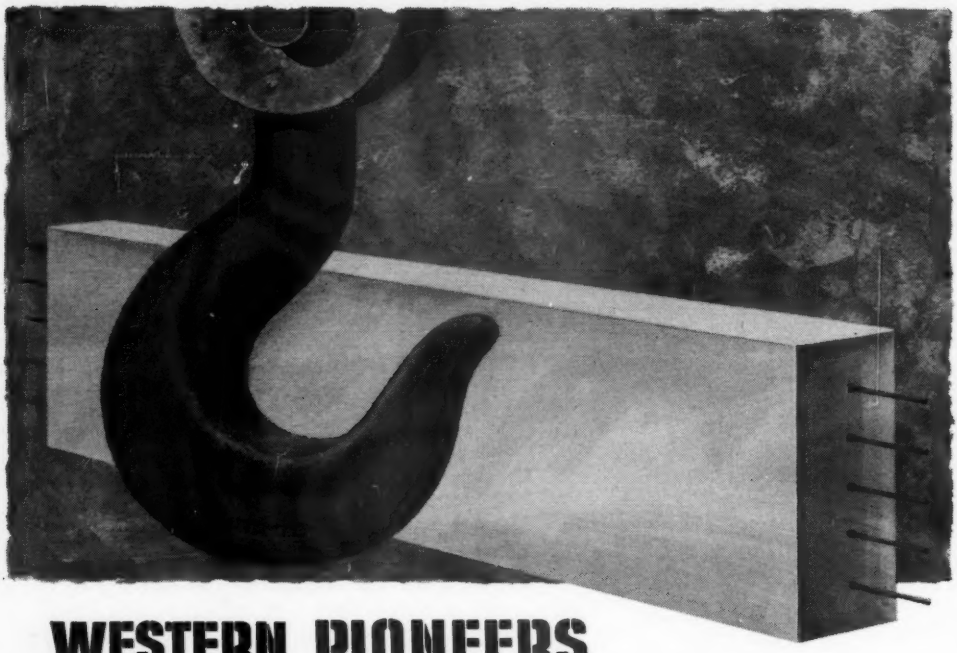

WESTERN PIONEERS FOR PRESTRESSED CONCRETE CONSTRUCTION

When Western construction experts needed a special-performance cement to meet the rigorous demands of prestressed concrete construction, they looked to Permanente. For no other cement company in the West could match Permanente's research, development and production facilities. It was with these facilities that Permanente produced "Pronto" Cement for prestressed concrete construction, thereby broadening the application of this time and money saving technique in the West. Pioneering new cements and improving existing standard types is a continuous effort of Permanente Cement Company.

KAISER Permanente CEMENT

PERMANENTE CEMENT COMPANY

Oakland • Los Angeles • Portland • Seattle • Pasco • Anchorage • Fairbanks • Honolulu

BEST FOR POST-TENSIONING . . .

DUOFLEX

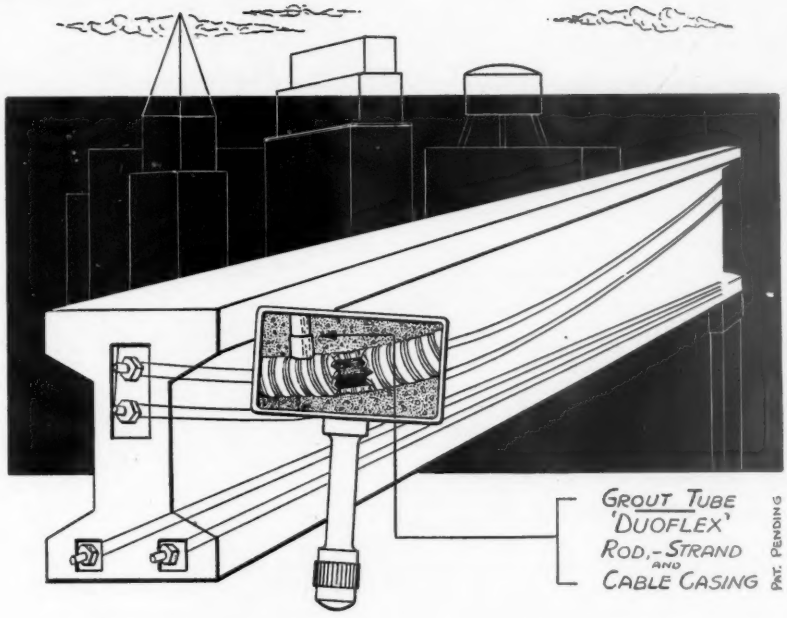

There is only one DUOFLEX casing specially designed for post-tensioning prestressed concrete used over bar, strand, or cable

DUOFLEX is designed for the greatest possible economy to keep your bids low — providing the best possible price for casing delivered to the job-site.

DUOFLEX casing has no peer. It is designed right and made right.
Specify DUOFLEX casing and Grout Connections and be right on all counts.

FLEXICO PRODUCTS, INC.

Flexible Metal Hose and Tubing for Industry

Metuchen, New Jersey

PRESTRESSED CONCRETE INSTITUTE

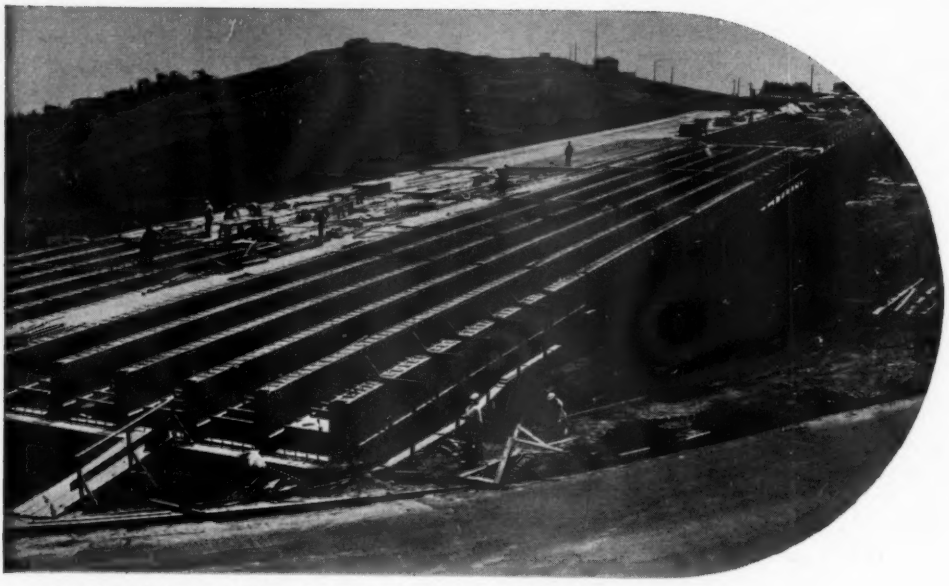

60′ bridge girders, Market Street Bridge, San Francisco, California. Precast by Basalt Rock Company, Inc., Napa, California. City and county of San Francisco, California.

when the job is done and all the facts are in— you'll find STRESSTEEL overall cost is lowest!

There is reason for the tremendous growth in the use of **STRESSTEEL** for prestressed concrete. Increasing numbers of users find . . .

- **STRESSTEEL** is the lowest in-place cost post-tensioning material.
- **STRESSTEEL** handles faster, providing lower labor costs for placing and tensioning.
- **STRESSTEEL** proof-tests every bar, assuring controlled quality.
- **STRESSTEEL** Wedge Anchor Units provide positive end anchorage. It is the fastest, safest and easiest post-tensioning method.
- **STRESSTEEL** tensioning equipment for rent and sale at nominal cost.

Write for new illustrated manual SS-3

STRESSTEEL CORPORATION
221 Conyngham Ave.
WILKES-BARRE, PENNA.

"takes it" as fast as you can "dish it out"!

WIDE OPEN PERIPHERY MEANS NO LIMIT TO SPEED OF CHARGE

Only the phenomenal Smith Turbine-Type Mixer has a full 360° charging area. *Whatever the speed of your charge — that's the rate this mixer accepts it!*

Discharge is just as fast: the mixer is available with up to four discharge doors, depending on requirements.

But that's not all to the story of speed. Because of "Live Mix" (no dead center area) mixing is at a peripheral rate of *600 feet per minute!*

Mixing is done in a doughnut-shaped drum. Blades set up a braiding action which breaks down centrifugal forces.

For detailed data write giving your type of application.

SMITH

Since 1900, the pioneer designer and foremost manufacturer of the world's finest mixers.

THE T. L. SMITH COMPANY • **Milwaukee, Wisconsin** • **Lufkin, Texas**

Affiliated with Essick Manufacturing Company • Los Angeles, Calif.

A8-4055-1P

A8-4055A-1F

This Hydrocrane uses its telescoping boom and jib to spot a 14-ft., 2,200-lb. slab at Waukesha, Wisconsin.

To give you a money makin' edge . . .

BUCYRUS ERIE HYDROCRANE

Hydrocrane's Busy Boom Picks Up Extra Jobs—Extra Profits

Boom swings left and right . . . telescopes in and out . . . moves up and down . . . independently, at the flick of a lever. That's how Bucyrus-Erie's *all-hydraulic* Hydrocranes can get in more lifts per day, build up extra profits. With this boom, you can change boom angle *and swing* or *telescope at the same time*, slip prestressed beams into position quickly, surely, safely — practically eliminates breakage of fragile concrete products — chalk up a real money-makin' edge on competition.

And, there's plenty of reach. Boom telescopes 8 feet on the 5-ton H-3, 12 feet on the 12-ton H-5. For longer reaches, three piece booms and 10 and 18-ft. jibs are available for the H-3 — 10 and 20-ft. jibs for the H-5.

Then, for fast between-job travel, the boom retracts neatly into a compact unit carried over the cab.

Your Bucyrus-Erie Hydrocrane distributor is ready to show you this busy boom that gives you a money-makin' edge on competition. 277H58

Other Hydrocrane money-makin' edges

- low-cost new or used standard commercial motor truck mounting
- short tail swing for close-quarter jobs
- quick setups and knock-downs, open road speeds up to 50 mph
- precise, smooth hydraulic control and power

Over 50% of Hydrocranes sold last year were repeat sales

BUCYRUS-ERIE COMPANY • SOUTH MILWAUKEE, WISCONSIN

JOURNAL

OF PRESTRESSED CONCRETE INSTITUTE

Vol. 3 June 1958 No. 1

OFFICERS AND DIRECTORS
1957-1958

Ben C. Gerwick, Jr.
President

Harold A. Price
Vice President

Peter J. Verna, Jr.
Secretary-Treasurer

DIRECTORS

Philip E. Balcomb
Forrest S. Burtch
Douglas P. Cone
Randall M. DuBois
George W. Ford
J. Ashton Gray
Prof. T. Y. Lin
Jacob O. Whitlock

EXECUTIVE SECRETARY
Martin P. Korn, M.ASCE

JOURNAL TECHNICAL EDITOR
Dr. A. M. Ozell

JOURNAL ASSOCIATE EDITOR
Douglas P. Cone

CHAIRMAN TECHNICAL ACTIVITIES COMMITTEE
Charles C. Zollman

•

The INSTITUTE is not responsible for any statements made or opinions expressed in its publications.

From the editor. . .

The teaching of the fundamentals and basic theories involved in the design of prestressed concrete members in our colleges and universities has lagged behind. Only a few engineering schools offer undergraduate and advanced courses in Prestressed Concrete Design. More and more civil engineering and architectural students should be given the opportunity to learn about this new material which has proven to be safe, functional, as well as economical, in many respects and under a variety of conditions.

Realizing the need of keeping the students and instructors of our colleges and universities abreast with the new developments, applications and research studies in prestressed concrete, the Board of Directors have decided to offer a free subscription to the Journal to every College of Engineering in the country.

The technical and semi-technical papers published in the Journal should serve well the new readers in acquainting them with the industry and the solution to the many design and application problems reported therein.

Beginning with the next issue, a new section will be introduced in the JOURNAL entitled "Readers' Comments." This section will be for technical and manufacturing questions only. All readers are invited to use it for an exchange of ideas. Questions should be sent directly to the Executive Secretary, PCI.

The **JOURNAL** is published quarterly by the **PRESTRESSED CONCRETE INSTITUTE, INC.**, 425 N. E. Fifth Street, Boca Raton, Florida. **TECHNICAL EDITOR:** Dr. A. M. Ozell, University of Florida, Gainesville, Florida. **ASSOCIATE EDITOR:** Douglas P. Cone, P. O. Box 11476, Tampa, Florida. **ADVERTISING, SUBSCRIPTION** and **PUBLICATION OFFICE:** 3132 N. E. Ninth Street, Fort Lauderdale, Florida. **DISTRIBUTION:** Available without cost to all members of the Prestressed Concrete Institute. **SUBSCRIPTION PRICES:** $6.00 per year for four issues. Single copy price: $2.00. For subscriptions outside the continental United States, add 20% to cover handling and mailing. Editorial contributions to the **JOURNAL** are welcomed, but publication cannot be guaranteed. All manuscripts should be submitted in duplicate and will be reviewed by the Technical Editor prior to publication. Advertisements of products, services and materials allied to the prestressed concrete industry are acceptable. Inquiries concerning advertising, and subscriptions should be directed to the Publication Office.

Copyright by the **PRESTRESSED CONCRETE INSTITUTE, INC.**, 1958.

SHEAR FAILURE OF TWO-SPAN CONTINUOUS PRESTRESSED CONCRETE BEAMS WITHOUT WEB REINFORCEMENT

By ISSAC ZEKARIA, *University of Manchester, England*

SYNOPSIS

Tests were made on 12 two-span continuous prestressed concrete beams of rectangular section without web reinforcement and without un-tensioned steel. Linearly transformed concordant cables were used, and all beams were post-tensioned and grouted.

It was shown by the present tests that such beams can fail in shear before the beam develops its full flexural strength. The mode and mechanism of such failures are described, and compared with flexure failures.

The validity of the elastic equations used in computing the principal stresses in concrete was checked experimentally, but these equations were found to fall short of describing precisely, or fully, the actual behaviour of the beams. They were, thus, found unsuitable as criteria for predicting the mode of failure.

Test results suggested that there is some degree of interaction between shear and bending, i.e., an increase in bending at a section reduces its shear-carrying capacity.

Analysis of the factors influencing shear failure in continuous prestressed concrete beams is presented, and a new concept, the Shear Susceptibility Number, is introduced the magnitude of which throws light on the vulnerability of a continuous beam to shear failures, and on the behaviour of the beam at failure. In addition, the difference in the internal behaviour of beams failing in shear and flexure is outlined by measurements of the variation of principal strains and the orientation of principal axes with loads in beams having high and low values of shear susceptibility number.

INTRODUCTION

The prediction of shear failure and the load at which such failure will take place is very important, and it becomes particularly so if we are to base our design on ultimate strength and load factor rather than on working stresses and a factor of safety. The importance of the study of shear failure in reinforced and prestressed concrete beams has long been recognized by engineers, but the study of the problem in prestressed concrete has started only recently. The literature available deals, in fact, with only one or two series of tests carried out on simply supported beams.[1] The present tests are believed to be the first attempt ever made to investigate the problem of shear failure in continuous prestressed concrete beams.

TESTS

Object of Tests

Because of the complexity of the problem of shear failure in general, and in continuous beams in particular, it was impossible to get information regarding the effect of all the variables, which are numerous indeed. Instead, the following study was made.

a—To determine the modes and characteristics of shear failures, and the fashion in which such failures differ from flexure ones.

b—To investigate the validity of the elastic equations for computing principal strains, principal stresses and the orientation of the principal axes, when applied to beams failing in shear and in flexure, and whether these equations can be used as criteria for predicting the mode of failure.

c—To study the effect of the following variables on shear strength of continuous beams:

i—Ratio of stressed longitudinal steel to cross-section of beam;

ii—Total prestressing force in reinforcement;

iii—Ratio of unit stress, lbs/sq. inch, at transfer to yield stress.

Materials

Cement: High alumina cement

Coarse aggregate: ⅜" Dorset Pea, and consisting mainly of rounded particles

Fine aggregate: River sand

Both coarse and fine aggregates were used in the dry state.

Concrete Mix: The same concrete mix was used throughout the tests.

water/cement ratio	0.45
aggregate/cement	4.0 : 1
coarse/fine	1.5 : 1

Compressive strengths are based on 2"x9" test cylinders.

Grout Mixture: In most beams the grout used had a water/cement ratio of 0.40, the cement being high alumina. Aluminum powder was used to improve bond characteristics, though this was found to reduce slightly the crushing strength of the grout.

Reinforcing Wires: High tensile steel wires were used with either 0.276-in. or 0.200-in. diameters. Typical stress-strain curves are shown in Figs. 1a and 1b.

Description and Classification of Test Beams

Table 1 gives the physical properties of the beams tested. They were all continuous over two spans, rectangular in section, 4"x8", post-tensioned and grouted. The beams are divided into three types according to span and cable profile, Figs. 2, 3 and 4. The choice of the small spans was made to simplify the problem by increasing the likelihood of shear failure. Shearing force and bending moment diagrams due to 1 ton external load are given in Fig. 5.

The amount of steel was varied from 0.1962% to 0.7425% . The lower limit resulted in failure of reinforcement before the concrete in the compression zone reached its limiting strain, and the upper limit in premature failure, by shear, before complete moment redistribution took place. The initial prestress was varied from zero to 132,000 lbs/sq. inch, corresponding to a variation in the ratio of f_e/f_y from zero to 0.645.

Strain Measurements

A mechanical demountable gauge was used, with 8-in. gauge length, based on 10:8 lever arm which actuates a dial gauge reading to 1/10,000 inch. Strain gauges were located over the depth of the beam at various sections as in Fig. 6.

The diagonal strains were measured in order to calculate the magnitude of the two principal strains, their orientation during loading and their direction at ultimate failure.

Testing Machine, Setting-up and Loading

The general set-up and loading arrangement are shown in Fig. 7. The ratio of shear span to depth, a/d, was kept constant at a value of unity throughout the series of tests to ensure that shear failure, if it did occur, would take place along a 45° direction with the axis of the beam. This was believed to be the loading most inducive to shear failure.

Prestressing

The wires were stressed individually, and were anchored by using grips composed of two wedges and an outer barrel. The wedges had serration to grip the wire. When the required load was reached the wedges were tapped home, and the pressure was released.

However, it was found that there was a certain amount of take-up in the wedges ranging from 1/16 to 3/16 inch when the pressure was released, causing the prestress to drop. It was thus difficult to predict exactly, or with any reasonable accuracy, the remaining prestress in the wire. To overcome this, a reaction frame was designed to be placed between the end of the beam and the prestressing jack. This frame was made-up of four 1-in. diameter rods, 13 inches long, with two end plates, a reaction plate and an anchor plate, and having holes for the wires to pass through, Fig. 8. The load in the wire at the prestressing end could be ascertained with accuracy from direct strain measurements on the wires using either the demountable gauge or an extensometer. On the other hand, losses due to friction could also be obtained by using a second reaction frame at the other end of the beam, and taking strain measurements on the wire. The load in the wire after anchoring was given by the final strain readings. However, it was possible to check the load in the wire by stressing it to a high force until the anchor grip was drawn clear of the anchor plate; and the pressure gauge reading, as well as the corresponding strain readings, were recorded. The jack was released, and strain readings again taken. The difference indicated the drop from the load to which the wire was stressed to the load at anchoring.

Because of the sharp curvature in the wire profile, losses in prestress due to friction were excessive. It was, thus, essential at times to prestress from both ends. On prestressing from the other end a special prestressing stool was used, and shims were slipped between the anchor grip and anchor plate of the reaction frame to give the required extra extension.

Control Beams

Plain concrete control beams, 4"x8" in section, obtained from the same mix as the test beams, were tested over a span of 24 inches, loaded at third points. Strain measurements were taken down the central section, and reflection recorded at mid-span, to determine values for E_c in bending and for the modulus of rupture.

FORMATION OF CRACKS AND MODES OF FAILURE OF TEST BEAMS

In all cases the test beams showed elastic behaviour before cracking, deflections and strain variation being linearly proportional to applied load. Residual deflections on removal of the load before cracking were almost negligible. The modes of failure observed can be grouped in the following categories:

Flexure Failures

a) Failure by crushing of concrete:

As the load was increased cracks appeared at the section most critical in bending, namely section B (Fig. 9) over the central support. These cracks widened and penetrated deeper into the compression zone with the increased load. Further cracks then appeared under the outside loading points, D and G, about 8"-10" from the end supports, either simultaneously in both spans or one after the other within an interval of 1 ton or less. As the load was further increased, the cracks at B and those at D and G continued to widen and to penetrate further into the compression zones, until the cracks at B showed no further change when they were 7" to 7.25" deep. At this stage cracks at D and G started to widen and penetrate more rapidly. The cracks went on widening until the beam failed by crushing of concrete under one or both loading points, D and G. In some beams cracks also appeared at mid-points of both spans, 2 to 4 tons tons before reaching ultimate load. Fig 9 (i) shows diagrammatically this mode of failure.

These observations are in agreement with the plastic theory and the modes of hinge formation. When after cracking of section B, more load was applied to the beam, the crack penetrated further until a state of a plastic hinge, or almost so, was formed over the middle support; and thus this section was carrying its full moment of resistance, and bending moment was constant. Beyond this stage redistribution of bending moment took place, and the rate of increase of bending moment with load at sections D and G, the next critical in bending, became steeper. For a complete collapse the beam had to be transformed into a mechanism which demanded the formation of at least another plastic hinge somewhere along the span; and if the beam was symmetrical both in strength and loading, plastic hinges would form at both spans.

It is to be remembered that the redistribution of moment from the elastic to the

ultimate load conditions seems to depend on the geometry of the section, on the form of loading and on the relative values of the moments of resistance at the critical sections[2]. Thus, it cannot be stated how fully developed those plastic hinges were in the present tests.

b) Fracture of reinforcement.

This happened in beam B10. The beam behaved in the same manner as above, but before enough plastic hinges could develop to transform the beam into a mechanism the wires failed at G.

Shear Failures

Beams which are grouped under this heading showed essentially the same initial pattern of crack formation as above. However, before concrete in the compression zone crushed or the reinforcement failed, i.e. before the beam reached its full flexural capacity, cracks of appreciable width and inclined at 45° to the centroidal axis of the beam appeared near the mid-support, Figs. 9 (ii) and 10. These cracks formed without exhibiting any warning, but rather suddenly. Their initial width was much wider and more apparent than the tension flexure cracks at their formation. The inclined cracks were wider near the centroidal axis than near the extreme fibres, and they penetrated the whole width of the beam. They did not close fully upon complete removal of the load following their formation. As the load was increased, the inclined cracks showed little change, and the width of the crack, as measured by a special crack-measuring microscope, showed very little increase. Final collapse of the beam was along the inclined crack by shearing the beam into two parts held only by the wires, Fig. 9 (iii) and 11. Whenever the inclined crack appeared final collapse was invariably along it, irrespective of the width of the flexure cracks or the state of the beam.

Failure of beams in the above fashion is referred to as "shear failure", i.e. a beam is said to have failed in shear when it fails along a diagonal crack before having developed its full flexural capacity.

TEST RESULTS

Load-Deflection Relationships

Figure 12 is given as an illustration of the load-deflection behaviour of the test beams. The zero deflection represents the prestressed state of the beam. The graphs start off along a curved line because the upward deflection due to prestressing was not restrained.

Slopes of load-deflection graphs before cracking depend mainly upon the values of $E_c I_{Tm}$ as shown in Fig. 13, whereas they do not show any consistent variation with the prestress. The mode of failure could not be predicted from the load-deflection characteristics. However, after cracking, these graphs are steeper in case of a shear failure than of a flexure one, which indicates that the load was steadily increasing when the first shear crack formed.

Comparison of Measured and Computed Cracking Loads

Cracking loads were computed from the i) the prestress, ii) the modulus of rupture of plain concrete as found from control beams, and iii) the properties of the section. The prestress at cracking was taken as the effective prestress at transfer. For the properties of the section, each beam was broken open after testing to ascertain the position of steel at the critical sections. E for the grout mix was taken the same value as for the concrete; E_s/E_c as 5.

It is assumed that when a beam cracks the fibre tensile stress in concrete equals the modulus of rupture. Therefore,

$$f_r = -\frac{P}{A} - \frac{Pey}{I} + \frac{My}{I}, \qquad \text{.....(1)}$$

where M is the cracking moment. In the case of a continuous beam with a linearly transformed concordant cable, we have:

$$M = M_D + M_L + M_T \qquad \text{.....(2)}$$

From (1) and (2), we have therefore,

$$M_L = -M_D - M_T + Pe + \frac{PI}{Ay} + f_r \frac{I}{y} \qquad \text{.....(3)}$$

The live load to give rise to M_L at mid-support, where the first cracks always appeared, was calculated by the method of moment distribution. Table 3 gives the results obtained.

Principal Strains and Principal Stresses

In the absence of any data regarding the shear failure of continuous prestressed beams, the first step in the present study was to check the validity of the design procedure which is based on the elastic equations for the state of stress under compound forces. With this in view, an attempt was made to:

1—Find the rate of increase of principal tensile strain with load, both in beams failing in shear and in flexure.

2—Find the orientation of the principal axes with loading in both modes of failure, and

3—Compare these experimental graphs with the theoretical ones as obtained from the elastic equation, and to find if these equations are in fact applicable to continuous beams.

To measure principal strains, strain readings were taken at 0°, 45°, and 135°; also at 0°, 60°, and 120° with the centroidal axis, arranged in a star, and on both sides of the mid-support (Fig. 6).

The theory of strain analysis due to compound stress is well-known[3], and only the main formulae are mentioned here.

Strains are positive when tensile and negative when compressive.

$$\epsilon\Theta = \tfrac{1}{2}(\epsilon_x + \epsilon_y) + \tfrac{1}{2}(\epsilon_x - \epsilon_y)\cos 2\Theta + \tfrac{1}{2}\epsilon_{xy}\sin 2\Theta \qquad (4)$$

$$\tan 2\Theta = \frac{\epsilon_{xy}}{\epsilon_x - \epsilon_y} \qquad (5)$$

$$e_1 = \tfrac{1}{2}(\epsilon_x + \epsilon_y) + \tfrac{1}{2}\sqrt{(\epsilon_x - \epsilon_y)^2 + \epsilon_{xy}^2} \qquad (6)$$

$$e_2 = \tfrac{1}{2}(\epsilon_x + \epsilon_y) - \tfrac{1}{2}\sqrt{(\epsilon_x - \epsilon_y)^2 + \epsilon_{xy}^2} \qquad (7)$$

From these measurements, the quantities known are: ϵ_x, $\epsilon\Theta_1$, $\epsilon\Theta_2$, Θ_1, and Θ_2.

From (4) ϵ_{xy} and ϵ_y are found, and (6) and (7) were solved for e_1 and e_2, the principal strains. The orientation was found from (5).

The graphs obtained are shown in Figs. 14, 15, 16 and 17.

The theoretical graphs are computed for ideal conditions by considering the initial prestress to remain the same throughout the loading, i.e. no slip, and the beam a homogeneous substance under compound stress. This is the normal design procedure[4].

The procedure is represented by the following formulae:

$$V_c = V - V_s \qquad (8)$$

$$v = \frac{V_c Q}{BI} \qquad (9)$$

$$p_t = \sqrt{v^2 + \left(\frac{f_c}{2}\right)^2} + \frac{f_c}{2} \qquad (10)$$

$$p_c = \sqrt{v^2 + \left(\frac{f_c}{2}\right)^2} + \frac{f_c}{2} \qquad (11)$$

The fibre stress, f_c, due to a total moment, M, a prestress P, with an eccentricity e, is given by

$$f_c = -\frac{P}{A} \pm \frac{Pey}{I} \pm \frac{My}{I}$$

Readings were, however, taken at the centroidal axis, therefore,

$$f_c = \frac{P}{A} \qquad (12)$$

The corresponding principal strains are obtained thus:

$$e_t = \frac{p_t}{E_c} - \frac{p_c}{mE_c} \quad \text{.....(13)}$$

$$e_c = \frac{p_c}{E_p} - \frac{p_t}{mE_c} \quad \text{.....(14)}$$

$\frac{1}{m}$ was taken as $\frac{1}{6}$

From the experimental graphs it is seen that the rate of strain increase with load in the case of shear failures is greater than in the case of flexure failures. This supports the view that shear failure is essentially a tensile one.

Also from Figs. 18, 19, and 20, it is seen that the beams failing in shear deviate from the theoretical graphs more than the ones failing in flexure, i.e. they exhibit the more advanced orientation of the axes.

The common features of shear failure are, therefore, (i) more severe principal strains, and consequently, stress, and (ii) the more advanced orientation. From the similarity in the general shape of the experimental and the theoretical graphs, it can be said that the state of stress in prestressed concrete under compound forces obeys, with reservation, the elastic equations, but these equations do not describe precisely, or fully, the actual behaviour of the beams as they show no distinction whether the failure is by shear or flexure.

Wire Stresses at Failure of Beams

An important connection was observed between the mode of failure and the wire stresses at failure of beam. In beams failing in shear, final wire stresses were below yield point, whereas, wires in beams failing in flexure were found to have been stressed beyond yield.

The final wire stress was found by taking strain measurements on the wire inside the reaction frame at each load increment. The sections of maximum deformation along the test beams, because of loading arrangement and cable profile, are D and G (Fig. 9) which are about 11 inches from the end of the beam. The wire strain is the greatest at these sections, and the loss in bond in these regions is the most severe. Under well developed, though not necessarily very severe cracks, the length along which bond is lost extends up to the end of the beam; and the wire stress, therefore, between either of these two sections and anchoring is the same, except for the friction between the reinforcements and the grout, which is almost negligible. Consequently, the extra load, after slip, is thrown on the anchor plates, and the recorded extra strain was added to the strain at transfer to find the total stress in the wires from the stress-strain graph of the steel. A graph of total stress versus load was plotted, and the stress at ultimate load was extrapolated. Fig. 21 is an example. The values obtained are listed in Table 2 for both ends of each individual wire. The final stresses were always higher at the end of the span where cracks were more severe in case of shear failure, or where flexure failure ultimately occurred.

It is seen that shear failure becomes unlikely once the wires enter the inelastic zone of the stress-strain graph. This is because when this happens, and especially if the beam is cracked, the deflection rate of the beam increases, thus causing the concrete in the compression zone to reach its ultimate compressive strain rapidly, i.e. with little increase in load.

Principal Tensile Stress at First Shear Crack and at Failure

As a further check on the validity of the elastic equations, equations 8, 9, 10 and 11 were used to calculate p_t at shear cracking load for beams failing in shear, and at ultimate load for beams failing in flexure. Values used for the prestress in this case were obtained from the total wire strain as measured directly inside the reaction frame. It is seen that the values (Table 3) are not as a rule high in case of shear failure, as would be expected; and that the mode of failure cannot be really predicted from these values. This shows that the elastic equations are unsuitable as criteria for predicting the mode of failure or the shear-carrying capacity of the beam.

DISCUSSION OF TEST RESULTS

Shear-Bending Interaction

The problem of whether there is any significant interaction between shear and bending is still a very controversial matter. The results obtained, however, show that there is ground on which the assumption of shear-bending interaction is very justifiable, though they cannot be claimed to give absolute proof.

It was observed that an increase in the value of steel area, for the same prestress, (B10 and B6, B7 and B9, B4 and B3, B14 and B12 also B14 and B11), changed the mode of failure from flexure to shear; and in case of two shear failures (B6 and B9, B11 and 12), the shear cracking load was the lower with the higher value of A_s.

To correlate these observations with the concept of shear-bending interaction, the following must be considered.

i—The maxiumu bending moment that can be reached over the mid-support of a continuous beam is the plastic moment of resistance of that section, and on reaching this condition the section will rotate under a fixed moment.

ii—The beam cannot fail unless (n+1) plastic hinges are formed, and in the present case, 2 plastic hinges must at least be formed. This means that the formation of a plastic hinge at mid-support is not the failure of the beam.

iii—The magnitude of M_p is dependent, among other things, upon A_s, and it increases, within certain limits, with the increase in A_s[5].

By increasing the area of steel the value of the ultimate bending moment at mid-support is increased, i.e. the moment acting at the section of maximum shear on formation of the inclined shear crack, becomes greater. This increase in bending moment seems to reduce the shear-carrying capacity of the section, and shear crack forms at smaller shearing forces. However, no conclusion can be arrived at from these results as regards the interaction in the other direction, i.e. the effect of shearing forces on the ultimate moment of resistance of the section.

To carry out quantitative study of this problem, the redundancy must be solved experimentally by finding the variation of an end reaction. This procedure enables the determination of the bending moment at mid-support at all loading, and also the evaluation of the shearing forces. A better picture of the shear-moment interaction can be had, and the variation of an end reaction with the applied load will indicate at what load the mid-support is transformed into a plastic hinge.

Analysis of the Factors Affecting Shear Failure

As the problem of shear failure has been found to be an irrational one, it is extremely difficult at this stage to arrive at a procedure by which to predict the shear strength of a continuous beam. Firstly, many more tests need be carried out, and secondly, the problem of shear-bending interaction must first be solved. However, a semi-empirical analysis was sought from test results and deductions made therefrom to find out the factors affecting the mode of failure, and the manner in which they do so.

i—Effect of f_e/f_y ratio.

As mentioned before, it was observed that shear failure became unlikely once the wires entered the inelastic zone of the stress-strain graph. Thus if f_e/f_y is high, only little deformation of the beam is needed for the wires to reach yield point, following which, the rate of deflection increased because the wires will not provide the beam with enough rigidity. As a result, the concrete reaches its ultimate compressive strain with little increase in load. It follows that by keeping f_e/f_y low there is more likelihood for the beam to fail in shear.

ii—Effect of p%

The effect of percentage of steel was fully described under Shear-Bending Interaction. However, in the absence of enough knowledge regarding this interaction, we can state that by increasing the area of steel, the beam is rendered more susceptible to shear failure.

iii—Effect of I_{Ts}

The inclined shear crack appears when the principal tensile stress p_t reaches a certain limiting value. Tests have shown that e_t, and consequently p_t, increase with the in-

crease in the nominal shearing stress, v. From equation 9, however, it is seen that by decreasing the value of I_{Ts}, v is increased, and failure in shear is more likely to occur in a beam with a low I_{Ts} than in one with a high I_{Ts}, all other factors being equal.

iv—Effect of E_cI_{Tm}

Deflection before cracking is inversely proportional to the value of E_cI_{Tm} (Fig. 13). Thus a beam with a high value of E_cI_{Tm} should suffer little deformation, and consequently little increase in steel stress would be caused. This means that yield of steel is retarded in a beam with high E_cI_{Tm}, and this has a similar effect to having a low ratio of f_c/f_y.

v—Effect of E_s

When the reinforcements have a high value of E_s little increase in strain, due to the deformation of the beam, causes a large increase in stress. Thus for the same yield stress, and all other factors being the same, reinforcements with a high E_s reach yield stress more rapidly than those with a low E_s, the beam consequently becoming less susceptible to shear failure.

vi—Effect of Span

The above factors refer to the properties of the beam section, independent of the span length. For the same system of loading, flexure failure is more likely to take place, for any specific section properties, with long spans than with short ones. This is obvious as the moment-to-shear ratio increases with span for the same load, the variation being very nearly linear as shown below.

Consider a continuous beam similar to the ones tested. From elastic analysis, we have:

$$M_b = \frac{3Wa}{2} - \frac{3\ Wa^2}{2\ L} \qquad (15)$$

W being ¼ the applied load.

$$V_b = W + \frac{3\ Wa}{2\ L} - \frac{3\ Wa^2}{2\ L^2} \qquad (16)$$

From equations (15) and (16), and simplifying, we have

$$\frac{M_b}{V_b} = \frac{2\ aL(L - a)}{2\,L^2 + 3\,aL - 3\,a^2} \qquad (17)$$

Differentiating (17) with respect to L, and simplifying

$$\frac{d}{dL}\left(\frac{M_b}{V_b}\right) = \frac{2\,a^2L(10L - 12a) + 6a^4}{(2L^2 + 3aL - 3\,a^2)^2} \qquad (18)$$

But L is always greater than 2a, therefore, $\frac{d}{dL}\left(\frac{M_b}{V_b}\right)$ is always positive.

Therefore 17 is an increasing function.

From (17), dividing throughout by L^2, and putting $\frac{a}{L} = x$, we have:

$$\frac{M_b}{V_b} = \frac{2\,a(1 - x)}{2 + 3x - 3x^2} \qquad (19)$$

Equation (19) is a curve with a large radius of curvature, and considering L to vary from 28″ to 80″, and with a = 8″, x ranges between, say, 0.3 and 0.1. Within these limits (19) is very nearly linear (Fig. 22).

It follows from the above that M_b/V_b depends upon the span, L, and it increases with the increase in L.

The above factors can thus be combined to describe the likelihood of a continuous prestressed beam failing in shear, as follows:

$$\frac{E_{cc}\,\frac{I_{Tm}}{I_{Ts}}\,p\%}{E_s\,\frac{f_e}{f_y}\,L} = Z,$$ the Shear Susceptibility Number, which has the dimension of in^{-1}.

It follows from the above that beams with high values of Z are relatively more susceptible to shear failure than those with low Z.

Computation of Shear Susceptibility Number of Test Beams

This criterion was applied to the beams tested by computing the Z values, Table 3. E_c is based on the values obtained from measurements of flexural strain on the control beam. I_{Tm} and I_{Ts} the transformed second moments of area, were computed at mid-span and at 4 inches from the mid-support respectively. The ratio E_s/E_c was taken as 5, and the grout was assumed to have the same E as the concrete. The value of f_e used was the average of the effective wire stresses at both ends of the beam, and f_y being the 0.1% proof stress. Span, L, is in inches.

From Table 3, Z is seen to vary from 1.62×10^{-3} to 13.5×10^{-3}. The lowest value corresponds to failure by fracture of reinforcements. Values up to 4.7×10^{-3} are for beams failing in flexure. The high values between 6.10×10^{-3} and 13.5×10^{-3} are for beams failing in shear.

The magnitude of Z was found to throw light on the prematurity of shear failures. For two beams failing in shear, the flexural deformations were less at the formation of the first shear crack in case of the beam having the higher Z.

The resulting mode of collapse illustrates the relationship between Z and shear failure.

So far as the present tests are concerned, the most effective terms on the value of Z, as well as being the ones that were quantitatively studied, are f_e/f_y, p% and L. The other terms changed but little. The concrete crushing strength, f_{cr}, can be taken to replace E_c, as it is believed that there is a certain relationship between the two[6]. This would be desirable as it is more convenient to work in terms of concrete crushing strength than of E_c.

Variation of e_t and Θ_p with Z

Figures 23 and 24 show the variation of the experimental tensile strain with Z, for loads 8, 12 and 16 tons. It can be seen that e_t increases with Z, irrespective of the mode of failure, though theoretically e_t is about the same for all beams. This shows that a beam with a high Z would reach a critical value of e_t at a faster rate than a beam with a low Z.

Also, beams with high Z show the more advanced orientation of the principal axes, under a certain load, than those with low Z, Figs. 25 and 26.

These observations show the relationship between the shear susceptibility number and shear failure by way of the internal behaviour of beams, in addition to the actual mode of failure.

CONCLUSIONS

1—It was found that continuous prestressed concrete beams of rectangular section can fail in shear before the beam develops its full flexural capacity. The cause of shear failures is the formation of an inclined crack at the zone of maximum shear as a result of the principal tensile stress in the concrete reaching a limiting value. Final failure takes place by sliding along the plane of the inclined crack.

2—Total prestress considered by itself was found to have no consistent effect on the mode of failure.

3—Beams failing in shear had the greater values of e_t, e_c and, consequently of p_t and p_c, than similar beams failing in shear at any given load. This observation supports the view that shear failure is essentially a tensile one.

4—The state of stress in concrete under compound forces obeyed, with reservation, the elastic equations, but these equations did not describe precisely, or fully, the actual

behaviour of the beam, as they fell short of showing any distinction whether the failure was by shear or flexure.

5—The design procedure accepted at the present for checking the shear strength of a prestressed beam was found unsuitable as a criterion to predict the mode of failure.

6—An important connection was observed between shear failure and final stress in reinforcement at failure of the beam. In beams failing in shear, final wire stresses were in the elastic range, whereas wires in beams failing in flexures were found to have been stressed beyond yield. It seems therefore that shear failure becomes unlikely once the reinforcements enter the inelastic zone of the stress-strain graph.

7—Test results were found to be in favor of the argument that there is interaction between shear and bending. Shear-carrying capacity of a section was found to decrease with the increase of bending moment operating on it.

8—The mode of failure was found, within the scope of the present tests, to be influenced largely by the shear susceptibility number of the beam: the likelihood of shear failure being the higher the larger is this number.

9—Principal tensile strains were found to increase with the increase of the shear susceptibility number of the beam, irrespective of the mode of failure.

ACKNOWLEDGMENT

The work was carried out in the Concrete Laboratories of the Engineering Department, Manchester University, under Professor J. A. L. Matheson.

The author is indebted to Mr. A. M. Neville, under whose supervision the work was carried out, for his valuable criticism and advise.

This paper is based on an M.Sc. thesis submitted by the author to Manchester University.

References

1. ZWOYER, E. M. & SIESS, C. P., "Ultimate Strength in Shear of Simply-Supported Prestressed Concrete Beams Without Web Reinforcement", Proceedings of the American Concrete Institute, Vol. 51, 1954-55.
2. MORICE, P. B. & LEWIS, H. E., "The Ultimate Strength of Two-Span Continuous Prestressed Concrete Beams as Affected by Tendon Transformation and Un-Tensioned Steel", Technical Report TRA/186, Cement and Concrete Association, May 1955.
3. CASE, JOHN, "The Strength of Materials", Edward Arnold & Co., 1938.
4. LIN, T. Y., "Design of Prestressed Concrete Structures", John Wiley & Sons, Inc., New York, 1955.
5. BILLET, D. F. & APPLETON, J. H., "Flexural Strength of Prestressed Concrete Beams", Journal of the American Concrete Institute, Vol. 25, No. 10, June 1954.
6. JENSEN, V. P., "Ultimate Strength of Reinforced Concrete Beams as Related to the Plasticity Ratio of Concrete," University of Illinois, Engineering Experiment Station Bulletin 345, June 1943.

NOTATION

a	—	shear span
A_s	—	area of stressed reinforcement
B	—	width of beam
C.A.	—	centroidal axis
d	—	overall depth of beam
e	—	strain in general, or eccentricity
e_1,e_2	—	principal strains, and are e_t when tensile and e_c when compressive
e_u	—	limiting compressive strain at which concrete crushes
E_c	—	modulus of elasticity of concrete
E_s	—	modulus of elasticity of steel
f_b	—	breaking strength of reinforcement, lbs/in^2
f_c	—	fibre stress in a concrete section at any level
f_{cr}	—	cylinder crushing strength of concrete
f_r	—	modulus of rupture of concrete

f_e — tensile stress in reinforcement at transfer
f_y — yield stress of reinforcement
f_u — tensile stress in reinforcement at ultimate conditions
f_x — stress in x-direction, positive when tensile
f_y — stress in y-direction, positive when tensile
I — second moment of area
I_T — transformed second moment of area
I_{Tm} — transformed second moment of area at mid-span
I_{Ts} — transformed second moment of area at section of maximum shear
L — span length in inches
$\frac{1}{m}$ — Poisson's ratio
M — bending moment in general
M_D — bending moment due to dead load
M_L — bending moment due to live load
M_T — secondary bending moment due to linear transformation of cable
Mp — plastic moment of resistance
M_{ult} — ultimate bending moment
n — number of redundancies
p — reinforcement ratio, A_s/Bd
p% — percentage reinforcement = $p \times 100$
p_t — principal tensile stress
p_c — principal compressive stress
P — prestressing force in general
P_e — effective prestressing force at transfer
P_u — prestressing force at ultimate conditions
q — shear stress
Q — statical moment, about the centroidal axis, of the cross-sectional area above (or below) any given level where shearing unit stress is required
v — unit shearing stress
V — shearing force
V_c — shearing force carried by the concrete
V_s — shearing force carried by the reinforcement
W — load in general
W_s — shear cracking load, i.e. the load at which the first inclined shear crack appears
W_u — ultimate load
Z — shear susceptibility number

$$X = \frac{E_c \dfrac{I_{Tm}}{I_{Ts}}\, p\%}{E_s \dfrac{f_e}{f_y}\, L}$$

Θ_p — orientation of principal axes, i.e. the angle, measured anti-clockwise, which the principal axes make with the x-axis
ϵ_x — strain in x-direction, positive when tensile
ϵ_y — strain in y-direction, positive when tensile
$\epsilon\Theta$ — strain in any direction, Θ, with the x-axis.
ϵ_{xy} — shear strain

TABLE 1

Beam No.	Section	Age at Test Days	Cylinders		Control Beams		Grout f_{cr}	Dia. of Reinforce't	A_s	p%	Cable Type	Effective Prestress at Transfer p_e* (lbs.)	f_e lbs/in^2	f_e / $f_{y0.1}$%
			f_{cr}	E_c—in Compres'n	E_c—in Bending	f_r								
3	8"x4"	14	4,610	3.93×10^6	4.63×10^6	750	5,520	0.276"	0.1188	0.3713	1	4,635	38,700	0.19
4	8"x4"	20	5,020	3.70×10^6	4.48×10^6	740	5,800	0.200"	0.0628	0.1962	1	5,070	82,800	0.394
8	8"x4"	67	4,425	5.38×10^6	6.00×10^6	651	4,020	0.276"	0.1188	0.3713	1	9,340	78,500	0.387
5	8"x4"	30	5,870	4.20×10^6	5.02×10^6	700	4,800	0.276"	0.1188	0.3713	2	9,975	83,600	0.410
6	8"x4"	44	5,150	4.40×10^6	5.68×10^6	797	3,250	0.276"	0.1188	0.3713	2	8,210	69,100	0.338
7	8"x4"	71	5,900	5.13×10^6	6.56×10^6	630	5,080	0.276"	0.1188	0.3713	2	11,900	100,300	0.490
9	8"x4"	53	5,540	5.30×10^6	5.38×10^6	865	4,620	0.276"	0.1782	0.5570	2	11,870	66,600	0.326
10	8"x4"	18	6,700	6.30×10^6	5.97×10^6	840	4,800	0.200"	0.0628	0.1962	2	8,300	132,000	0.645
13	8"x4"	46	6,800	5.80×10^6	5.70×10^6	862	3,020	0.276"	0.1188	0.3713	2	0	0	0
11	8"x4"	75	6,370	5.50×10^6	5.40×10^6	820	2,900	0.276"	0.1782	0.5570	3	12,630	71,000	0.348
12	8"x4"	79	6,220	5.31×10^6	5.53×10^6	766	4,200	0.276"	0.2376	0.7425	3	12,050	30,700	0.248
14	8"x4"	14	6,850	6.00×10^6	6.78×10^6	754	3,700	0.276"	0.1188	0.3713	3	11,750	98,950	0.485

* Average of both ends of beam

TABLE 2

Stresses in Wires at Ultimate Loads

Beam No.	LEFT END		RIGHT END		Load§ Ton	W_u	Mode of Failure	Location of Failure
	Wire 1	Wire 2	Wire 1	Wire 2				
3	42,700	83,500	48,500	46,000	28.0	29.25	Shear	B(L)‡
3*	43,800	85,500	50,500	47,300	29			
4	202,000	202,000	186,000	200,000	20	20.50	Flexure	D&G
8	133,000	132,000	136,000	152,000	31	32.00	Shear	B(L)
8*	139,000	138,000	142,000	160,000	32			
5	143,000	151,000	86,000	93,500	28	30.00	Flexure	D&G
5*	173,000	180,000	89,000	97,500	30			
6	136,000	110,000	168,000	174,000	33.5	33.5	Shear	B(L)
7	193,000	190,000	138,000	135,000	31	31.2	Flexure	D
9	94,000	94,200	134,000	122,000	30	31.0	Shear	B(L)
	91,000		142,000					
9*	103,000	104,000	144,000	133,000				
	102,000		152,000					
10	204.000	190,000	234,000	232,000	20.5	20.6	Rupture of Wires	G
13	126,000	125,000	94,000	104,000	23	24.0	Flexure	D
11	108,000	135,000	125,000	125,000	34	36.0	Shear	B(L)
	122,000		125,000					
11*	124,000	149,000	141,000	143,000	36			
	136,000		142,000					
12	64,500	58,700	94,000	94,000	29	29.5	Shear	B(L)
	61,000	67,000	87,500	77,500				
14	190,000	196,000	172,000	195,000	36.5	39.5	Flexure	D&G
14*	214,000	206,000	195,000	202,000	38			

* Stress values are obtained by extrapolation
‡ B(L) = Shear failure occurred on the left of section B
§ Load = Load at which stresses are calculated
f_y = 160,000 lbs. per sq. inch for B4 and B10, for rest of beams the value is 176,000 lbs. per sq. inch

TABLE 3

Behaviour of Test Beams

Beam No.	Mode of Failure	Measured Cracking Load Tons	Computed Cracking Load Tons	Measured / Computed	Shear Cracking Load	Ultimate Load Tons	Principal Stresses			Computation of Shear Susceptibility Number			
							p_t lbs./sq. in.	p_c	Load*	$\frac{I_{Tm}}{I_{Ts}}$	$\frac{p}{f_e/f_y.L}$	Z	Comparison %
3	Shear	11	10.6	1.04	29.25	29.25	810	1,020	29.25 (W_s)§	1.02	6.95×10^{-2}	11.5×10^{-3}	710
4	Flexure	10	10.7	0.94	—	20.50	390	796	20.50 (W_u)†	1.01	1.80×10^{-2}	2.58×10^{-3}	160
8	Shear	13	13.8	0.94	32.50	27.50‡	683	1,217	32.50 (W_s)	1.02	3.41×10^{-2}	7.25×10^{-3}	450
5	Flexure	14.5	13.8	1.05	—	30.00	715	1,209	30.00 (W_u)	1.02	2.50×10^{-2}	4.45×10^{-3}	274
6	Shear	15.0	14.0	1.07	29.00	33.50	720	1,126	29.00 (W_s)	1.02	3.02×10^{-2}	6.10×10^{-3}	376
7	Flexure	13.5	14.8	0.92	—	31.20	670	1,296	31.20 (W_u)	1.02	2.10×10^{-2}	4.70×10^{-3}	290
9	Shear	15.0	16.7	0.90	24.00	31.00	511	979	24.00 (W_s)	1.03	4.75×10^{-2}	9.15×10^{-3}	565
10	Flexure (Rupture of wires)	14.7	13.5	1.09	—	20.60	421	869	20.60 (W_u)	1.00	0.85×10^{-2}	1.62×10^{-3}	100
13	Flexure	7.0	6.8	1.02	—	16.00	236	654	14.0	1.02	—	—	—
11	Shear	20.0	19.6	1.02	32.20	36.00	618	1,222	32.20 (W_s)	1.05	3.56×10^{-2}	7.02×10^{-3}	435
12	Shear	20.0	18.7	1.07	25.00	29.50	493	937	25.00 (W_s)	1.06	6.64×10^{-2}	13.50×10^{-3}	834
14	Flexure	18.7	18.0	1.04	—	39.50	734	1,526	39.5 (W_u)	1.03	1.69×10^{-2}	3.98×10^{-3}	246

*The load at which the principal stresses are computed

‡The beam was unloaded when the first shear crack appeared at 32.5 tons. On reloading the beam failed at 27.5 tons.

§W_s = Shear cracking load, i.e. the load at which the first shear crack appeared.

†W_u = Ultimate load

Note: Z for B13 is omitted because beam was not prestressed.

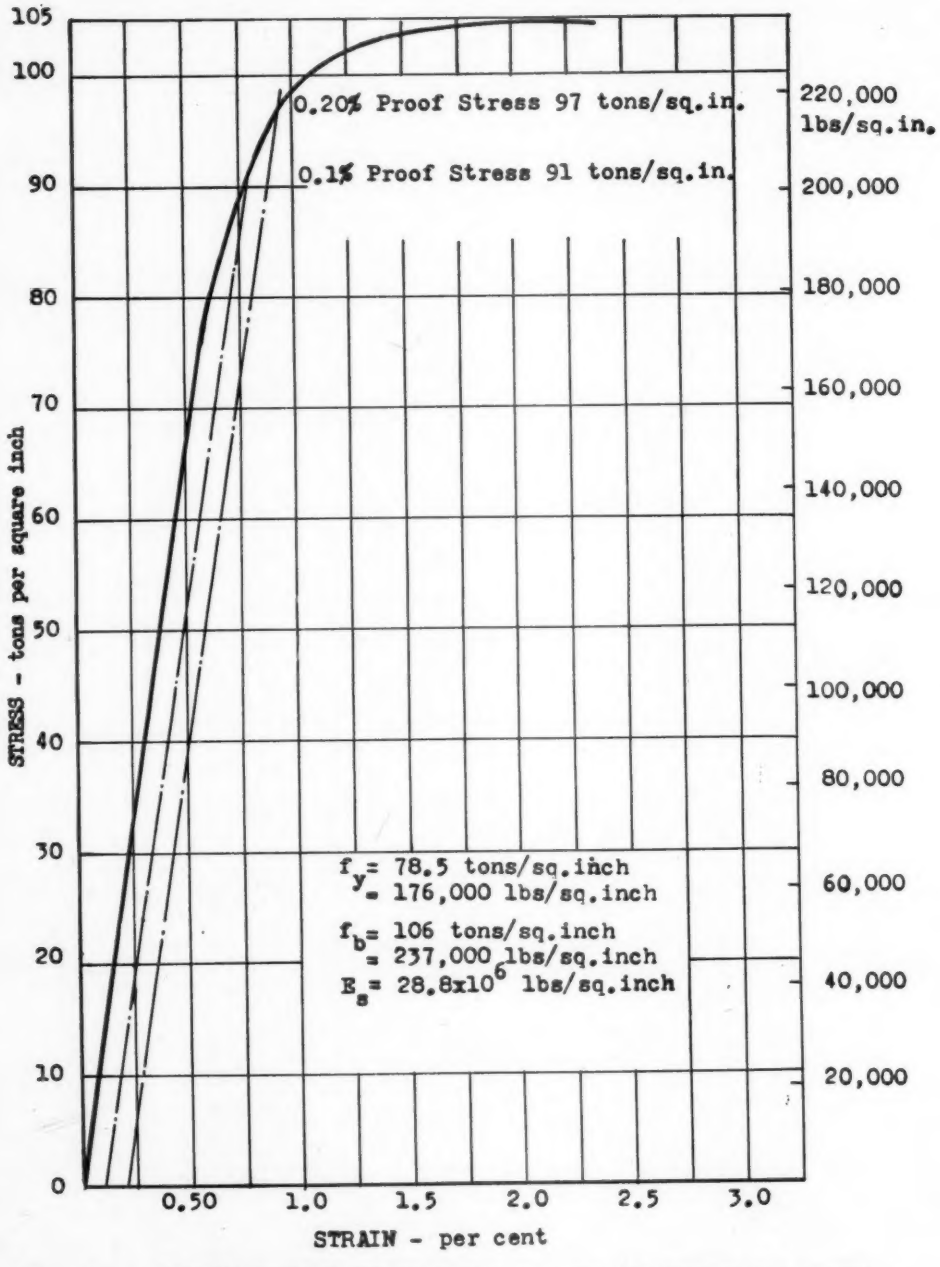

Fig. 1a: STRESS-STRAIN CURVE FOR 0.276 IN. DIAMETER H.T. STEEL

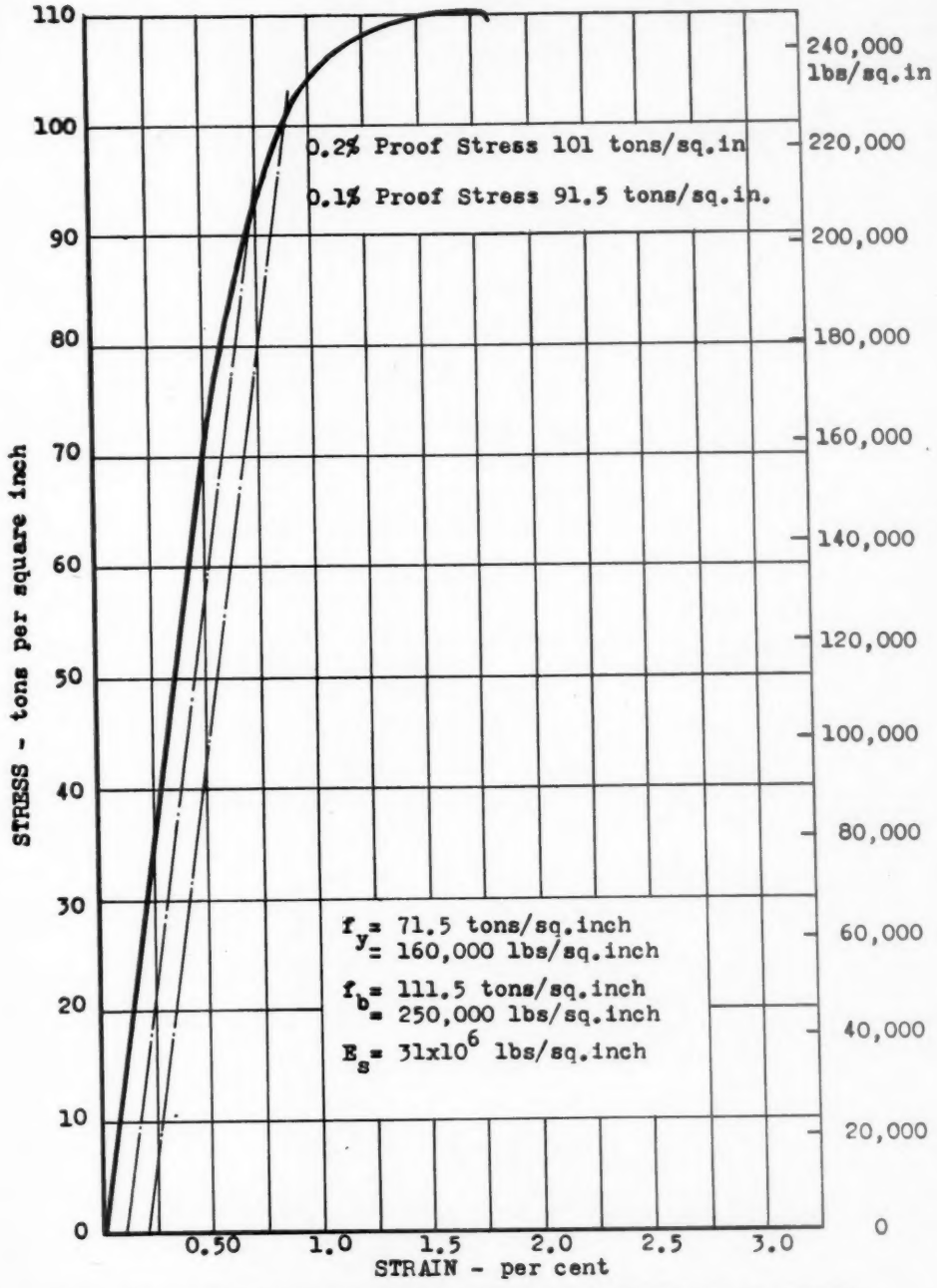

Fig. 1b: STRESS-STRAIN CURVE FOR 0.2" DIAMETER H. T. STEEL

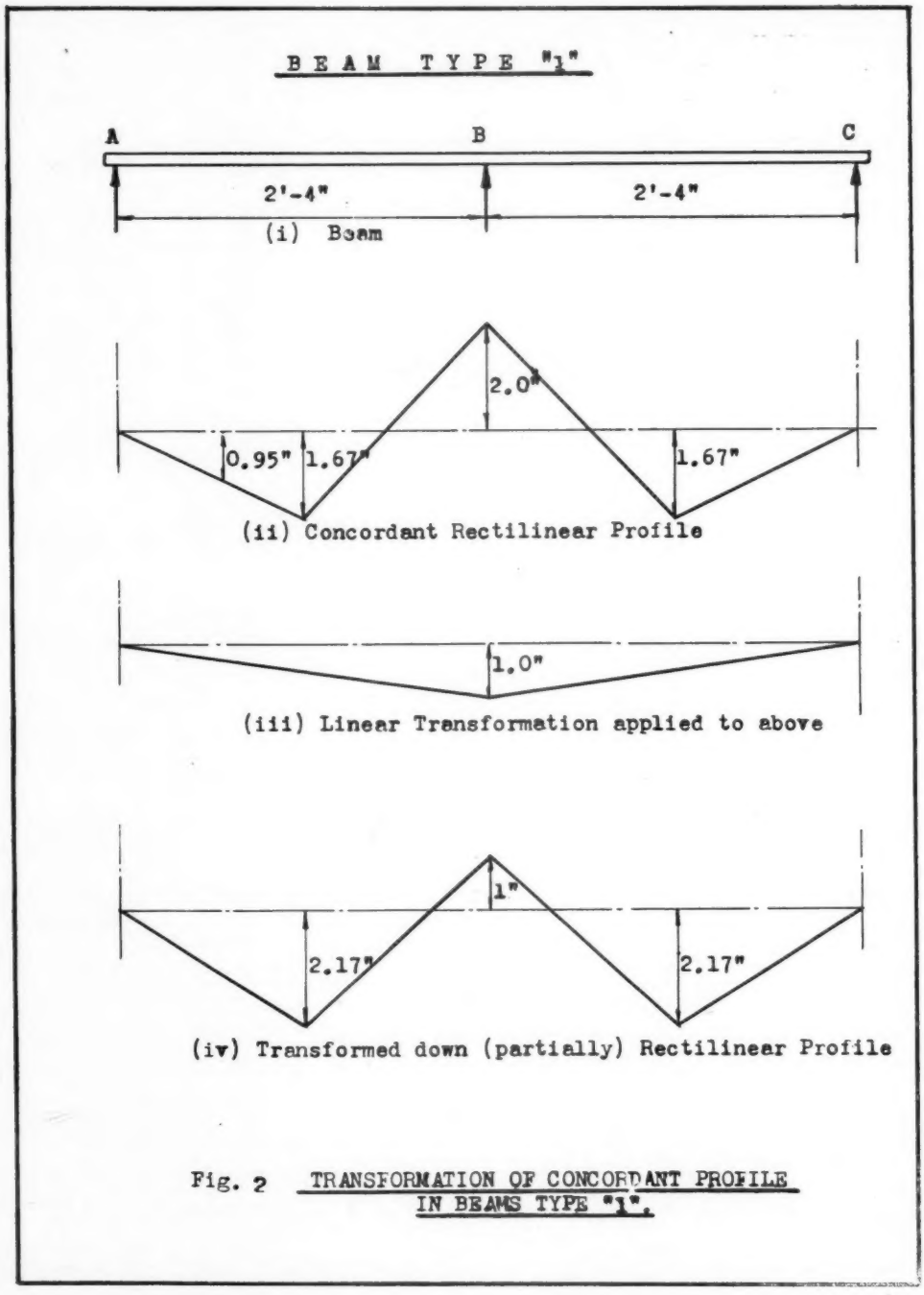

Fig. 2 TRANSFORMATION OF CONCORDANT PROFILE IN BEAMS TYPE "1".

BEAM TYPE "2"

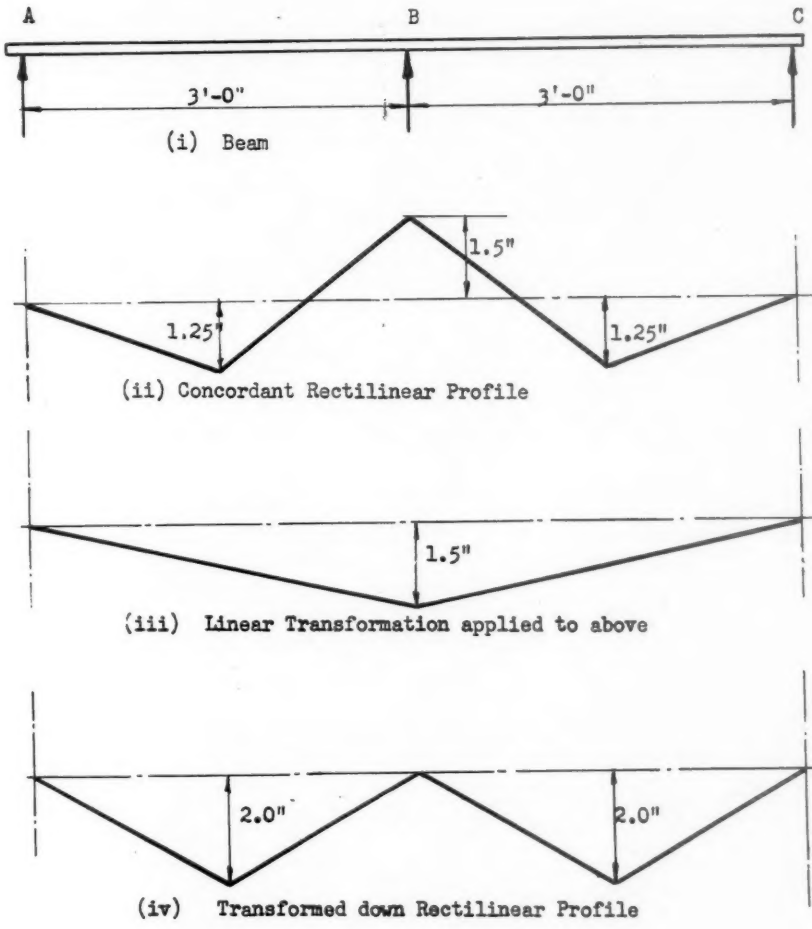

Fig. 3 TRANSFORMATION OF CONCORDANT PROFILE IN BEAMS TYPE "2"

BEAM TYPE "3"

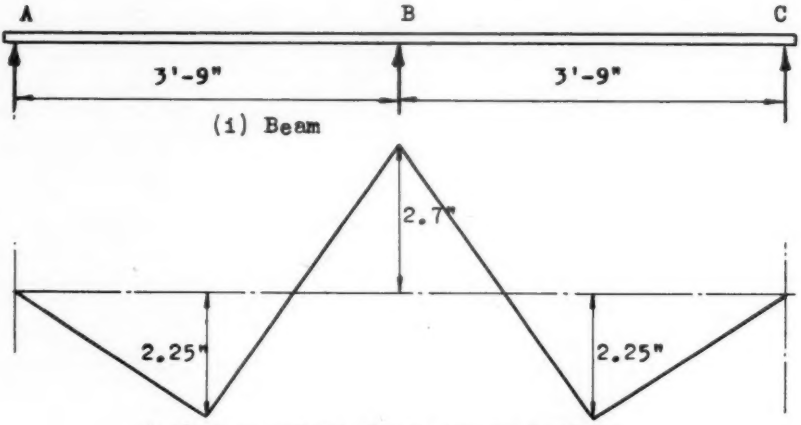

Fig. 4 TRANSFORMATION OF CONCORDANT PROFILE IN BEAMS TYPE "3"

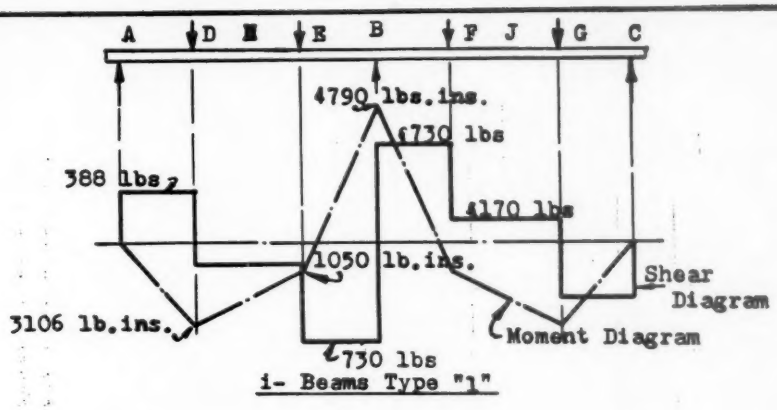

i- Beams Type "1"

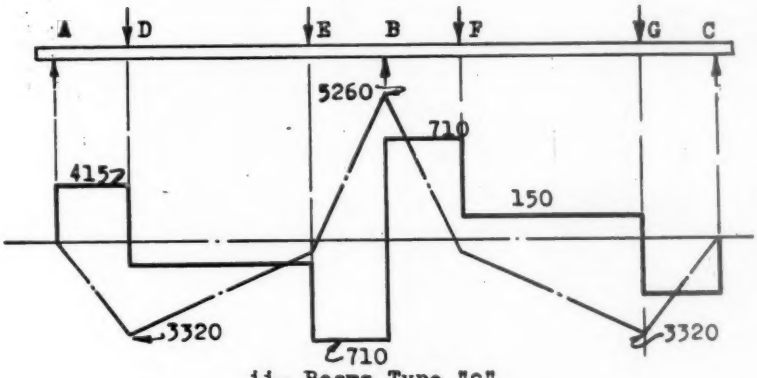

ii- Beams Type "2"

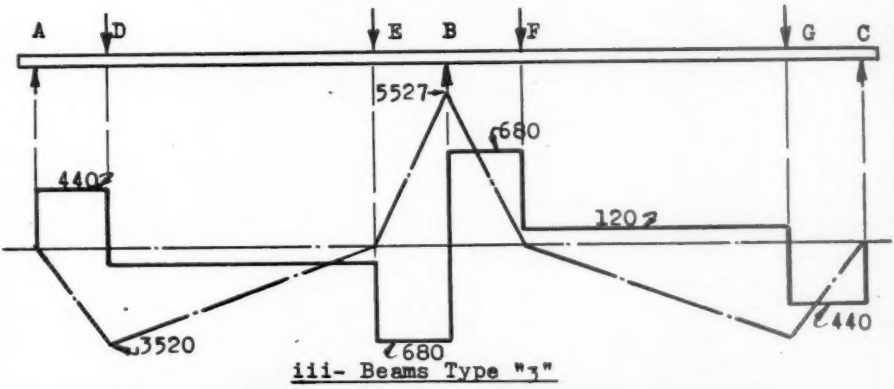

iii- Beams Type "3"

Fig. 5: BENDING MOMENT AND SHEAR FORCE DIAGRAMS DUE TO 1 TON LIVE LOAD.

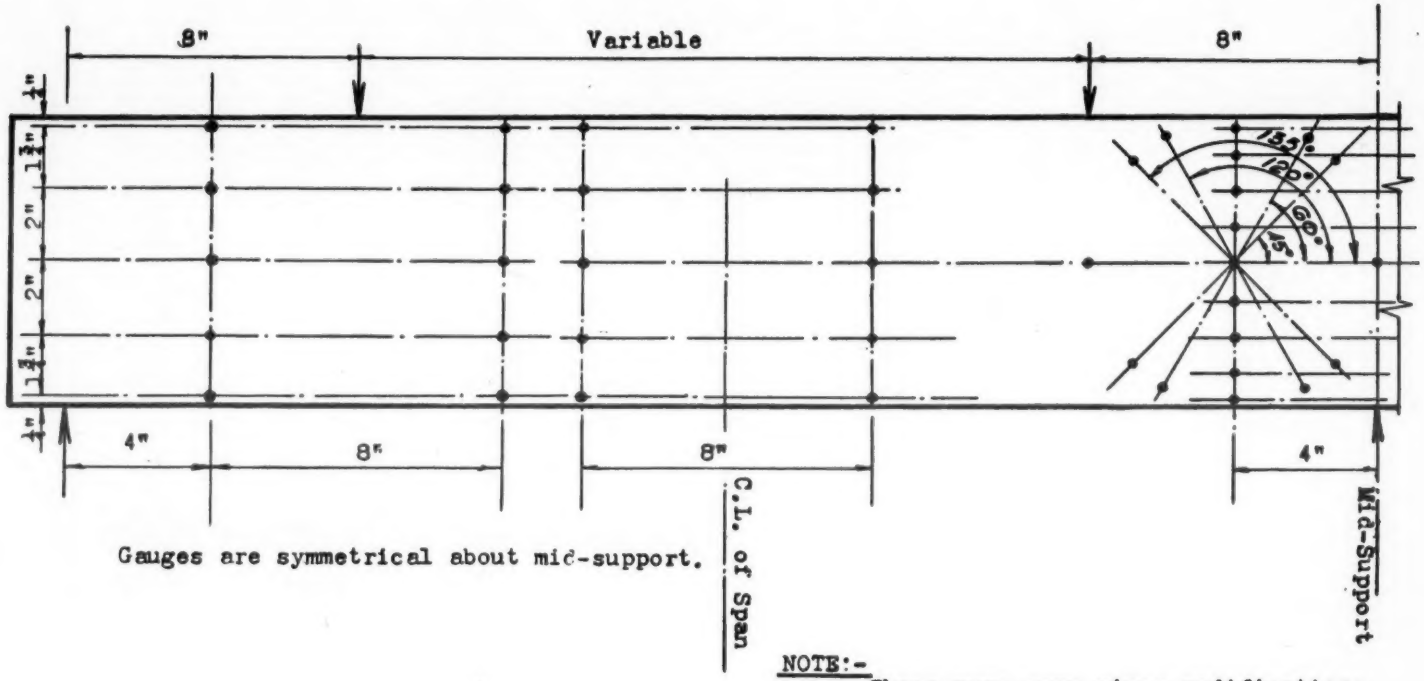

Gauges are symmetrical about mid-support.

NOTE:- There were some minor modifications on the above in some beams.

Fig. 6 LOCATION OF GAUGES ON SIDE OF BEAMS

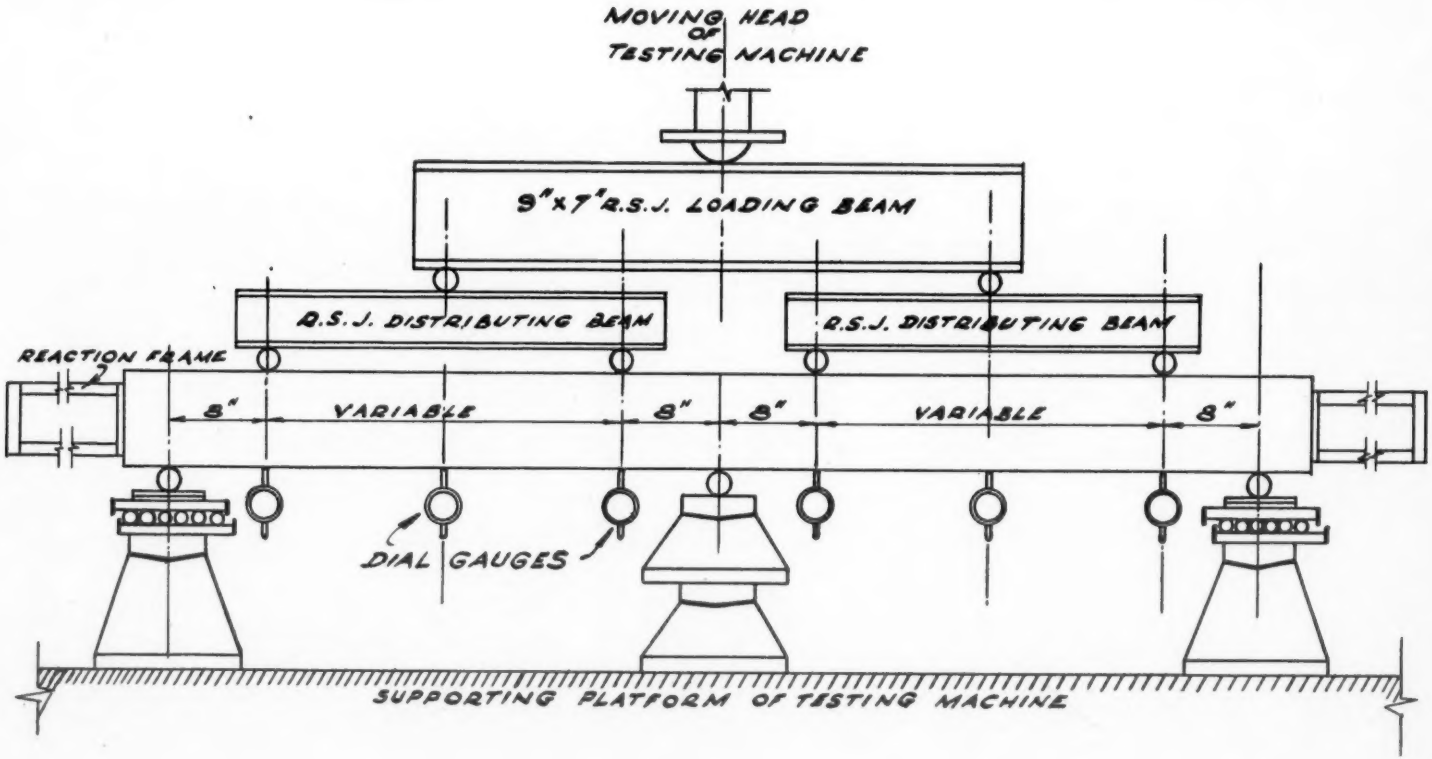

FIG. 7 - GENERAL TEST SET-UP

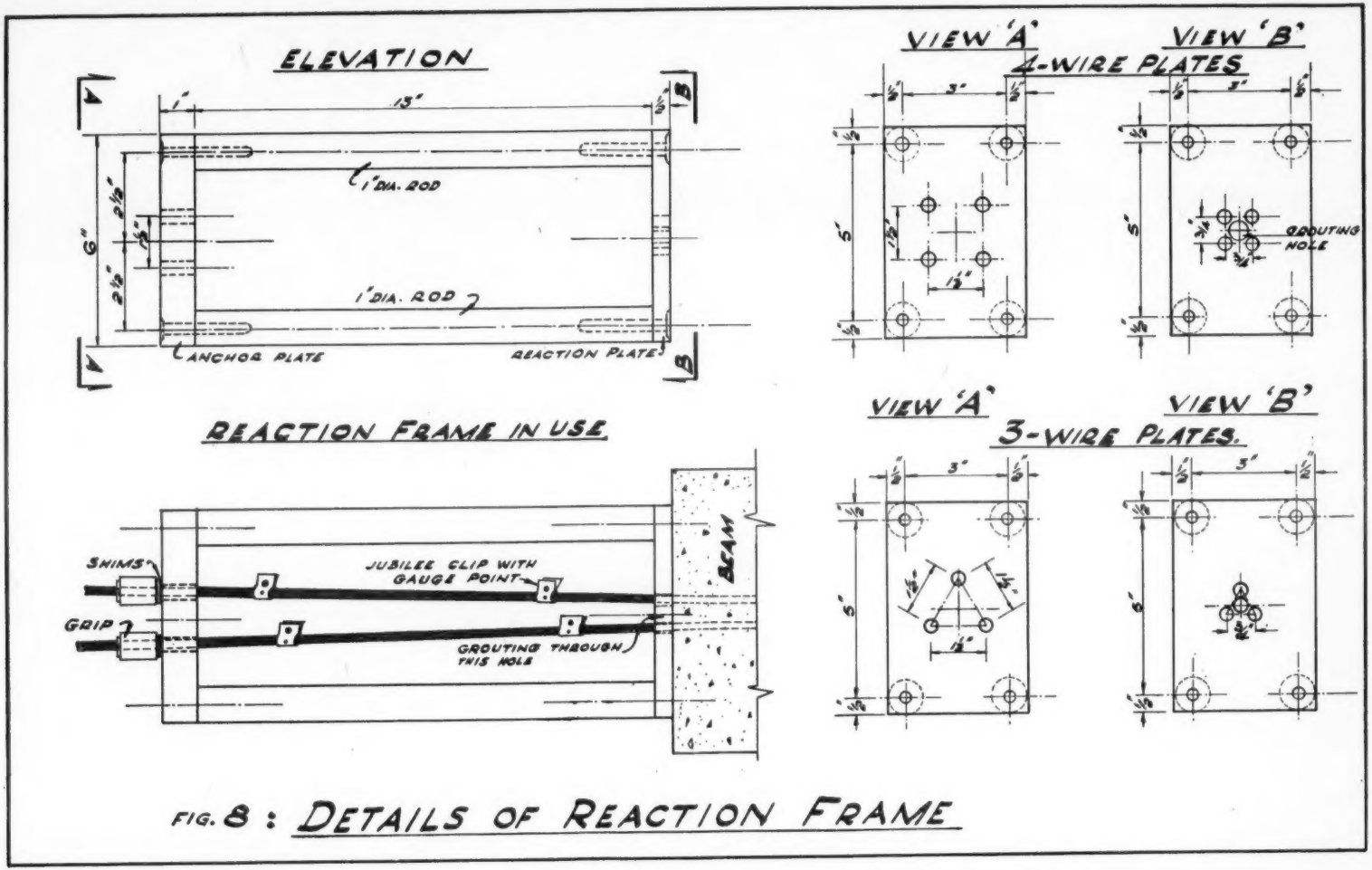

FIG. 8 : DETAILS OF REACTION FRAME

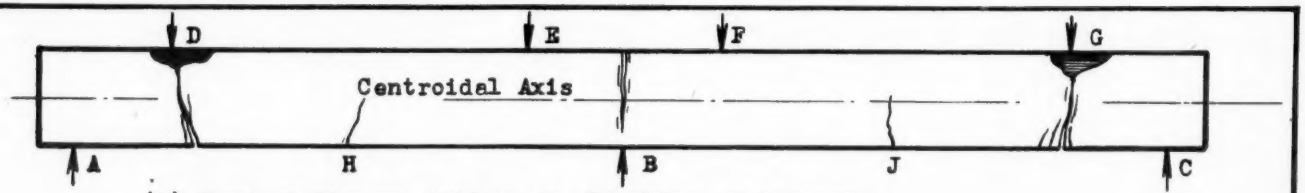

(i) Typical Flexure Failure by Crushing of Concrete

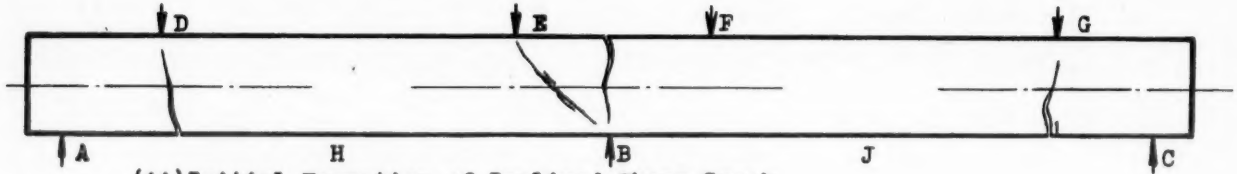

(ii) Initial Formation of Inclined Shear Crack

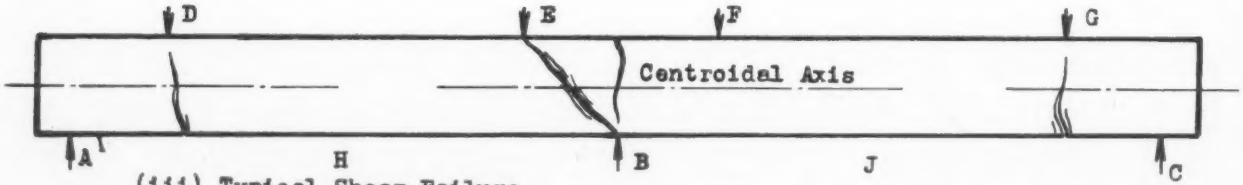

(iii) Typical Shear Failure

Fig. 9 : MODES OF FAILURE OF TWO-SPAN BEAMS

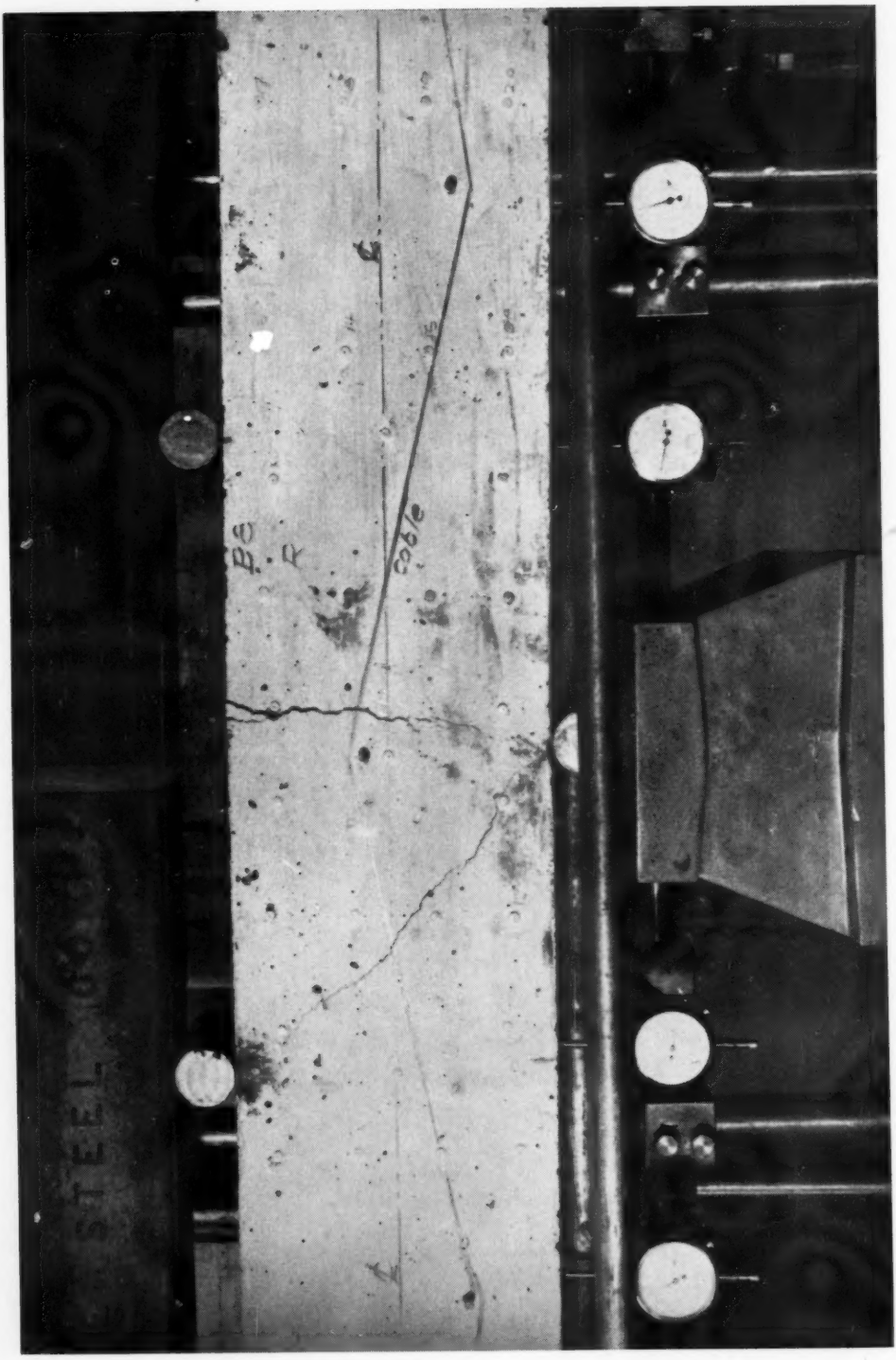

Figure 10—Initial formation of inclined shear crack

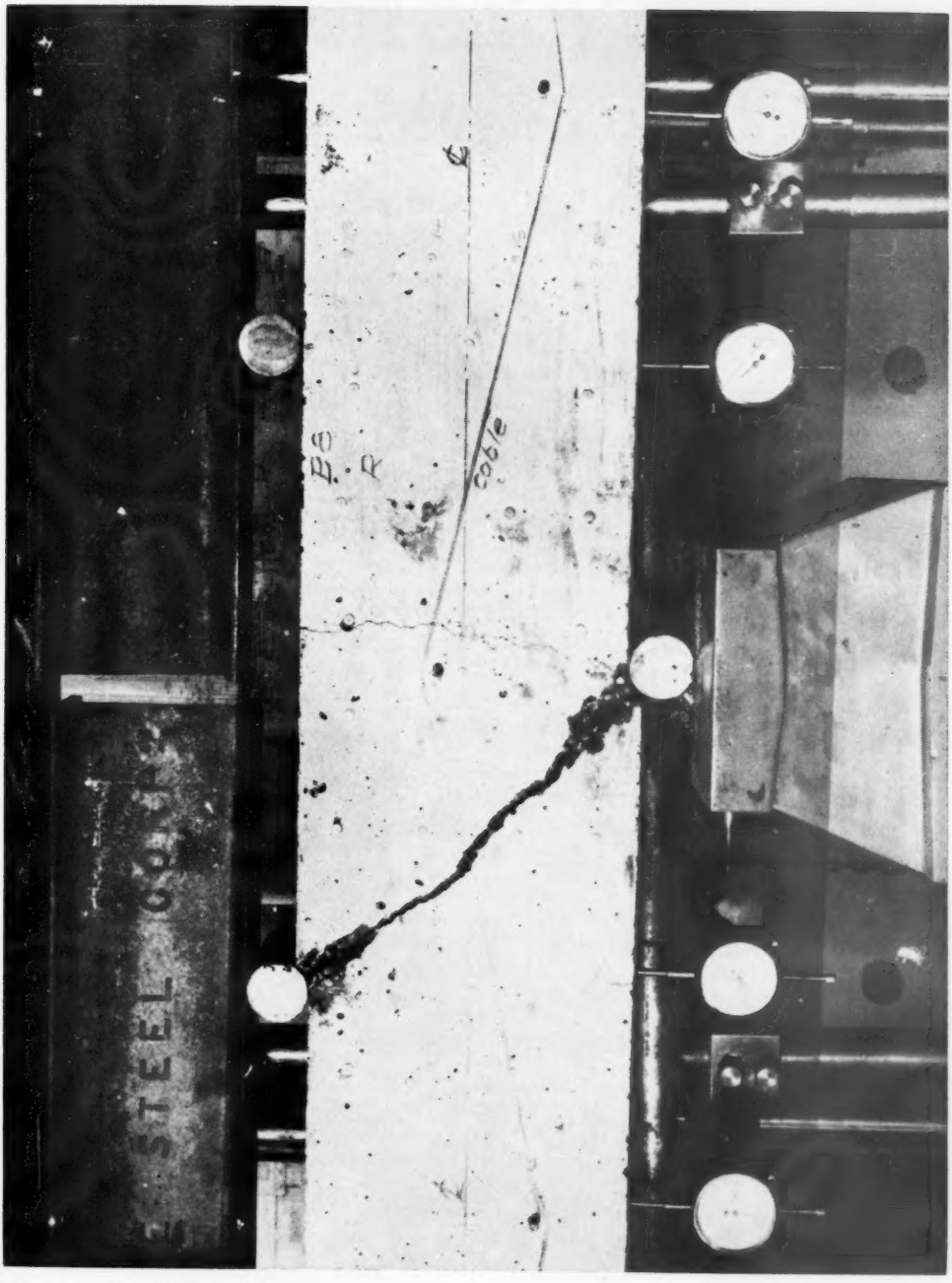

Figure 11—Typical Shear Failure

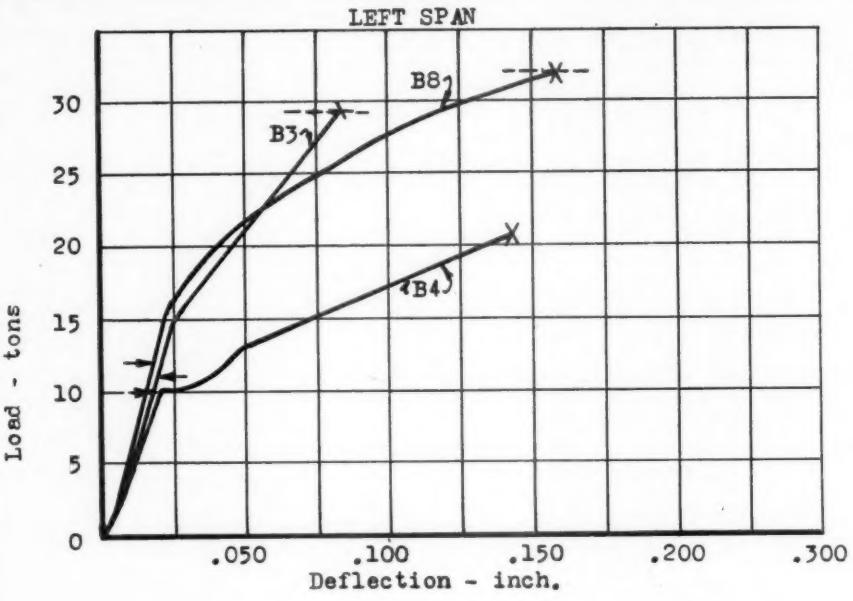

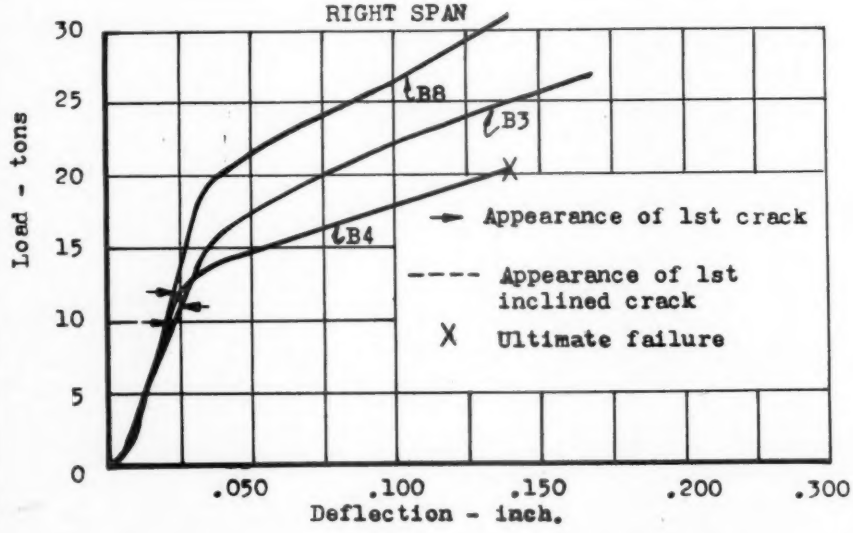

Fig.12 : LOAD-DEFLECTION GRAPHS FOR MID-SPAN BEAMS TYPE "1".

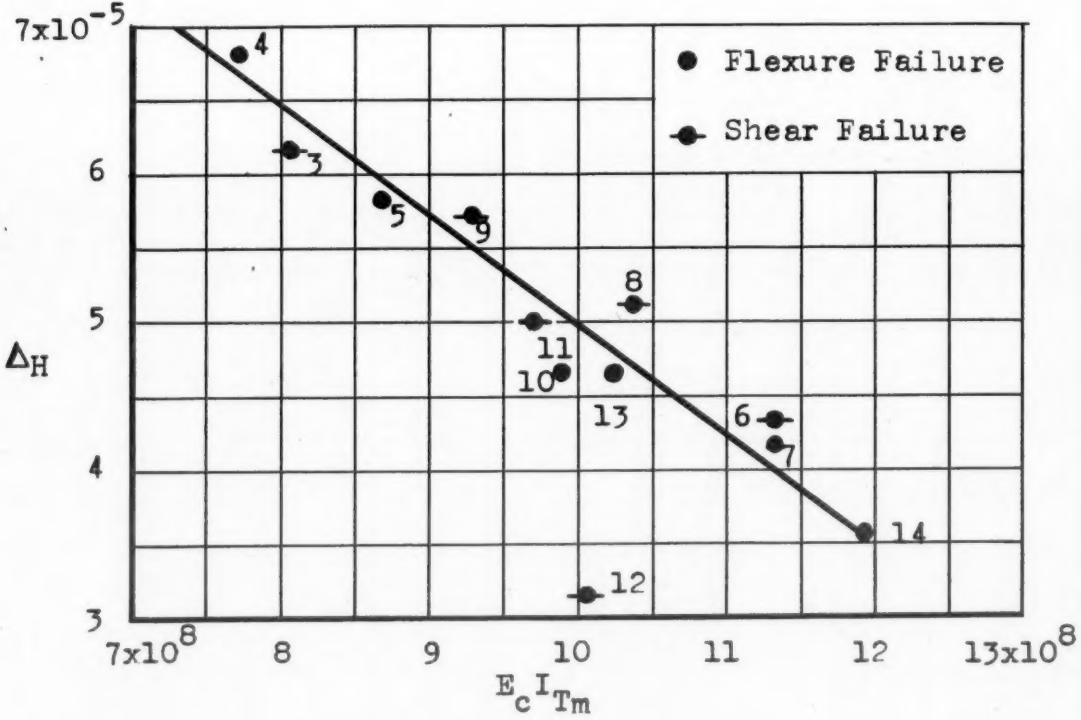

Fig.13: Δ_H v. $E_c I_{Tm}$

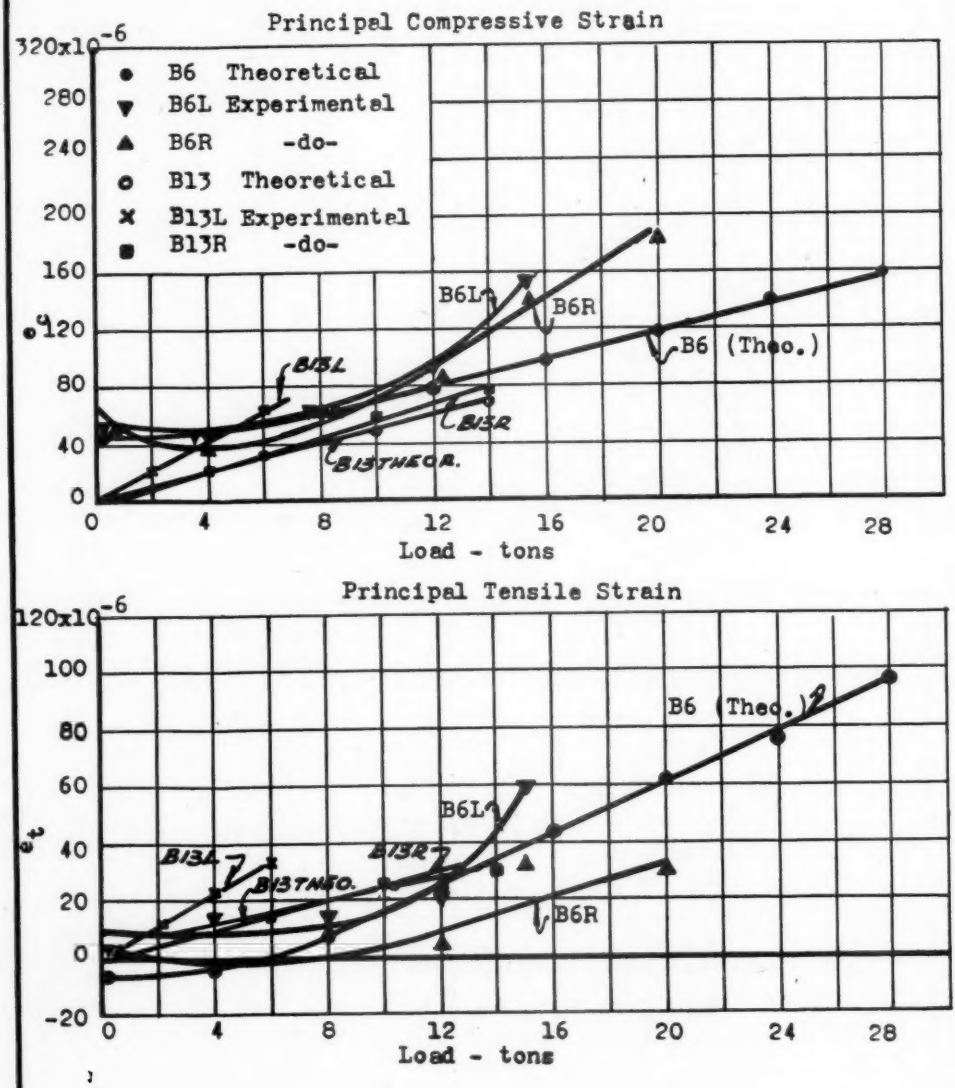

Fig. 14 : PRINCIPAL STRAINS v. LOAD
BEAMS "B6" & "B13".

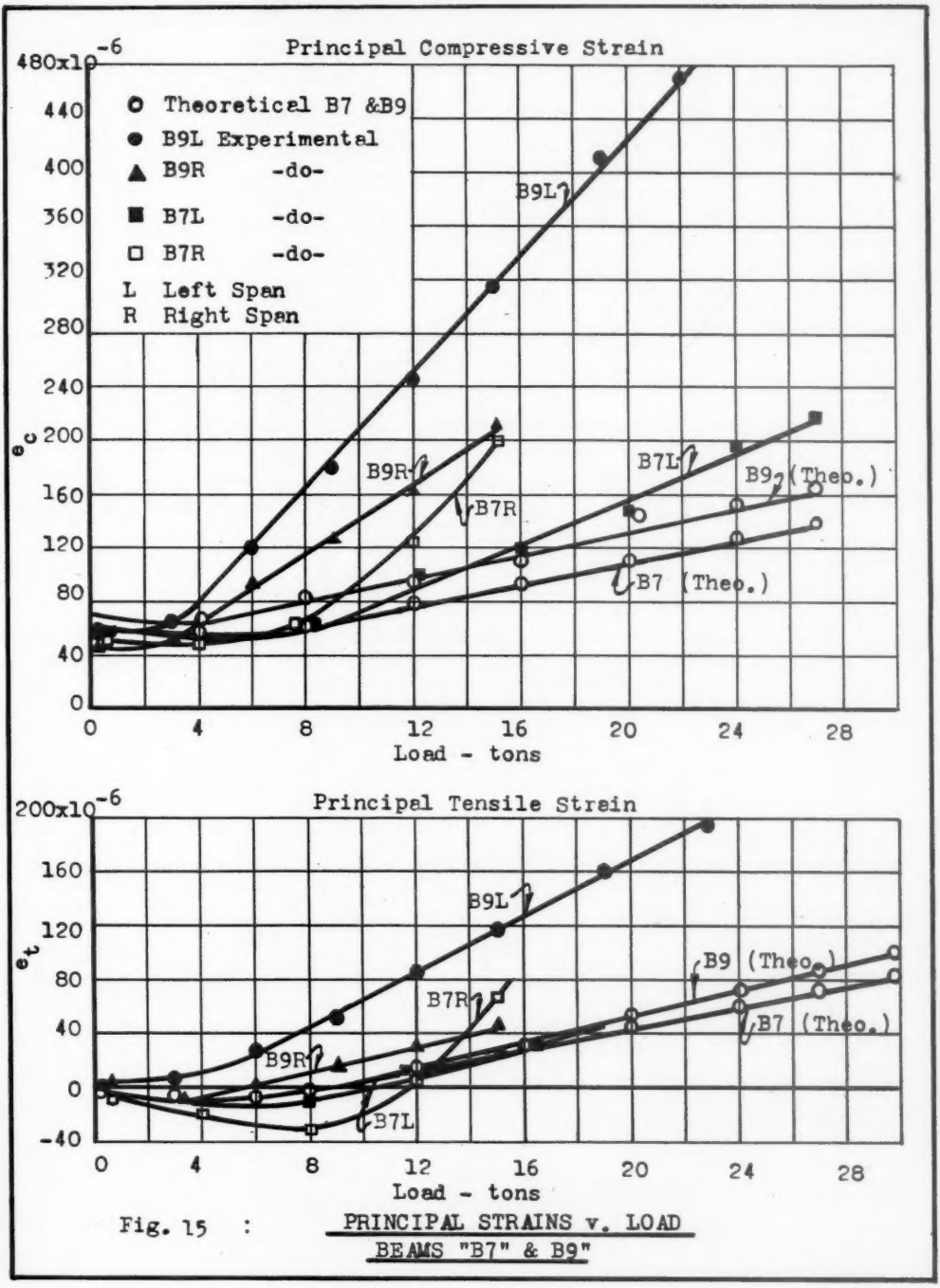

Fig. 15 : PRINCIPAL STRAINS v. LOAD
BEAMS "B7" & B9"

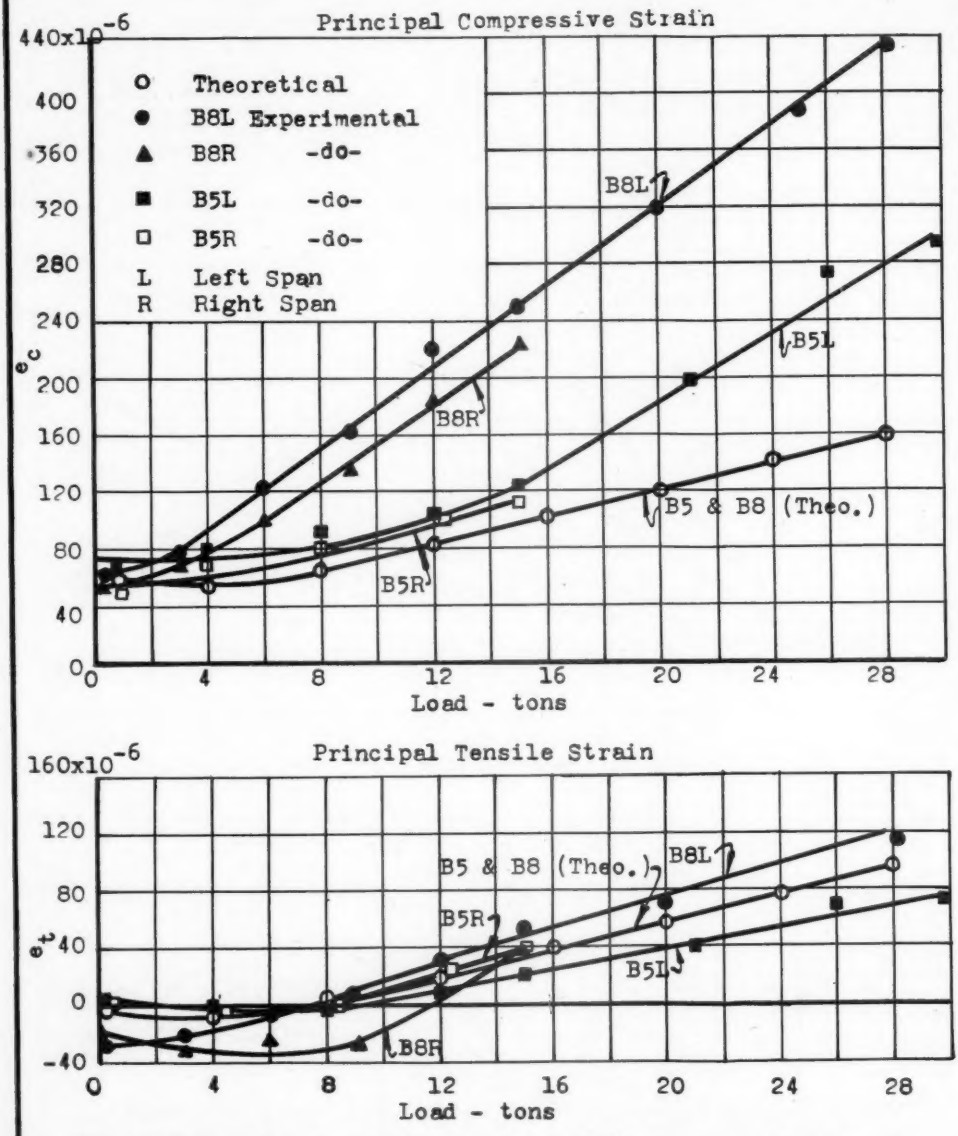

Note:- Theoretical Graphs for B5 and B8 are very identical

Fig.16 : PRINCIPAL STRAINS v. LOAD BEAMS "B8" & "B5".

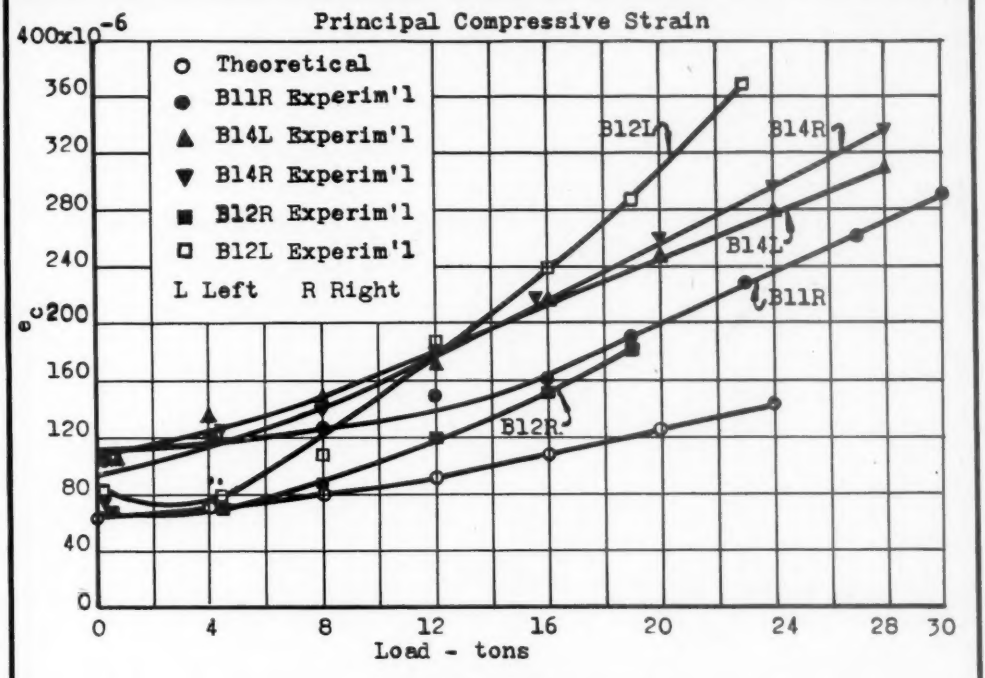

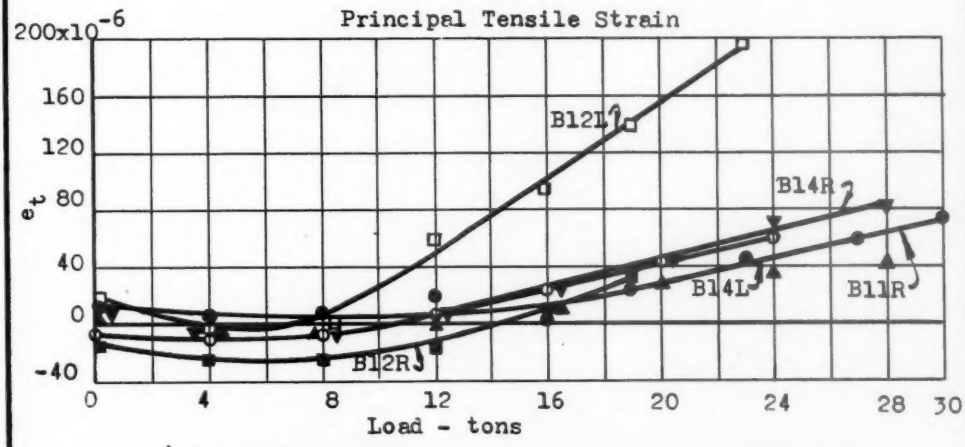

Note:- Theoretical Graph is the same for B11, B12 and B14.

Fig.17 : PRINCIPAL STRAINS v. LOAD BEAMS "B11", "B12" AND "B14".

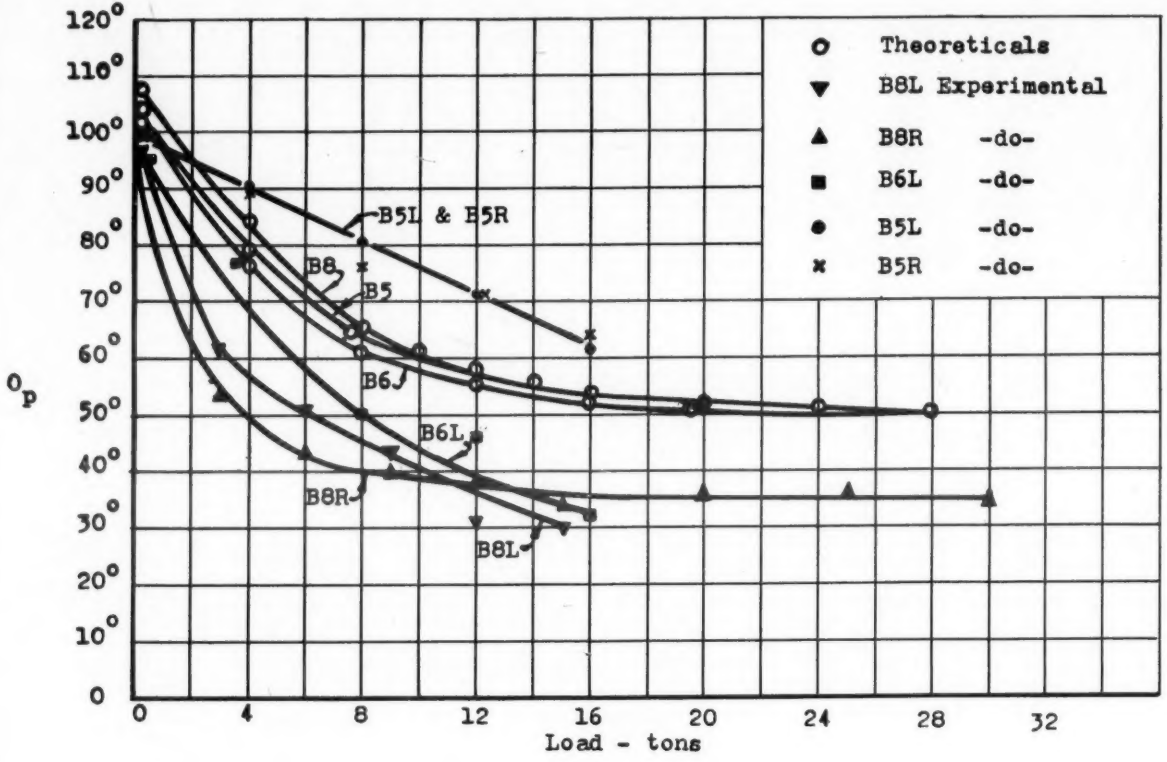

Fig.18 : ORIENTATION OF PRINCIPAL AXES v. LOAD BEAMS "B5", "B6" AND "B8".

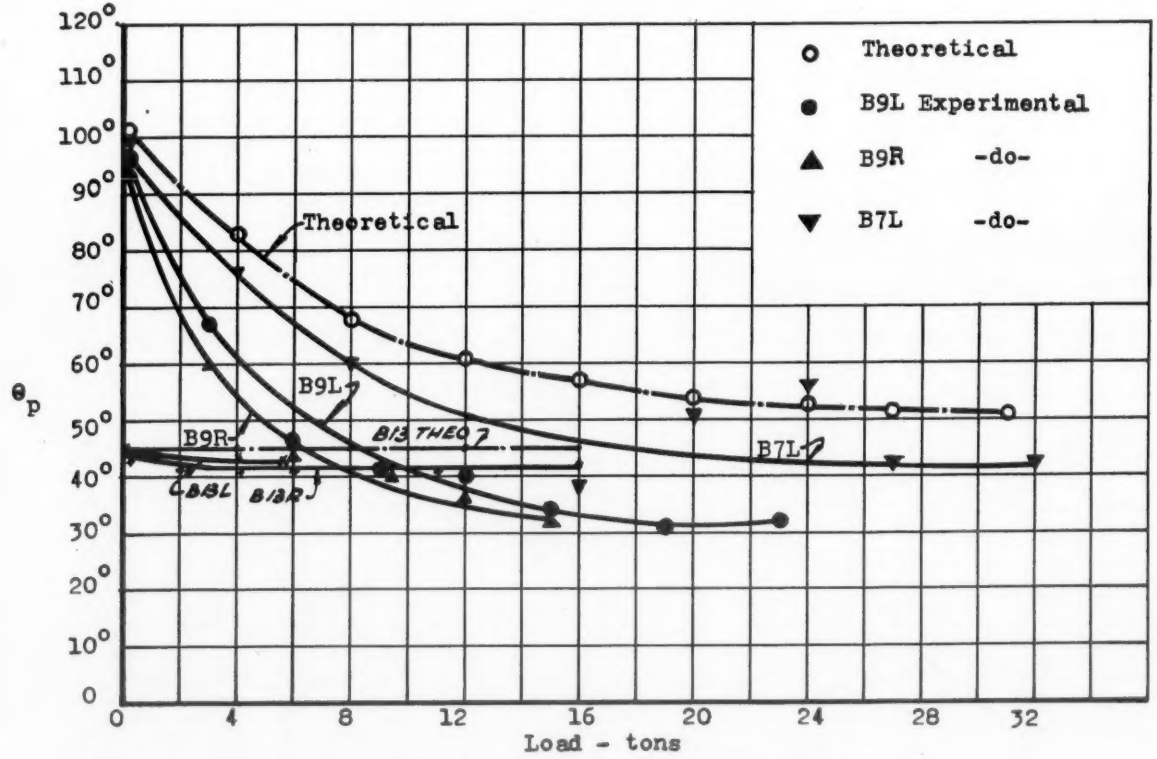

Note:- Theoretical Graphs for B7 and B9 are identical.

Fig. 19 : ORIENTATION OF PRINCIPAL AXES v. LOAD
BEAMS "B7", "B9" & "B13".

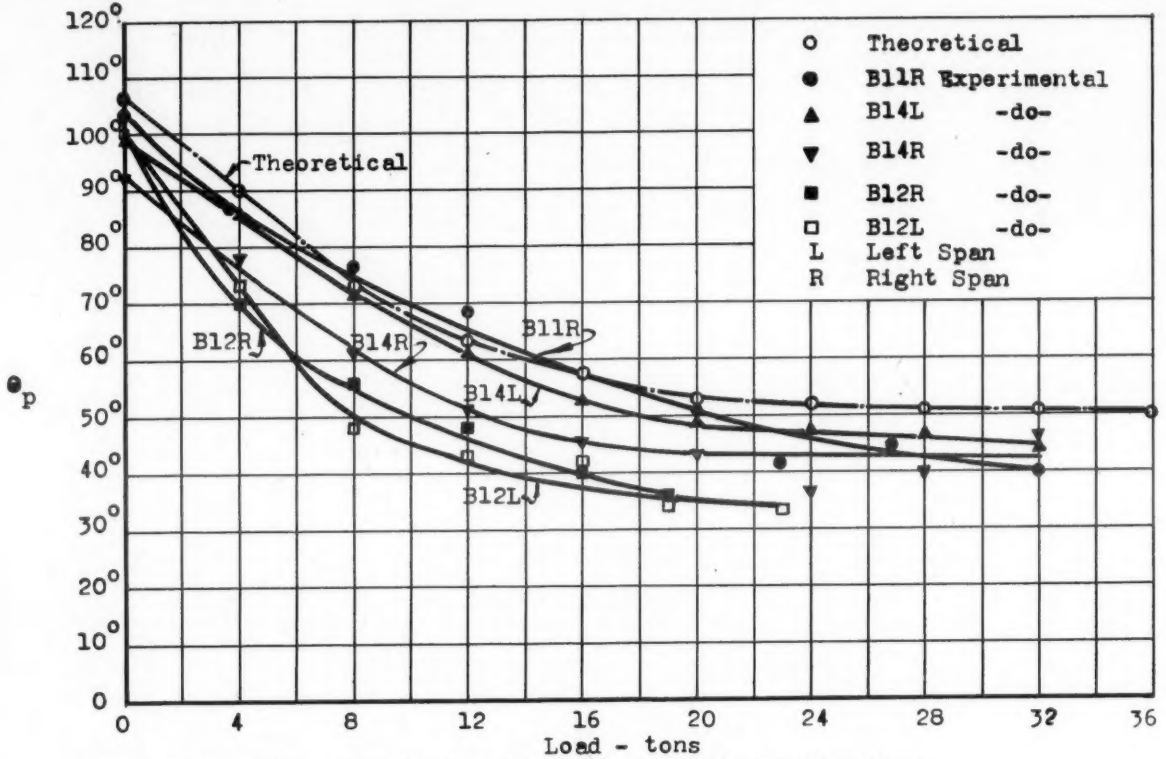

Note:- Theoretical Graphs for B11, B12 and B14 are identical.

Fig. 20 : ORIENTATION OF PRINCIPAL AXES v. LOAD
BEAMS "B11", "B12" & "B14".

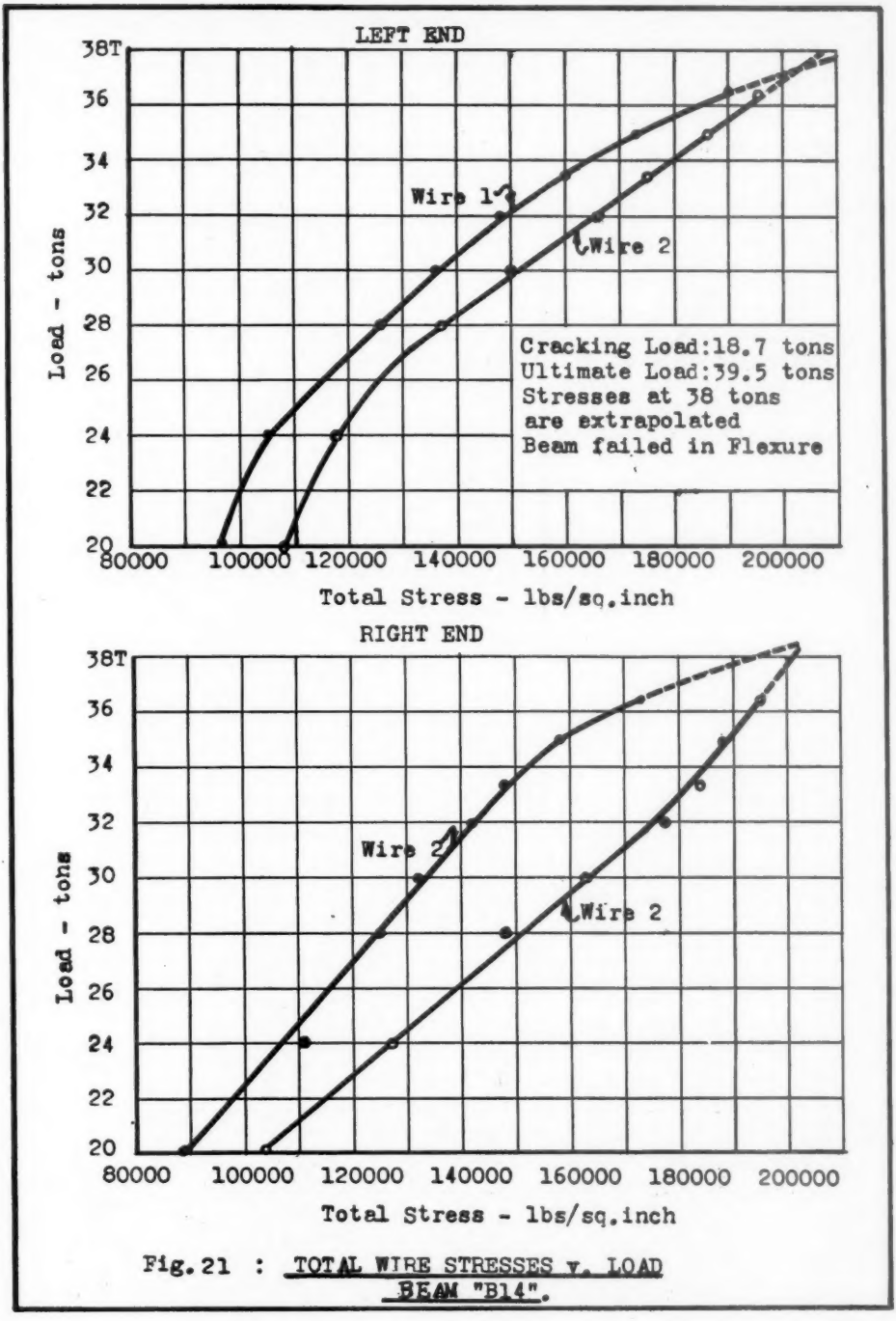

Fig.21 : TOTAL WIRE STRESSES v. LOAD
BEAM "B14".

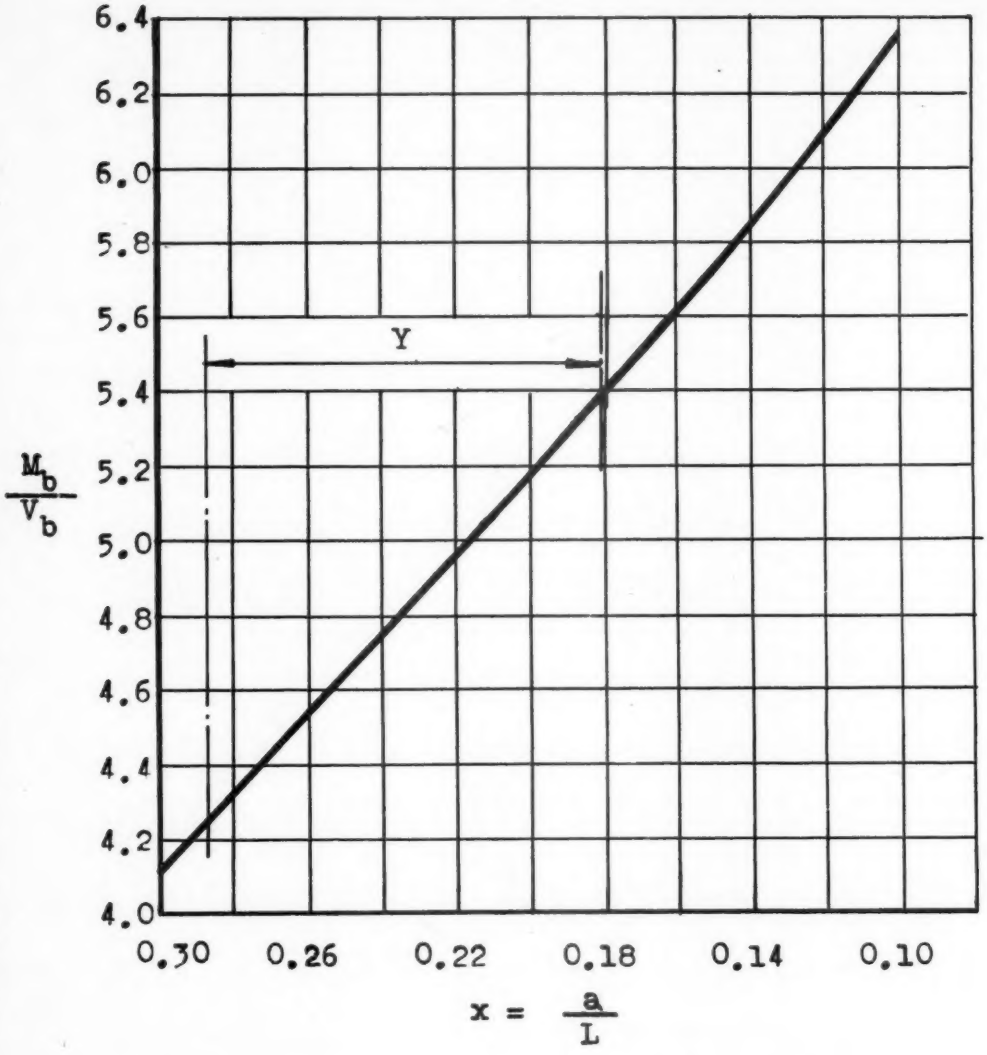

Notes

1- Y = Range of present tests

2- Equation of curve: $\frac{M_b}{V_b} = \frac{2a(1-x)}{2 + 3x - 3x^2}$

Fig.22: VARIATION OF $\frac{M_b}{V_b}$ WITH $\frac{a}{L}$

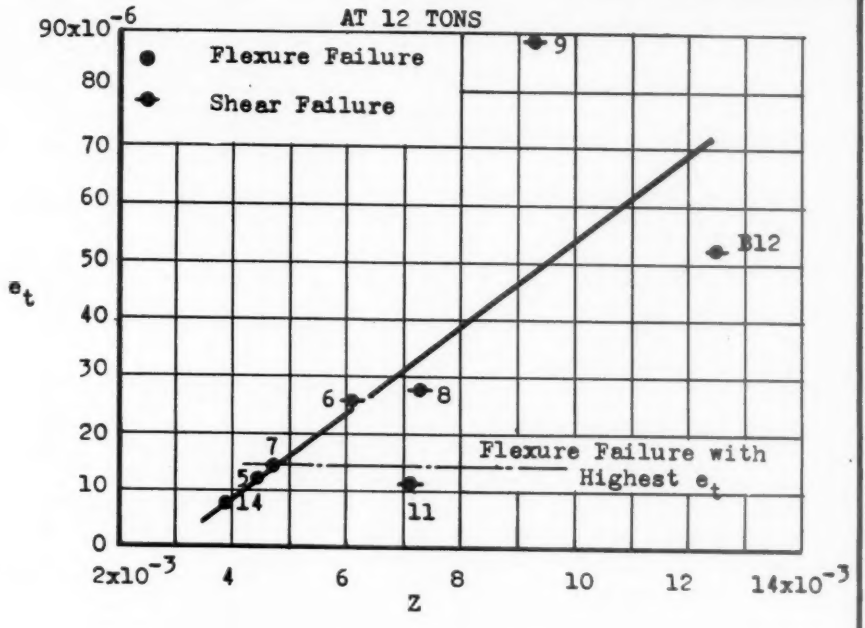

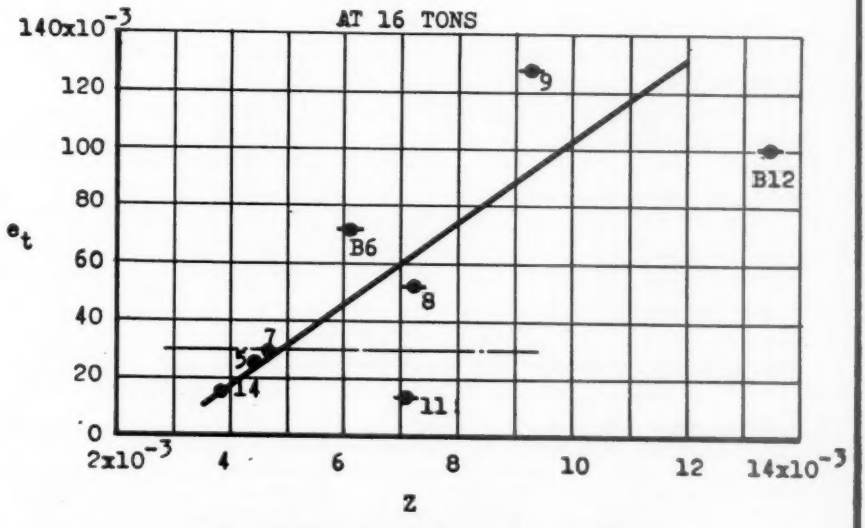

Fig. 23: PRINCIPAL TENSILE STRAIN v. SHEAR SUSCEPTIBILITY NUMBER

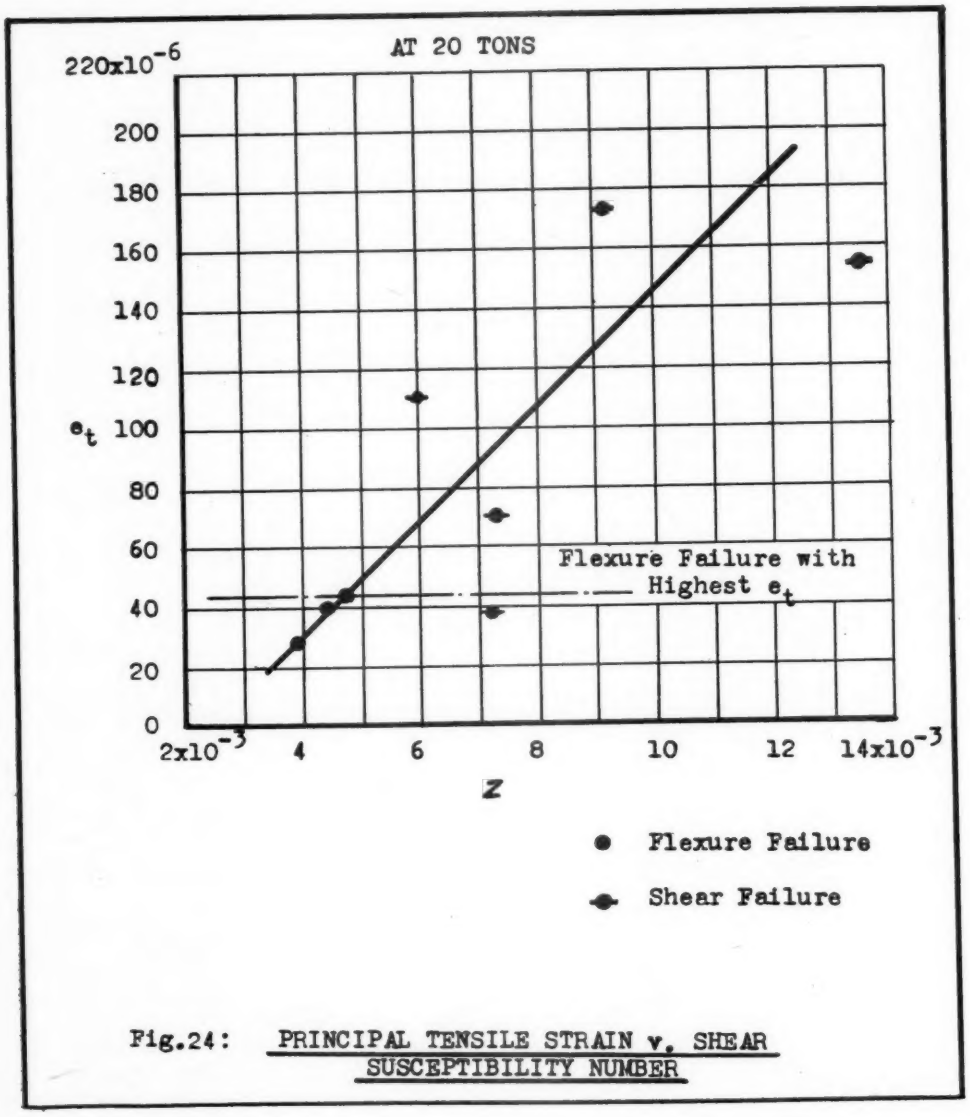

Fig.24: PRINCIPAL TENSILE STRAIN v. SHEAR SUSCEPTIBILITY NUMBER

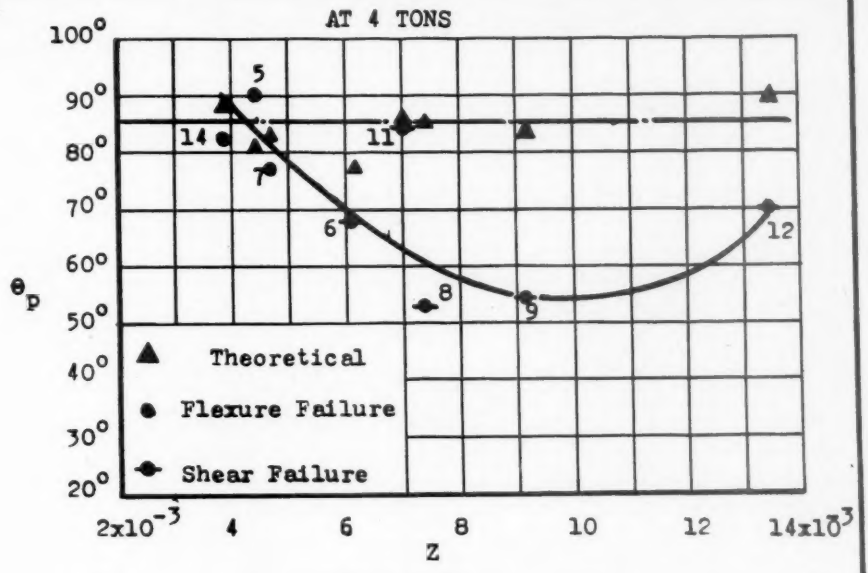

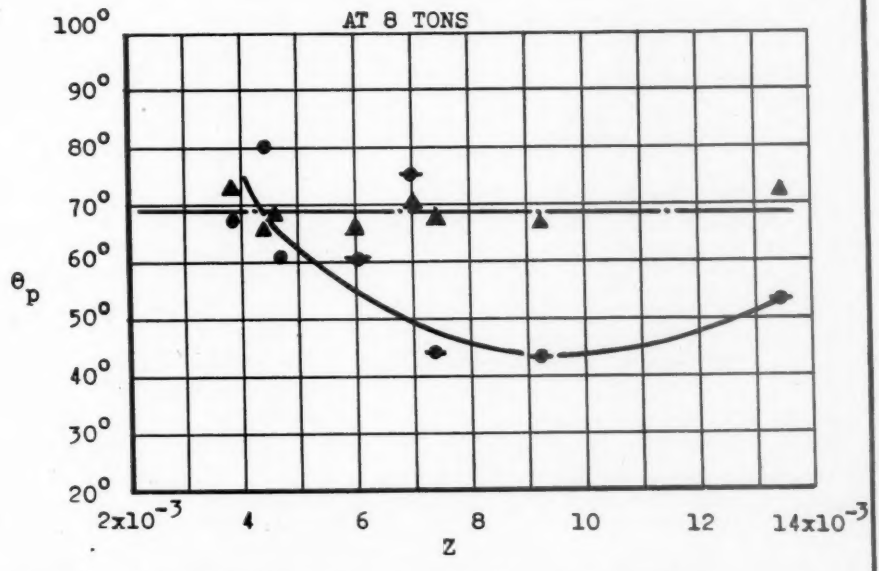

Fig. 25 ORIENTATION OF PRINCIPAL AXES v. SHEAR SUSCEPTIBILITY NUMBER

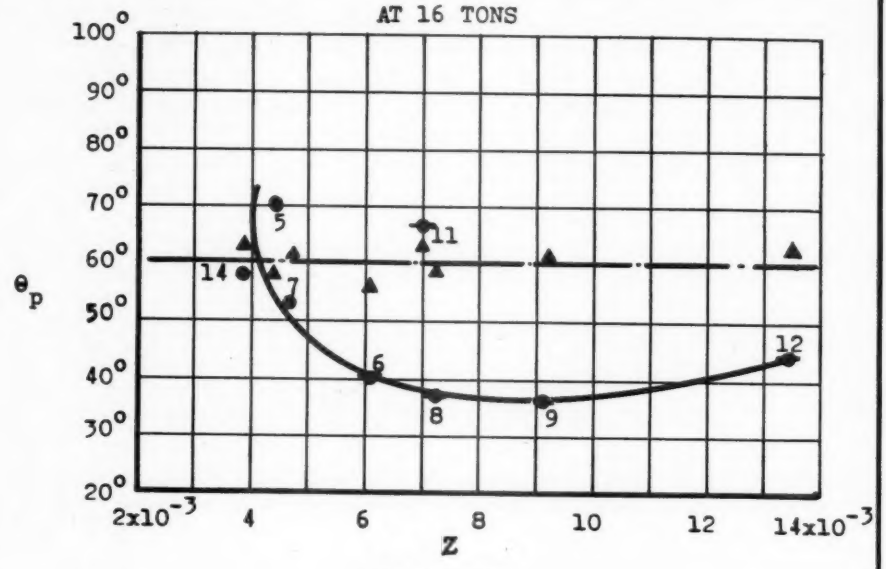

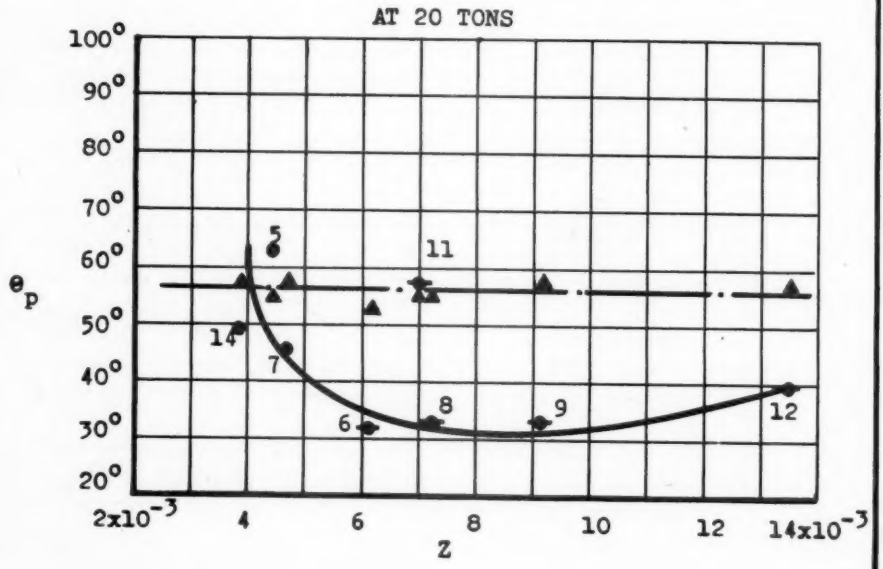

Fig. 26 : ORIENTATION OF PRINCIPAL AXES v. SHEAR SUSCEPTIBILITY NUMBER

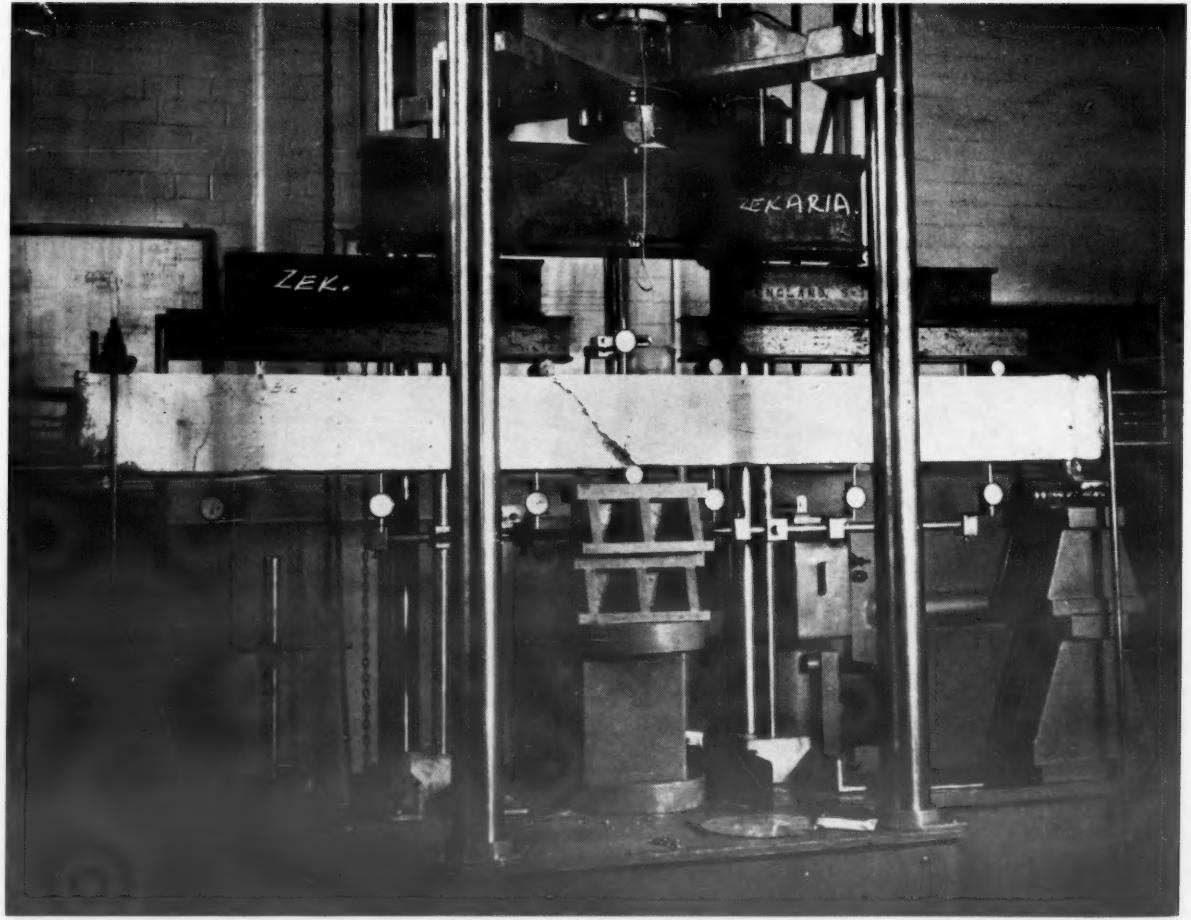

Figure 27—General test set-up

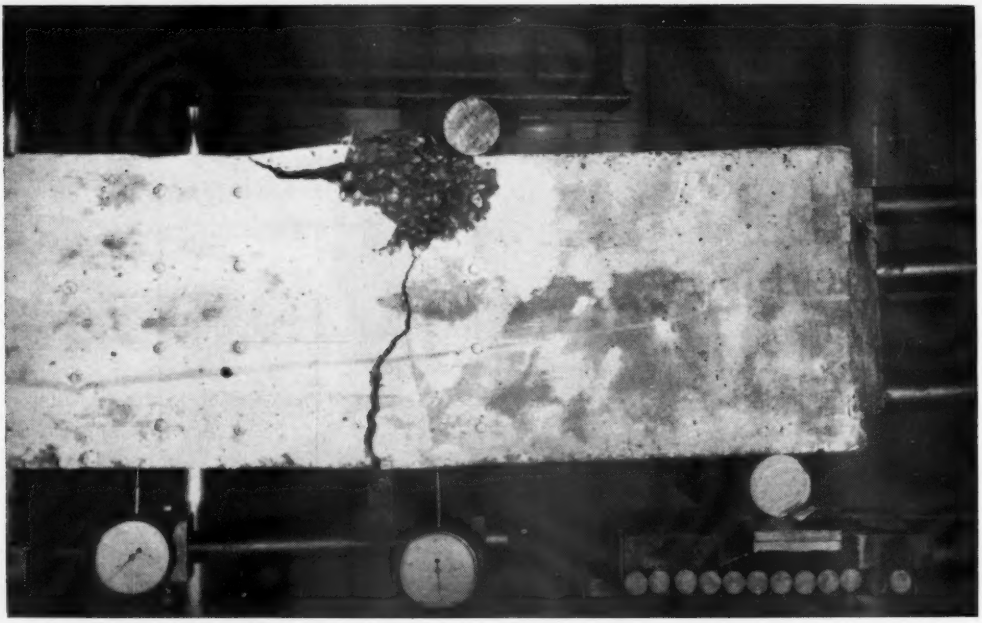

Figure 28—Typical flexure failure

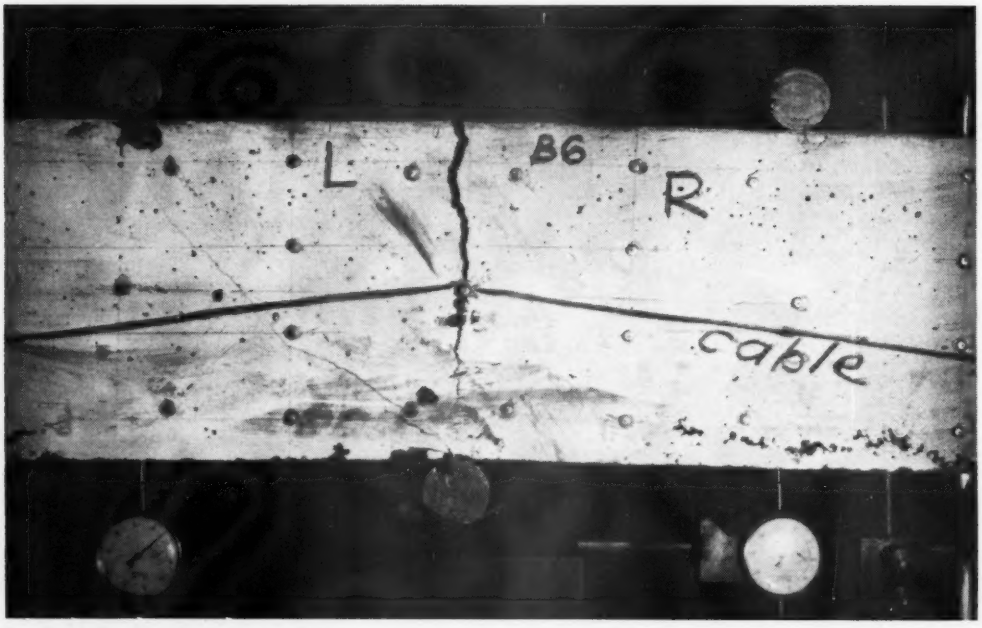

Figure 29—First shear cracks in B-6

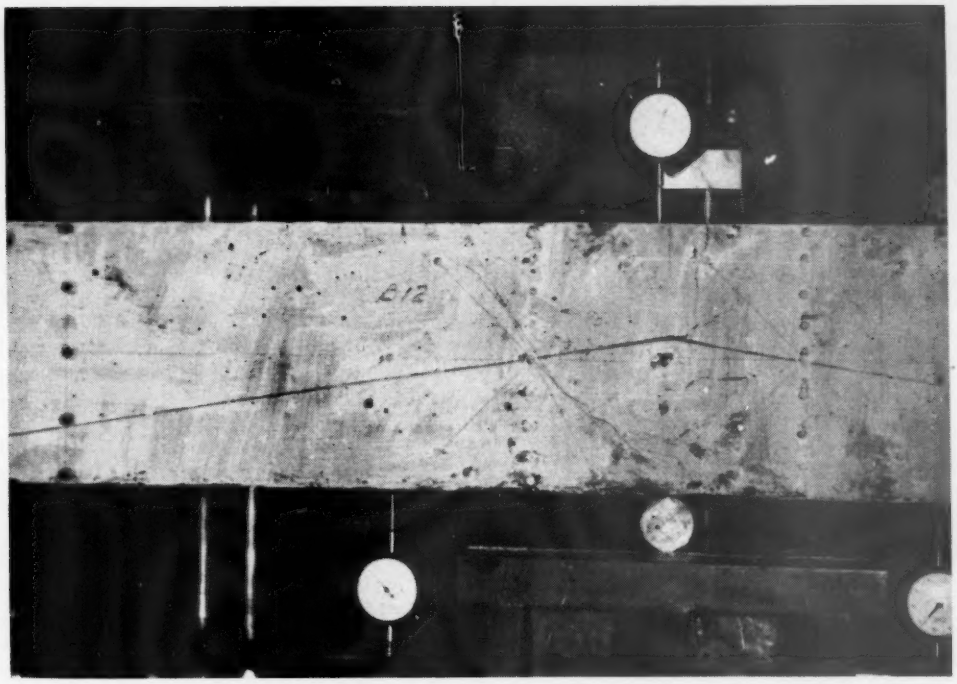

Figure 30—Formation of first shear crack in B-12

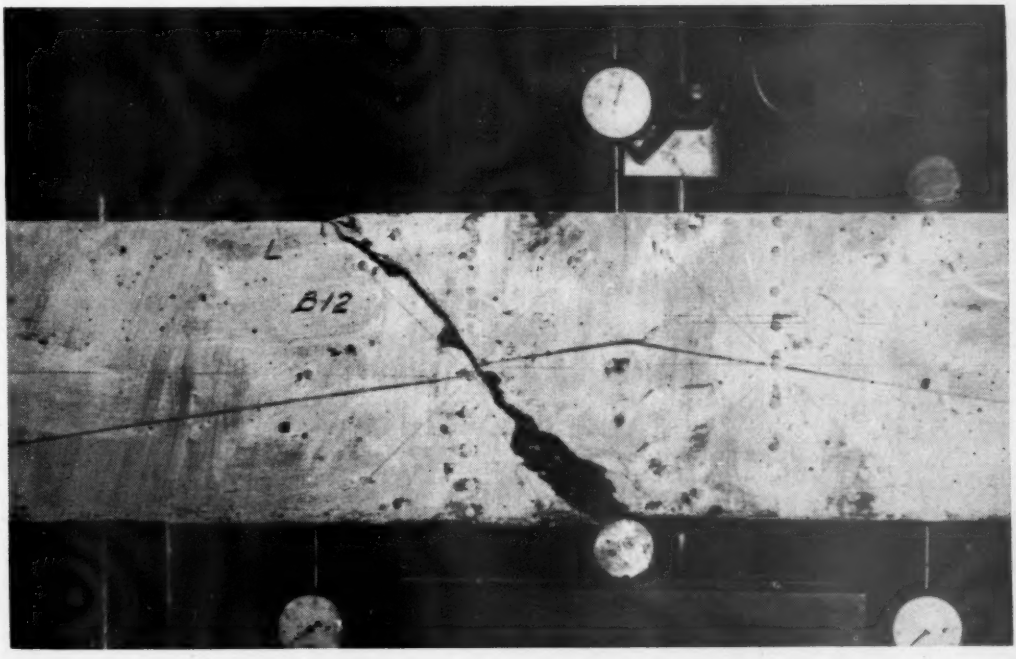

Figure 31—Shear failure in B-12

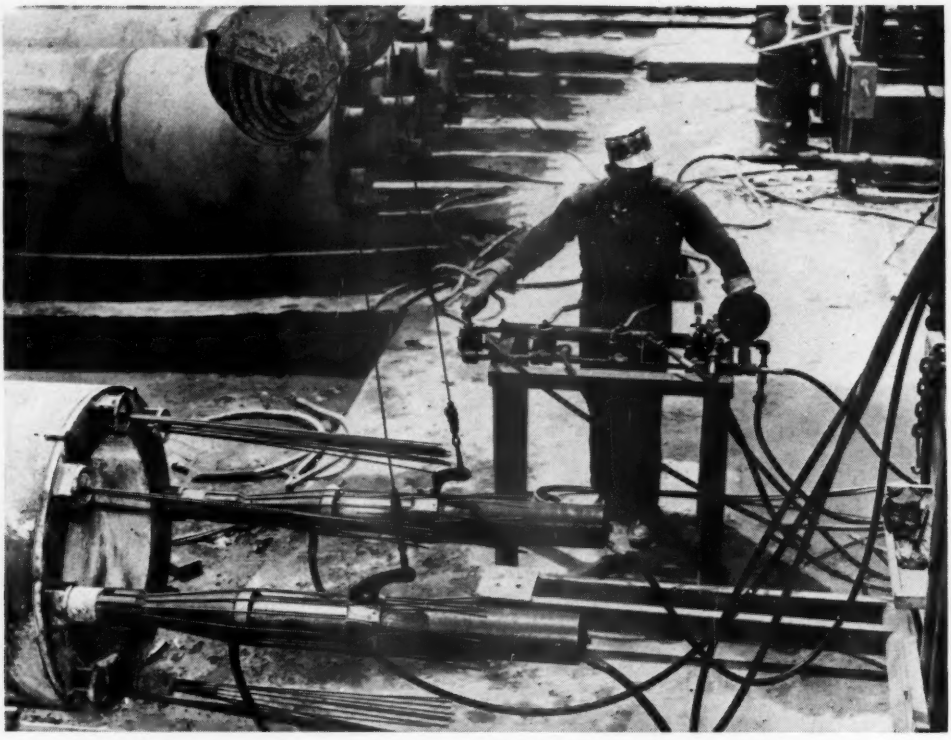

Figure 1—Simultaneous tensioning with two jacks, from a semi-permanent hydraulic control panel. Jacks are suspended from balancer units which are set to counteract jack weight.

Photo courtesy: Raymond Concrete Pile Co.

POST-TENSIONING OPERATIONS

E. M. SMITH, *Freyssinet Company Inc., New York, N. Y.*

Pretensioning and post-tensioning offer the prestressed concrete industry two major methods of production. The choice of techniques is further broadened by modifications such as pretensioned deflected strands and the combination of pretensioning and post-tensioning. Each has its advantages and its disadvantages which must be balanced by the designer and by the producer to achieve the most economical solution for a given project.

The rapid advance in the number of pretensioning facilities has been well dscribed in a variety of talks and articles. Perhaps less well known is the fact that the application of post-tensioning is also increasing, with many of the pretensioning plants making frequent use of post-tensioning methods, especially for the longer, heavier members. To evaluate the relative costs of post-tensioning and pretensioning, alternate designs must be made. The result will be wasteful of materials if post-tensioning tendons are merely substituted in a member designed for pretensioning with its heavy bottom flange and relatively low center of gravity. A post-tensioned design may permit use of a lighter member, less steel (which is also less expensive per pound) smaller form investment, more versatile production scheduling, etc.

In any repetitive operation, careful planning and scheduling can achieve economies and reduce labor requirements. This is universally recognized as applicable to any pretensioning operation. Perhaps it has even more significance in post-tensioning work because of the relatively discontinuous operations of placing tendons, stressing, burning off ends of tendons, grouting the ducts, and patching the anchorage block outs. Advance planning should serve to eliminate a variety of possible manpower wastages:

—Crews will be of the correct size, neither too small to perform their work quickly nor too large to do it efficiently;

—Materials and equipment will be available when and where required. Some plants have mounted all necessary items on carts so that the men do not have to search for hand tools, tie wire, anchorages, etc.;

—The workmen will be fully instructed in their assigned tasks and accept a degree of responsibility for proper performance. This not only helps eliminate expensive corrective measures, but also reduces the demands on the time of the foremen.

—The equipment used will be properly serviced and maintained and will have whatever accessories may be necessary for efficient operation.

In the following discussion of the highlights of the various aspects of post-tensioning, an attempt is made to touch on the considerations and techniques which tend to reduce labor costs and maintain good workmanship.

PREPARATION OF TENDONS

With the variety of post-tensioning systems, it is difficult to draw any general conclusions on tendon handling and preparation. However, for the wire systems, a user who anticipates any volume of post-tensioning work will probably find it best to purchase wire, ducts, anchorages, etc., separately, and prepare the tendons at his plant. This will result in savings in freight and re-handling. It will also permit him to stock the necessary items, to be prepared for tight scheduling and to be relatively independent of shipping delays.

All high tensile steel should be properly stored for protection against excessive oxidation. However, it should be remembered that normal rusting is not harmful.

Personnel in the plant should be cautioned against subjecting the high tensile steel to the heat of burning or welding equipment, even through arcing from a welder's ground system. Excessive heat from this equipment may ruin the steel, and cause it to break under the tensioning load.

FORMS

The forms for a girder should be properly designed, surfaced and braced to assure satisfactory finish and dimensional tolerances, and to strip easily.

The soffit form may require special consideration. It must be supported throughout its length to bear the relatively uniform load of the fresh concrete. Upon tensioning, the girder will both camber and shorten. In its cambered condition, all the weight of the member will be distributed to the bearings, and the soffit supports under these points must be adequate. If the bearing plates protrude through the bottom of the member, the soffit form must be designed to permit the motion of these plates due to the shortening of the member.

PLACING OF DUCTS AND TENDONS

It is necessary to position the tendon accurately in the forms, and to minimize accidental curvatures or "wobble" along the length of the tendon. Perhaps the technique most frequently used is to perform all the measuring and tying operations on the soffit form. However, serious consideration should be given to the advance positioning of spacers and supports, prior to bringing the tendon or duct to the mild steel cage. This is especially applicable if the mild steel cage is jigged. Good duct supports will eliminate the possibility of the tendon floating or being pushed out of position during concrete placing and vibration.

Flexible metal hose is frequently used to form the duct. Stretching this metal hose to the limit of its flexibility will usually result in a smoother trajectory. As it is placed, care should be taken that no punctures or flattened portions exist. If they do, the punctures can be sealed with tape and the flattened portions can usually be rounded out by light

tapping. Care should also be exercised that sand, dirt or other foreign material is not allowed to enter the hose and interfere with the subsequent grouting operation.

It is a good policy to move the tendons in their ducts several hours after the placing of concrete. If there were any mortar leaks into the duct, this movement will serve to break the mortar clots while the concrete is still green.

There is a growing trend to preforming ducts in the member by re-usable rubber or neoprene hose, which may or may not be pneumatic. This not only saves some of the cost of the flexible metal hose, but also reduces the difficulties of handling the long, relatively awkward tendons, with a consequent reduction in labor requirements. Some time after the concrete has been placed, the rubber hoses can be withdrawn, and the tendons inserted in the preformed holes.

Anchorage units should be properly and accurately positioned and securely held. All connections between anchorage and forms, between anchorage and metal hose, etc., should be mortar tight and reliable enough to withstand the vibration.

TENSIONING

The plans should clearly specify the force required in a tendon. Since the force in a tendon will vary with time (due to the gradual losses of creep, shrinkage and stress relaxation), and will vary along the length of the tendon due to friction, the plans should indicate the time and location of the force specified. From the producer's point of view, perhaps the easiest combination is to have specified the initial force at the center line (of a simple span member). Tensioning calculations may then be prepared, giving consideration to the frictions and the effect of the anchorage set.

One end stressing, of course, reduces the labor and equipment requirements. In many cases it is also preferable from structural considerations, since it may result in a better distribution of stress along the length of the tendon.

The jacks should have a stroke adequate to achieve the entire elongation in one pumping operation. Since this necessitates a relatively heavy unit, an efficient method of suspension is required, one which will permit easy movement of the jack in any direction: vertically; from side to side; toward or away from the member.

The equipment used for tensioning should be completely mobile. A wheel-mounted frame used to support the jack at the member can also carry the jack, the pump unit,

Figure 2—Skid mounted, gasoline powered, positive displacement grout pump.

Photo courtesy: Precrete, Inc., New York, N. Y.

the necessary hand tools, etc., from member to member, thereby reducing the number of trips to the storage area. The frame should be complete so no extra rigging is required at each member.

The frame, equipped with wheels or castors, should have a horizontal arm well above, and in line with the member. This horizontal arm should be capable of some degree of lateral motion, or swing. On it, a small trolley, may be mounted, from which is hung a hand joist or balancer unit for the support of the jack. The balancer, commerially available, is pre-set for the weight of the jack, and permits almost effortless raising or lowering of the jack. Thus, the combination of trolley and swinging arm permit horizontal motion, and the balancer permits vertical motion.

The pump unit should be power operated, and properly valved for the simultaneous operation of at least two jacks. A wide variety of adequate units are available, with a choice of power sources—air, gasoline or electricity. Calibrated gauges should be used. Close calibration of the jacks is not usually necessary because the tendon force is ordinarily more accurately measured by elongation of the tendon, with hydraulic pressure serving as a check. The average friction in a jack is accurate enough for this use.

The tensioning procedures should be in accordance with the manufacturer's recommendations and the Engineer's instructions. If there is any conflict between these, the conflict should be settled prior to the start of work. The crews should know exactly what they are to do, and should not be confused because of any unresolved differences of opinion.

Throughout the tensioning operations, adequate safety precautions should be taken since the forces involved are very high. Personnel should not stand or walk behind the jacks while stressing is in progress. Other crews should be kept from the area, or else adequate barricades should be erected. A suitable barricade may easily be incorporated in the jack frame.

After the stressing operation, the ducts are usually grouted to protect the tendons and to increase the strength of the member. To perform effectively, the grout must be of good quality, and must be as free from voids as possible. This requires a well-designed mix, high quality mixing and pumping equipment, good technique and conscientious performance.

Figure 3—Winter production of precast post-tensioned girders.

Photo courtesy: Precast Concrete Ltd. Calgary Canada.

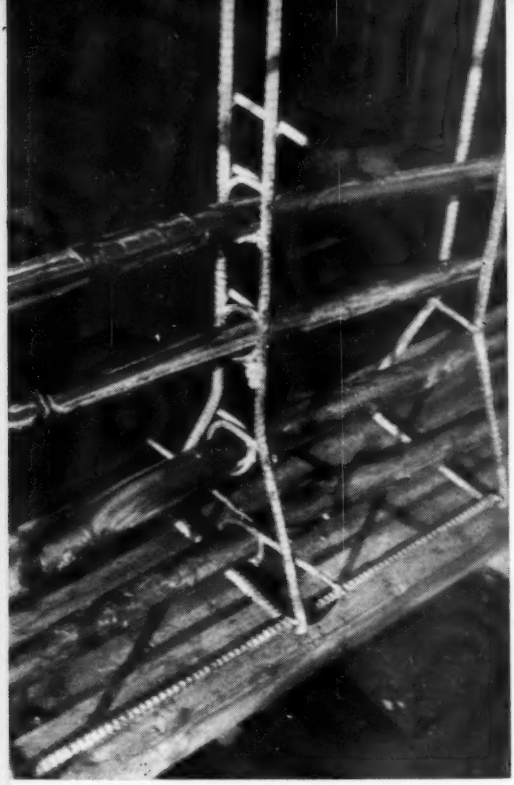

Figure 4—Pneumatic hose used to preform tendon ducts. Bent bars properly position hose, and minimize field work.

Photo courtesy: Precast Concrete Ltd. Calgary Canada.

The water cement ratio should be as low as possible, yet the mix must be sufficiently fluid for pumping. The addition of a suitable admixture and the use of a good mechanical grout mixer will help to get the maximum fluidity from a given w/c ratio. Fly ash and fine sand may also be added to the mix.

The mix should be such that the bleeding of free water is minimized. Mixes can be compared for bleeding by letting samples stand in sealed jars and measuring the percentage of free water that comes to the top. An efficient mixer and adequate mixing time will help reduce the amount of bleeding.

Screening the grout prior to putting it in the grout pump will eliminate lumps and help avoid possible clogging. If excessive amounts of grout are left on the screen, it may be an indication of inefficient or inadequate mixing.

The duct should have one access hole for injection, and another hole for air and water escape. For the longer ducts it may be advisable to have an extra escape hole. To permit pressure-tight grouting, other possible points of leakage—around the wires, under bearing plates, etc.,—should be sealed prior to the start of the grouting operation.

The duct should be flushed with water to remove foreign matter and then blown out with air, or drained, to remove the water.

Grout is introduced into the access point and continuously forced into the cable until all the air and water is forced through and an uninterrupted flow of clean undiluted grout emerges at the escape hole. The escape hole should then be sealed and a moderate pressure built up by the pump, at which point the access point is also sealed off.

As in all concreting operations, special precautions must be taken in cold weather. Grout used under these adverse conditions must be kept reasonably warm until it has had time to achieve adequate strength. This will require the heating of the member. If freezing temperatures are expected prior to the grouting operation, one must be sure that the ducts are free of water, to avoid the possibility of cracking the member due to freezing and expansion of the water.

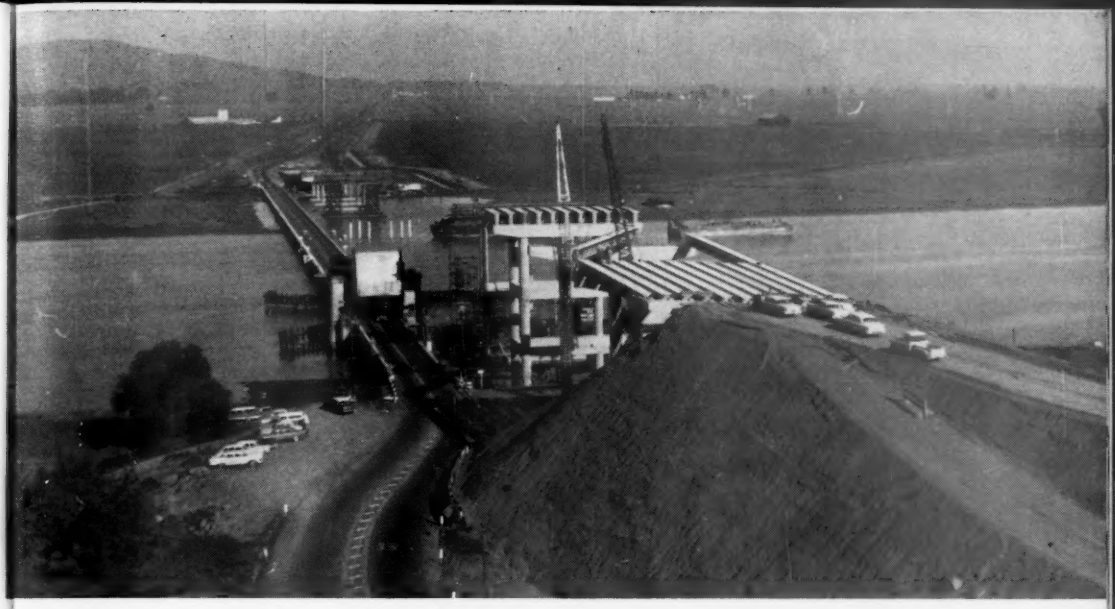

Figure 1—Petaluma Creek Bridge looking east.

Prestressed Concrete Units Of The Petaluma Creek Bridge At Black Point, California

By HERBERT BRAUNER, Ben C. Gerwick, Inc.

INTRODUCTION

A California State Highway overcrossing of Petaluma Creek at Black Point is being built by a joint venture of Ben C. Gerwick, Inc. and J. H. Pomeroy.

Prestressed components include 188 piles 26" square ranging in length from 40 ft. to 85 ft., and 264 pretensioned "T" girders 79'-2" in length. All members were pretensioned in the Gerwick Yard located at Petaluma, California.

PILE MANUFACTURE

The piles were manufactured on a 340 ft. bed. The 26" square piles were pretensioned with 34' ⅜" HTSR strands arranged in a square pattern. The piles contained a 12" dia. hollow core except for a 5'-0" solid head and 9'-0" tip. A 14" 184 lb. WF was cast in the tip, 6' within the pile, and a minimum of 2' protruding. This composite section was welded at the jobsite to previously driven steel piles up to 120' in length.

PRETENSIONING PROCEDURE

Thirty-four reels of strand set up at the far end of the pretensioning bed made it possible to pull all strands in one operation. Each strand was threaded into a small pulling template and held by a strand vise. At the jacking end of the bed a ⅜" wire

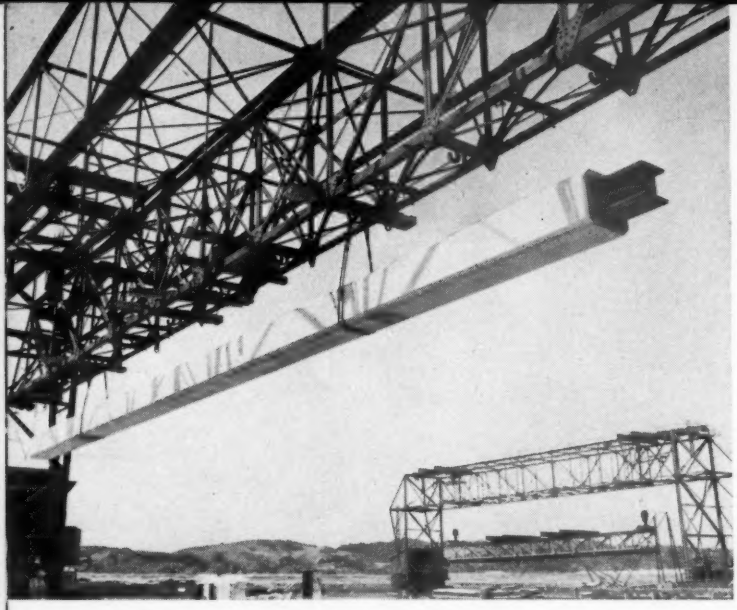

Figure 2 — Pretensioned 26" square pile with 14" WF 184 Lb. H-stub. Pile has 12" hollow core.

rope was pulled from the drum of an air tugger. Attached to the pulling template, this tugger line provided the means of pulling all 34 strands the length of the bed.

When the jacking end of the bed was reached it remained to thread all strands into the main pulling head, and at the fixed end to burn all strands and similarly install in the fixed head.

The main pulling head was attached to the jacking head by threaded rods passing through abutment piles. Nuts on these threaded rods bearing on the abutments retained the tension in the strands after jacking.

Individual strands were given an initial load of 1000 lbs. using a dynamometer to measure the force. At this point, the steel pile stubs were positioned in the tips, the hollow core tubes placed and the spiral reinforcement spread along the length of the pile.

The 34 wire group was next stressed to 14 kips/strand utilizing two Rogers Hydraulic Rams, each of 200 ton capacity and 4 ft. ram travel. Elongation of the strands was measured from the initial 1000 lbs./strand to the final 14,000 lbs./strand. The wire group was actually pulled to this calculated elongation and the gage pressure

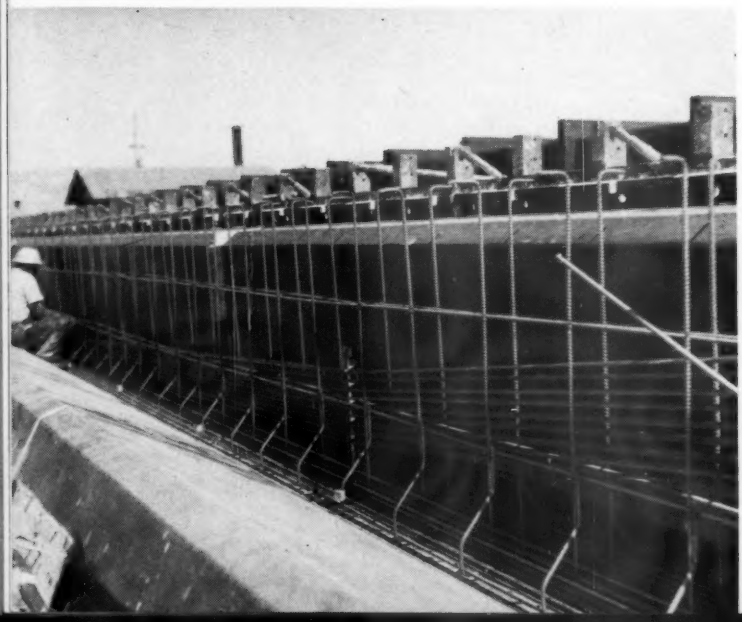

Figure 3—Deflected strands for Petaluma Creek girders. Girders are 80'-0" long and have three strand deflection points.

Figure 4—Closeup of composite prestressed concrete/steel H-pile for Petaluma Creek bridge.

read as a check. Variance in this respect never exceeded 3%.

Finally, spirals were accurately positioned, core tubes secured and all remaining form work completed prior to placement of concrete.

After steam curing to required strength —in this case 4500 psi—forms were broken down and transfer of stress accomplished by releasing all strands simultaneously on the hydraulic rams.

GIRDER MANUFACTURE

The manufacture of the "T" girders is being carried out on four short beds set up especially for this job. The four beds, side by side, are situated between and perpendicular to the rails of an existing 75-ton capacity traveling gantry. In addition to the four casting beds, the total area between rails includes sufficient work space for prefabricating mild steel cages, storage for re-steel and strand, as well as storage room for approximately 90 completed girders. The gantry is utilized in most every phase of the operation, including placing cages within forms, moving jacks, lifting forms, pouring concrete, placing and removing steam hoods, removing girders to storage and loading out—whether by truck or barge.

Each bed has a complete hinged type form set up. As a result of this single unit parallel bed set up, several phases of manufacture will be evident at any given time and each bed will be independent of work on adjacent beds.

The 264 "T" girders are 79'2" long and conform to a state standard for this type member.

36 7/16 strands are used in pretensioning these girders, 18 of which are straight and 18 deflected. The operation begins when 18 strands are pulled simultaneously from as many reels on to a bench parallel with the beds. The bottom group of 18 is threaded through two templates at this time to keep the strands in proper relationship when placed in the pulling heads. —The strands are cut on the bench and the group then placed in a prefabricated steel cage which includes all mild reinforcing except end block and deck steel.

The top group of 18, when pulled on the bench, is also threaded through templates. After entering this second group of 18 strands in the mild steel cage, the entire cage is picked up by the gantry and placed on a soffit within the hinged steel form.

One side of this form had previously been raised, aligned and secured. The strands are threaded into the fixed and jacking end heads and strand vises affixed. Each of the 36 strands is individually tensioned to 1000 lb. using a dynamometer to insure uniformity. The 18 straight

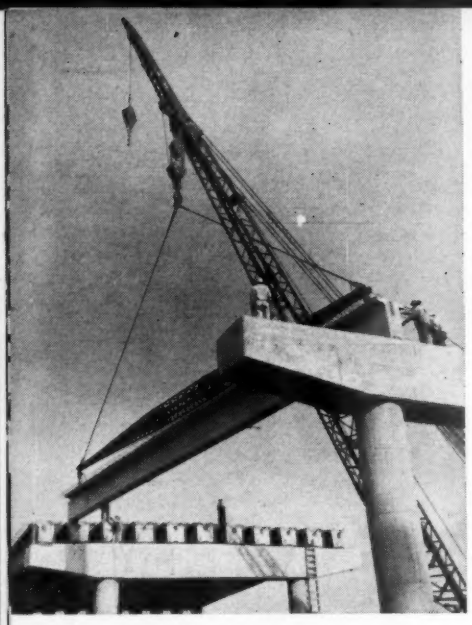

Figure 5—Erecting 80'-0" girders at Petaluma Creek bridge.

strands are tensioned to 18.9 kips/strand using two 150 ton hydraulic rams. Gage pressure is checked against elongation.

The top strands are tensioned to 9.7k/strand using two 150 ton rams, elongation vs. gage pressure checked as before. The quarter and center point strand deflectors are then positioned and all three deflectors attached to pull down cables which enter through holes in the soffit. Metal strands are placed at girder ends to support pins over which the strands bend when deflected.

The deflecting mechanism is simply a fixed horizontal screw on which travels a threaded rectangular steel block guided by tracks. Attached to this block is the pull down cable which makes a 90 degree change in direction from horizontal to vertical around heavy sheaves under the soffit. The screw and driving gear, threaded block, guides and sheaves are all contained in a heavy metal frame which is held down to the casting bed with bolts and inserts in the bed. An especially adapted air boring gun is used to drive the screw.

The quarter points are deflected first, each to within three inches of their final position. The mid point is next deflected to three inches from final position. The sequence is repeated taking each point to final position. Two operations are used so as to minimize the loads on the deflecting mechanisms and hold down inserts.

After deflecting the strands, the hydraulic rams are extended so as to take the full load of the group, and the gage pressure is read as a check on total load. This total load must indicate 18^9 kips per strand.

End block reinforcement is added, following which the open hinged side form is raised and secured. Placement of deck steel, diaphragm steel and end bulkheads readies the girder for concrete placement. Low slump concrete (under 2") is consolidated within the forms utilizing internal and external vibration.

After the pour, a one piece steam box of insulated redwood is placed over the girder form. Approximately three hours after completion of the pour, steam is introduced into the hood and allowed to reach a temperature of 150 degrees F. When specified strengths are obtained the hoods are then removed.

After removal of the steam hood and stripping the forms, tension in all 36 strands is simultaneously released on the stressing rams—the strands are burned flush with the concrete, deflecting devices released, and the girder removed to storage. The forms are cleaned and oiled, one side raised and aligned, and the bed is ready to repeat the entire cycle.

Field Studies of Prestress Loss Due to Shrinkage and Creep *

By RALPH W. KLUGE
Head Professor of Civil Engineering
University of Florida, Gainesville, Florida

Stress losses in the tensioning elements of prestressed concrete result from causes such as anchorage losses, friction losses, creep of the tensioned steel, elastic deformation for pretensioned members, and losses resulting from the combined effect of shrinkage and creep of the concrete. The stress loss caused by the latter is perhaps the greatest single loss that occurs. The effects of shrinkage and creep are concomitant and not always readily separated. However, as far as the designer is concerned the total effect is the important one.

Considerable data have been accumulated over the past 25 to 30 years on creep of plain and reinforced concrete, but practically all of it has been concerned with ordinary concrete strengths of 2500 psi to 4000 psi. For strengths above this, there are relatively little data. Such information which has been obtained for higher strength concretes has been, quite naturally, associated with prestressed flexural members, but almost all such data have been based on laboratory observations. Since the element of shrinkage is such an important factor in the total shortening of a long concrete member, the surrounding atmospheric conditions would be expected to affect materially the stress losses from this source. That is, it is to be expected that such losses would be somewhat greater under laboratory conditions where the air is drier than it is in the field, particularly where exposure is over water areas. The codes have recognized this and have recommended shrinkage coefficients based on the best knowledge available.

The rate of creep also seems to depend upon the moisture content of the air surrounding the concrete, but probably not to as great an extent as in shrinkage. It depends upon several other factors as well. For example, the rate of creep is approximately proportional to stress; it is affected by strength of the concrete and the greater the age of the concrete at application of load, the less extensive the creep. Practically all of this basic creep information has been obtained from test specimens subjected to uniform stresses over the concrete. Such is not the case with prestressed flexural members. Consequently there is much to be learned about its effect on prestressed concrete.

The Tentative Recommendations for Prestressed Concrete as reported by the Joint ACI - ASCE Committee indicates that values between 0.0002 and 0.0003 in. per in. are commonly used for the calculation of prestress loss caused by shrinkage and that 100 per cent to 300 per cent of the elastic strain should be assumed for creep, the particular values depending upon atmospheric conditions. Where atmospheric conditions are very dry, the latter value is recommended.

To the knowledge of the author there have been only two other attempts in this country to determine the stress loss resulting from these factors under field conditions, although some data on total shortening in bridge structures have been reported in the German technical literature.

Ulrich Finsterwalder, in an article published in "Beton und Stahlbetonbau,"* re-

*Paper presented to the Second National Prestressed Concrete Short Course, Daytona Beach, January, 1958.

*Vol. 50, No. 1, January, 1955, pp. 44-50.

ported the total shortening resulting from shrinkage and creep of nine different types of prestressed bridges, about half of which were single-span and the remaining, triple-span structures.

It was not clear from this report whether these bridges were pre-tensioned or post-tensioned, but the latter method of prestressing was probably employed. No attempt was made to separate shrinkage or creep from the total shortening. Comparisons were made between the measured maximum shortening and calculated values based on a creep factor of 150 per cent of the elastic shortening and a shrinkage coefficient of 0.00011 — a value somewhat less than is commonly used for design in this country. Table I shows these comparisons.

Based upon these creep and shrinkage factors and assuming an initial tensioning stress in the reinforcement of 100,000 psi, the loss of stress in these bridge girders would be no greater than 10 per cent, if no creep occurred in the steel.

With this background information, some of the meager data obtained in this country for post-tensioned bridge girders under similar conditions might be examined. One investigation of very limited scope was made on two girders during the construction of the Sunshine Skyway Bridge, crossing lower Tampa Bay.

The measurements were rather crude and undoubtedly were recognized as such, but were made in order to obtain some scale on the extent of stress loss that might be anticipated in girders placed in the bridge. These observations were made in the casting yards and extended over a period of about nine months. The technique for determining the loss of stress in the tensioning bars was to apply a jack to one end of each of the bars at stated intervals and to determine the jacking force necessary to barely loosen the washer between the anchorage nut on the bars and the end bearing plates. These observations revealed that the average loss of stress at the end of the nine-month period was of the order of 12 per cent of the initial stress. Although it was reported that most of this loss occurred in the first 60 days, subsequent observation on similar girders

BRIDGE	ACTUAL TOTAL SHORTENING mm	CALC. TOTAL SHORTENING mm	RATIO ACTUAL / CALC.	COMMENTS
1	31	23.8	1.30	3-SPAN CURVED SOFFIT SOLID RECTANGULAR SECTION GIRDER.
2	40	37.7	1.06	SINGLE SPAN - CURVED SOFFIT SOLID RECTANGULAR SECTION GIRDER.
3	30	30.1	1.00	SIMILAR TO BRIDGE NO. 2.
4	20	19.1	1.05	3-SPAN UNIFORM DEPTH SOLID RECTANGULAR SECTION GIRDER - 2 LAND SPANS.
5	13	15.9	0.82	3-SPAN CURVED SOFFIT BOX GIRDER.
6	25	14.0	1.78	SINGLE SPAN UNIFORM DEPTH SOLID RECTANGULAR SECTION GIRDER.
7	40	31.3	1.28	3-SPAN - WITH TWO VERY SHORT LAND SPANS - CURVED SOFFIT RECTANGULAR SOLID SECTION.
8	30	29.8	1.01	3-SPAN UNIFORM DEPTH SOLID RECTANGULAR SECTION GIRDER. SHORTENING MEASURED IN TWO LAND SPANS ONLY.
9	55	65.7	0.84	3-SPAN - CURVED SOFFIT BOX GIRDER - LAND SPANS.

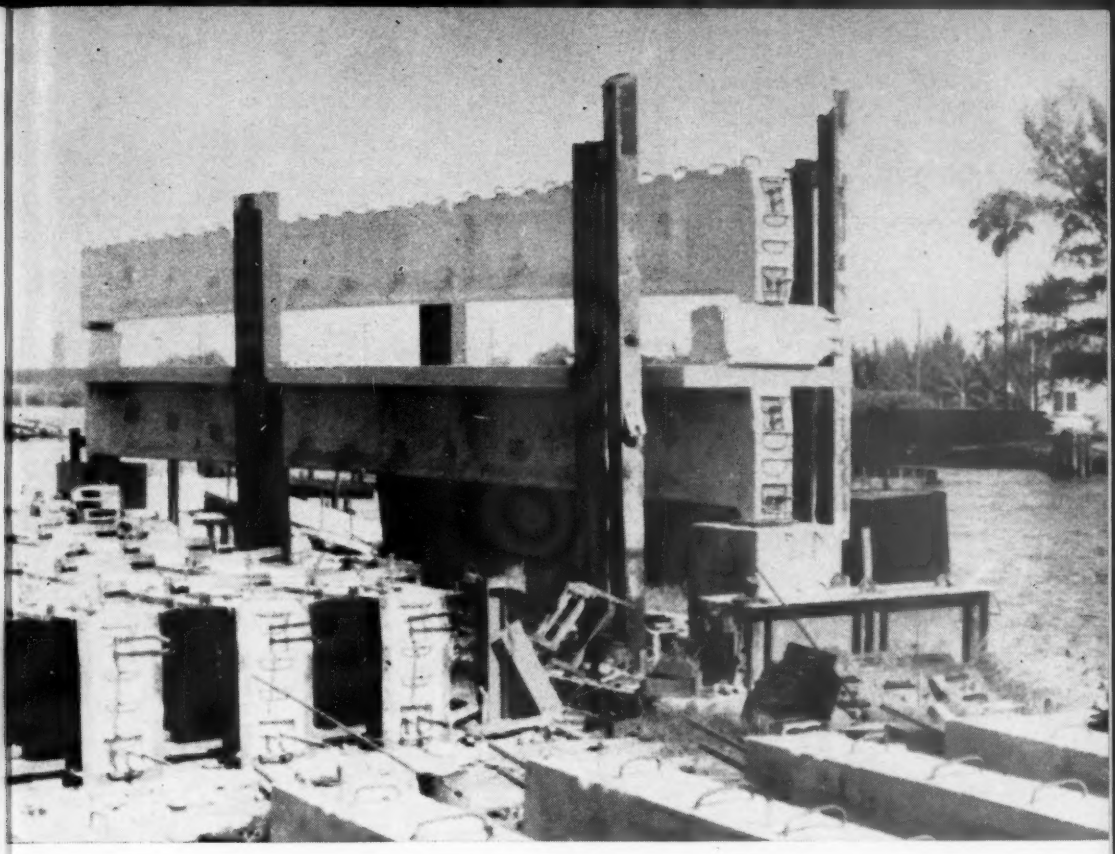

Figure 1

indicates that a somewhat greater loss might be expected at the end of another year.

In the summer of 1953 another investigation was initiated to determine stress loss in six girders of the same lower bay bridge. After a period of about four months the readings indicated an unaccountable erratic behavior of the structure. Subsequently it was discovered that the abutment supporting one end of the girders was tipping and causing the erroneous readings. After this unsuccessful attempt, a similar study was planned in connection with the construction of the Gandy Bridge crossing Tampa Bay between St. Petersburg and Tampa. Eight girders were selected for this study, all cast at the same time. Four were subsequently placed in the bridge, two remained in the casting yard and two were shipped to the Materials Laboratory of the University of Florida (Fig. 1). These eight identical girders were observed during the same period under laboratory, field, and service conditions. In an attempt to separate the effects of shrinkage and creep, two 4-ft. shrinkage specimens shown in Fig. 2, containing approximately the same quantity of reinforcement per foot as the prototype girders, were cast in the girder forms. One of these remained with the girder specimens in the casting yard and the other was sent to Gainesville to be stored with the laboratory girders. The ends of these unstressed specimens were sealed with a mastic and aluminum foil so that the sides were primarily exposed to drying.

Strain loss, in the girder specimens, was measured directly on the two horizontal tensioning bars and on the lower concrete flanges of the girders at the level of the rods on 10-in gage lines located at approximately the quarter points of the span. A Whittemore Strain Gage was used for this purpose. The same gage was used to observe shrinkage on 16 gage lines spaced from top to bottom on both sides of the shrinkage specimens. In order to minimize

Figure 2

differential temperature effects between the embedded steel and exposed concrete as well as such effects on the bridge structure itself, all field observations were made in the morning hours just before sunrise. Temperature readings taken in the concrete adjacent to the bars were generally found to vary not more than one degree from air temperature at this period of the day.

In order to provide access to the bars for strain readings, stainless steel box shields through which the bar and its flexible tube passed were cast into the girder. Immediately after the girders were post-tensioned and the grout surrounding the bar had its initial set, the girders were lifted from the casting beds and supported at their ends so that the portion of the flexible tube within the box could be cut away and the bar exposed. Special bar clamps were then fastened to the exposed portion of the bar and the strain gage applied to the ends of these bar clamps. Figure 3 shows the box and a bar clamp and Figure 4 indicates how the strain gage was applied to the bar clamps after their installation. Figure 5 is a section of the girder at approximately the same location as the strain gage lines.

The specimen girders were post-tensioned seven days after they were cast, at which time concrete control cylinders indicated a strength of approximately 4000 psi. Initial strain readings were taken on the concrete flanges immediately before and after tensioning of the bars, thus providing a measure of the elastic deformation in the concrete caused by this prestressing force. Initial strain readings were obtained on the bars within 24 hours after stressing. Thus the strain history for each girder reached to within a day of prestressing and within eight days of casting.

Figure 6 shows the rate of strain loss in the bars over a period of two years and also indicates that most loss, if not all, has taken place during this period. The values shown represent the total loss, namely, that caused by both shrinkage and creep in the concrete and creep in the bars, if such creep occurred. The data for the girders in the bridge and one in the casting yard supporting the slab, have been corrected for the strain caused by the weight of the slab. This was accomplished by noting the difference in strain readings taken immediately before and after the slabs were cast in both the bridge and on the single girder in the casting yard. A decided difference in stress loss was evident between the girders in the bridge and those in the laboratory. The bars in the bridge experienced a maximum loss of approximately 10,000 psi and those in the laboratory about twice this value or approximately 20,000 psi, and, since the bars were initially stressed to 100,000 psi, this represents 10 per cent and 20 per cent losses respectively. The surprising feature of this study was that the girders in the casting yard consistently lost more stress than those in the bridge, although the climatic conditions were quite similar. It is of course possible that their losses may approach each other over a longer period of time, and it is also possible that stress losses in the bridge girders could be influenced by deformation stresses in the bridge structure itself. After two years the girders in the casting yard had lost about 12 per cent of their initial stress.

If it is assumed that shrinkage of a 4-ft. length of the girder, as an independent

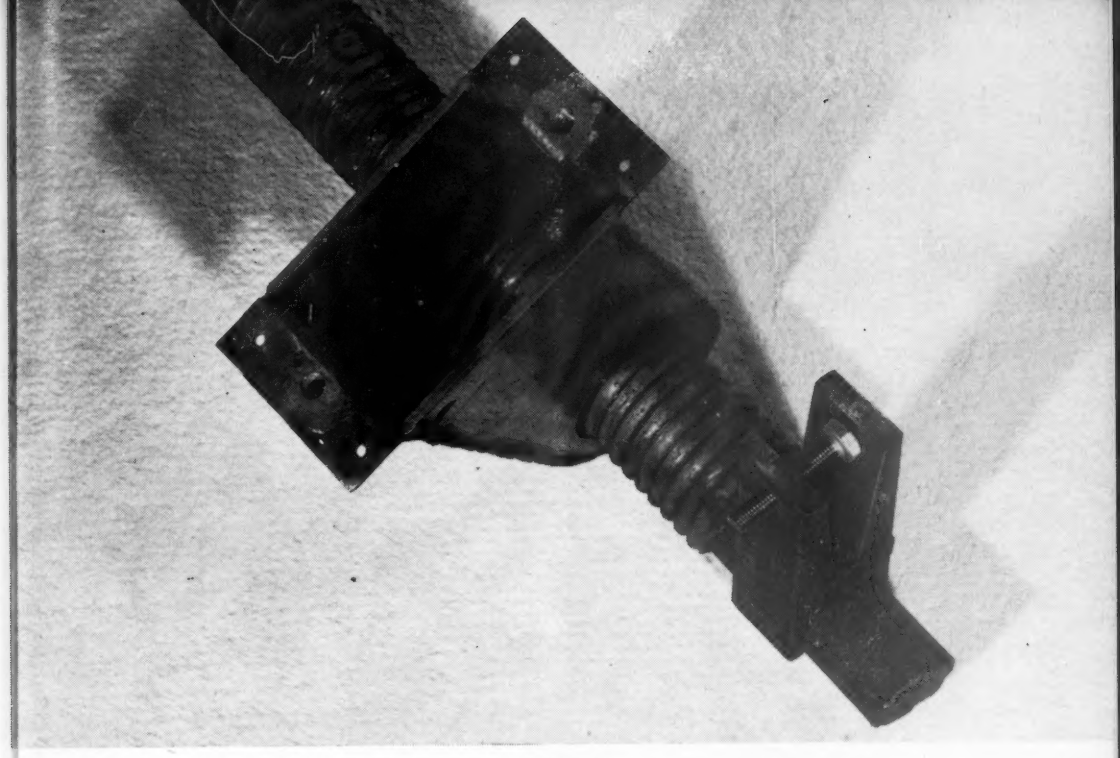

Figure 3

Figure 4

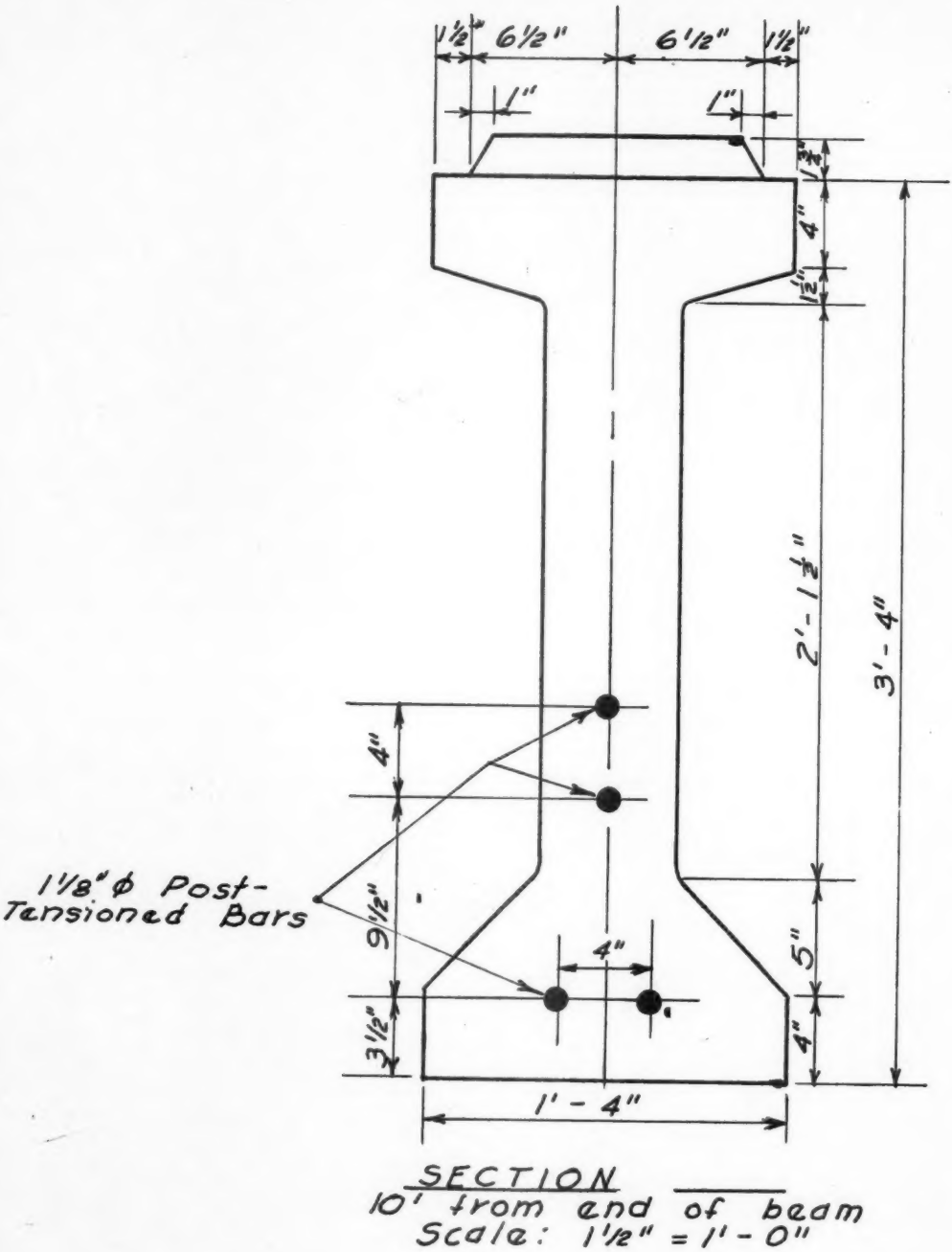
1½"
6½"
6½"
1½"
1"
1"
4"
2'-1¾"
3'-4"
4"
1⅛" ϕ Post-
Tensioned Bars
9½"
4"
5"
3½"
4"
1'-4"
SECTION
10' from end of beam
Scale: 1½" = 1'-0"

Figure 5

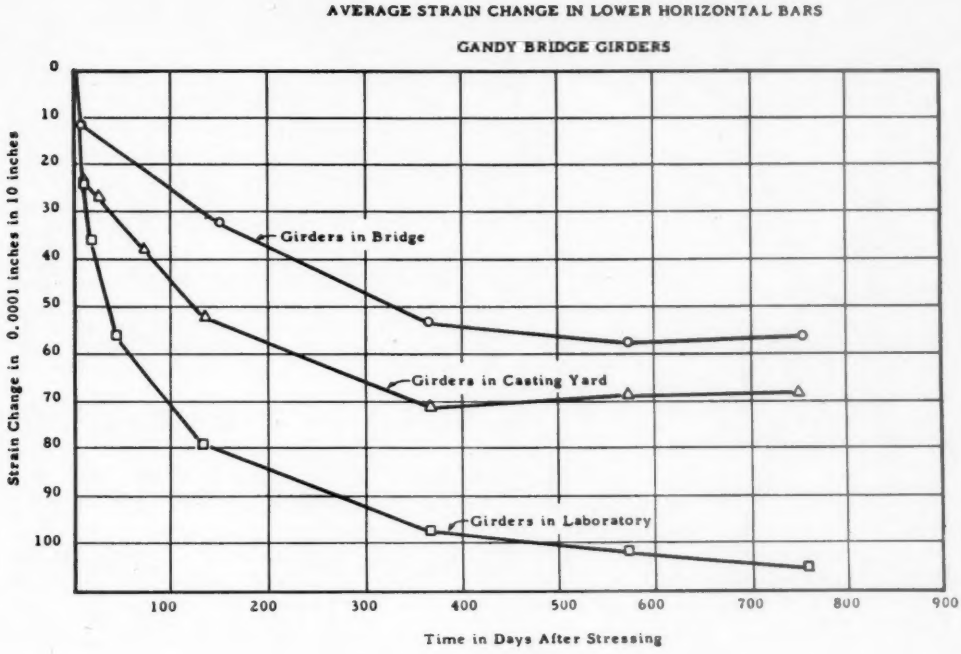

Figure 6

unloaded shrinkage specimen, is a measure of the shrinkage actually occurring in the girders, then about 25 per cent of the total stress loss in the field girders resulted from shrinkage and about 50 per cent of the total loss in the laboratory girders was caused by shrinkage. Deducting the shrinkage deformation from the total shortening leaves the creep deformation, if it is assumed that no creep occurred in the steel.

The magnitude of creep thus determined was approximately the same for the laboratory and field girders, the difference in the surrounding atmosphere notwithstanding. The comparison here is limited only to those girders in the laboratory and in the casting yard, since the magnitude of the shrinkage occurring in the bridge girders is not known with any degree of certainty. Although it appears that less shrinkage occurred in the bridge girders, this is not conclusive, at least at this stage of the study.

Based on this data, the creep coefficient or ratio for these girders is very close to 1.0 as compared with a value of 1.5 for the German bridges and a recommended value of 1.0 to 3.0 in the ACI - ASCE Committee report. A shrinkage value of 0.0002 was indicated for the field shrinkage specimen and a rather high value of 0.0005 for the laboratory specimen. This compares with 0.0001 from the German report and 0.0002 to 0.0003 recommended by ACI - ASCE.

The data reported here are obviously not conclusive evidence of the correctness of the factors presently being used. They indicated, however, that recommended code values are probably not far in error either way. They also add to our limited knowledge of shrinkage and creep under service conditions.

Acknowledgment. The author wishes to acknowledge the services of various members of the Civil Engineering Department of the University of Florida for their generous assistance in the preparation of the girders for strain readings throughout the period of observation. The study is one of the research projects in prestressed concrete financed by the Florida State Road Department and was made possible through the excellent cooperation of W. E. Dean, Assistant Highway Engineer.

TEST OF A prestressed CONCRETE HYPERBOLIC PARABOLOID SHELL

T. Y. Lin
Professor of Civil Engineering,
University of California, Berkeley

R. Itaya
Assistant Engineer,
University of California, Berkeley

I. Synopsis:

A prestressed concrete hyperbolic paraboloid shell 15 ft. square by 1 in. thick was tested to failure. Strain and deflection measurements, the cracking load, crack pattern and the ultimate load were recorded. Experimental results were compared with those obtained by both the classical membrane theory and an approximate ultimate theory.

II. Purpose

The purpose of this investigation was to determine the behavior and strength of a prestressed concrete hyperbolic paraboloid shell, as shown in Figure 1.

One advantage of a hyperbolic paraboloid shell is its efficiency in carrying uniformly distributed loads. Formwork for this type of shell can be constructed without excessive work because the form of the shell is generated by two systems of straight lines.

The edge beams were prestressed to increase the elastic and ultimate strength of the shell as well as to control deflections and limit cracks.

III. Description of the Shell

The shell was composed of four identical hyperboloid surfaces, each of which was 7.5 by 7.5 ft. square in horizontal projection with a vertical drop of 2.5 ft. at one corner. A center column 10 in. square supported the shell. Thus the shell resembled an inverted umbrella or a funnel. Fig. 2.

Reinforcement for the shell consisted of wire mesh (2 by 2 in. No. 14 gage) with some No. 2 bars in the valleys. Each of the 3 by 3.5 in. edge beams was post-tensioned with a cable made of two ¼ in. high strength steel wires.

Normal thickness of the shell was 1 in. The corners, the center and the valleys were slightly thickened to resist stress concentrations in these areas.

IV. Materials

Concrete for the shell consisted of Santa Cruz Type I cement, Fair Oaks sand, and ¼ in. roofing gravel in the proportion of 1:3.4:2.0 by weight, with a water cement ratio of 0.67 by weight. The average 28-days compressive strength of 3 by 6 in. cylinders was 4240 psi. The modulus of rupture averaged 438 psi as obtained from 6 by 6 by 20 in. beams loaded at third points on an 18-in. span. The secant modulus of elasticity at 1000 psi was 3,400,000 psi.

Each of the prestressing cables consisted of two ¼ in. diameter cold drawn wires wrapped with Gilsonite coated Sisal-kraft paper. The ultimate strength of the wires was 250,000 psi; the proportional limit, 160,000 psi; and the yield point at 0.2% offset, 230,000 psi. The modulus of elasticity was 27,000,000 psi.

The 2 by 2 in. No. 14 gage wire mesh had a yield strength of 48,000 psi and an ultimate strength of 64,000 psi. The steel area provided was 0.03 square inches per linear foot.

The No. 2 intermediate grade smooth bars had a yield strength of 48,000 psi and an ultimate strength of 75,000 psi.

Figure 1—Hyperbolic paraboloid shell 15 ft. x 15 ft.

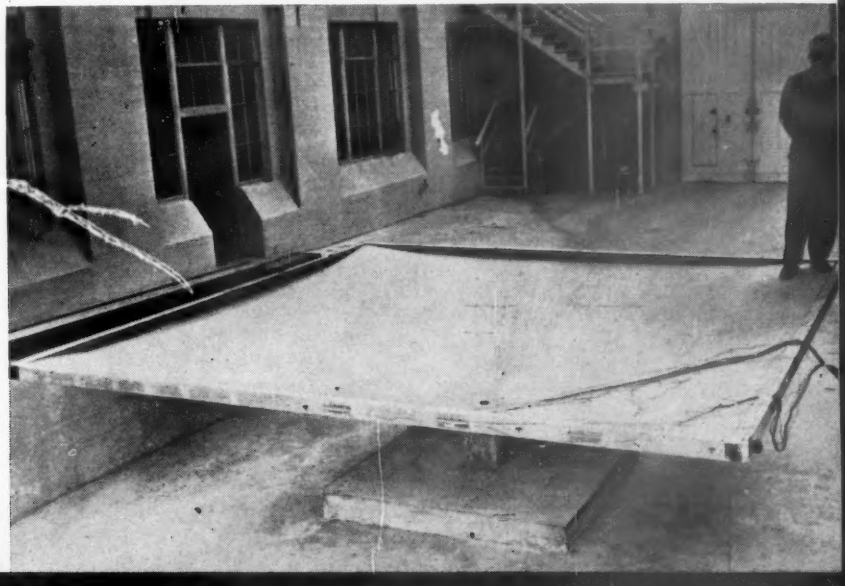

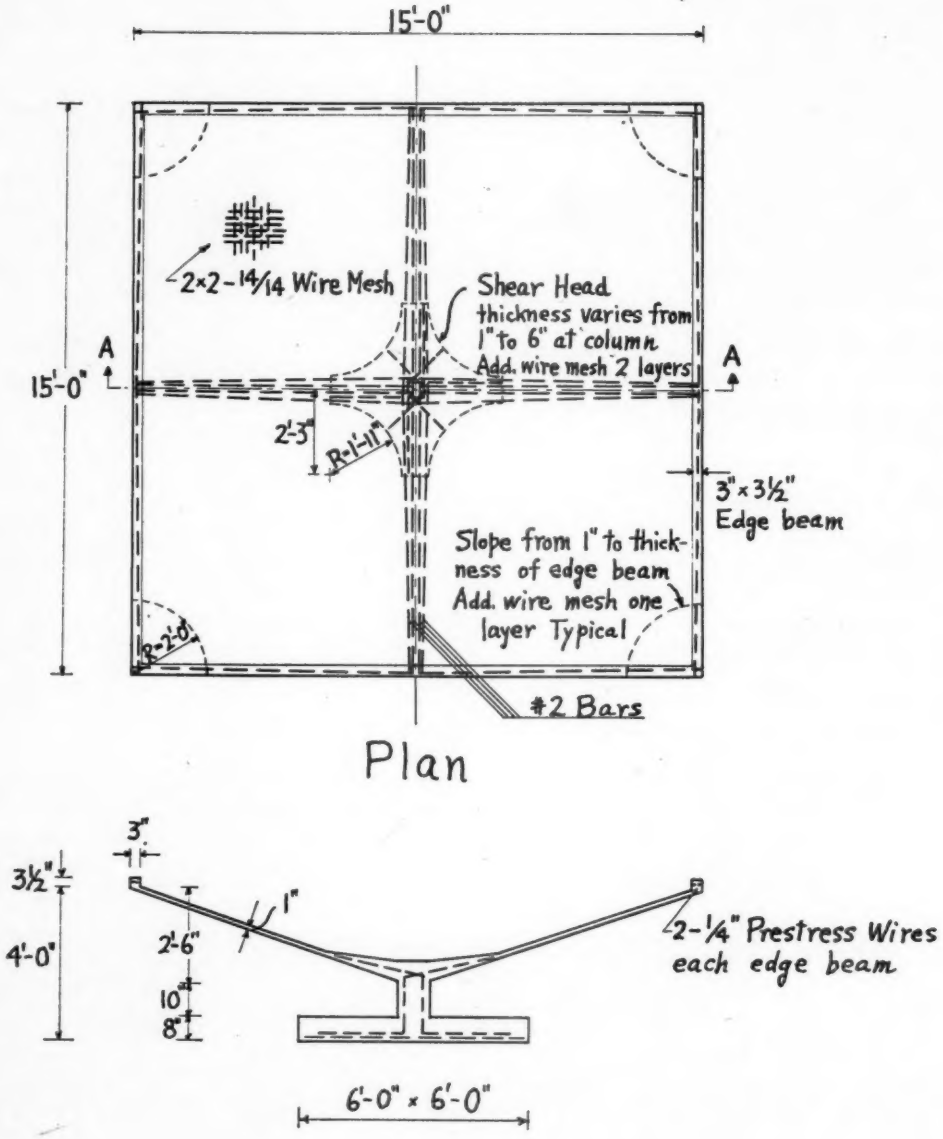

Figure 2—Details of a hyperbolic paraboloid shell

V. Construction

Forms were made with 1 in. lumber on 2 x 4 in. timber framing. As mentioned previously, only straight lumber was used for the forms.

The prestressing cables were supplied by Western Concrete Structures, Inc. The end anchorages consisted of 3 by 3 by ½ in. bearing plates and a standard 7-wire stressing washer. Steel shims of predetermined height were used to maintain the prestress.

Concrete was placed in two half-inch lifts to obtain the necessary smoothness and to minimize air voids. Artificial fog spray was applied to the shell for 12 hours; then it was cured with wet burlap for 7 days. An excellent surface was obtained with no shrinkage cracks.

VI. Test Procedure:

Uniform load was applied over the whole shell with moist sand. The sand was made to conform to the surface of the shell by screeding. The test consisted of four stages:

1. At 21 days an initial prestress of 5 kips per cable was applied so that forms could be removed.
2. At 27 days prestress was increased to 13 kips per cable in two increments.
3. At 28 days uniform load was applied with sand, in increments of 10 kips. A total of 40 kips was placed and remained on the shell.
4. At 142 days additional load was applied in increments of 10 kips until total failure took place.

VII. Instrumentation

The instrumentation was designed to obtain a distribution of strains and deflections in the shell so that results could be compared with theoretical studies. The strains in the shell were measured with SR-4 Type AR-1 strain rosettes. The strains in the valleys and the edge beams were measured with SR-4 Type A-9 strain gages. The deflections were measured with dial gages until the final stage of loading when scales attached to the shell were used. Gage locations are shown in Figure 3.

VIII. Test Results

Strain readings were taken during the first three stages.

Strain readings in the shell proper were in the order of magnitude of 100 millionths. Considering the effects of temperature and moisture on such a thin member, the probable error in reading the strain gages was likely 20 to 50 millionths. Hence the strain readings in the shell were considered inaccurate.

Deflection measurements were more reliable. The load-deflection curves for points along the edge beam are shown in Figures 4, 5, and 6. As expected, the deflection due to prestress was upward while the deflection due to load was downward. Note that the load-deflection curve was linear until cracking took place.

The crack pattern is shown in Figure 7. The first cracks became visible at a live load of about 170 psf. At a load of 180 psf, the major cracks were about 0.04 in. wide. Just prior to failure at 247 psf. some cracks were close to 1 in. wide. It might be noted that the cracks did not materially change during the 114 days, with sustained load of 180 psf.

The ultimate live load at failure was 55,660 lbs. or 247 psf. The pattern of failure indicates that final failure of the shell occurred by punching shear around the column after considerable cracking had taken place. The final zone of failure was around the outside edge of the thickened shear collar.

IX. Analysis

A. Membrane Theory

The behaviour of the shell before cracking is usually described by the membrane theory. Using Cartesian coordinates with axes parallel to the generatrices of the shell, Figure 8, the equation of the surface is

$$z = \left(\frac{h}{ab}\right)xy$$

Assuming edges $x = a$ and $y = b$ are prevented from moving horizontally, but not vertically, the deflection of the corner $x = 0$, $y = 0$ with respect to corner $x = a$, $y = b$ is given by*

$$\Delta = \frac{2w}{Gt}\left(\frac{ab}{2h}\right)^2$$

where G is the shear modulus and t, the thickness of the shell.

Both the theoretical corner deflections

*Reissner, E., "On Some Aspects of the Theory of Thin Elastic Shells," Journal of the Boston Society of Civil Engineers, April, 1955.

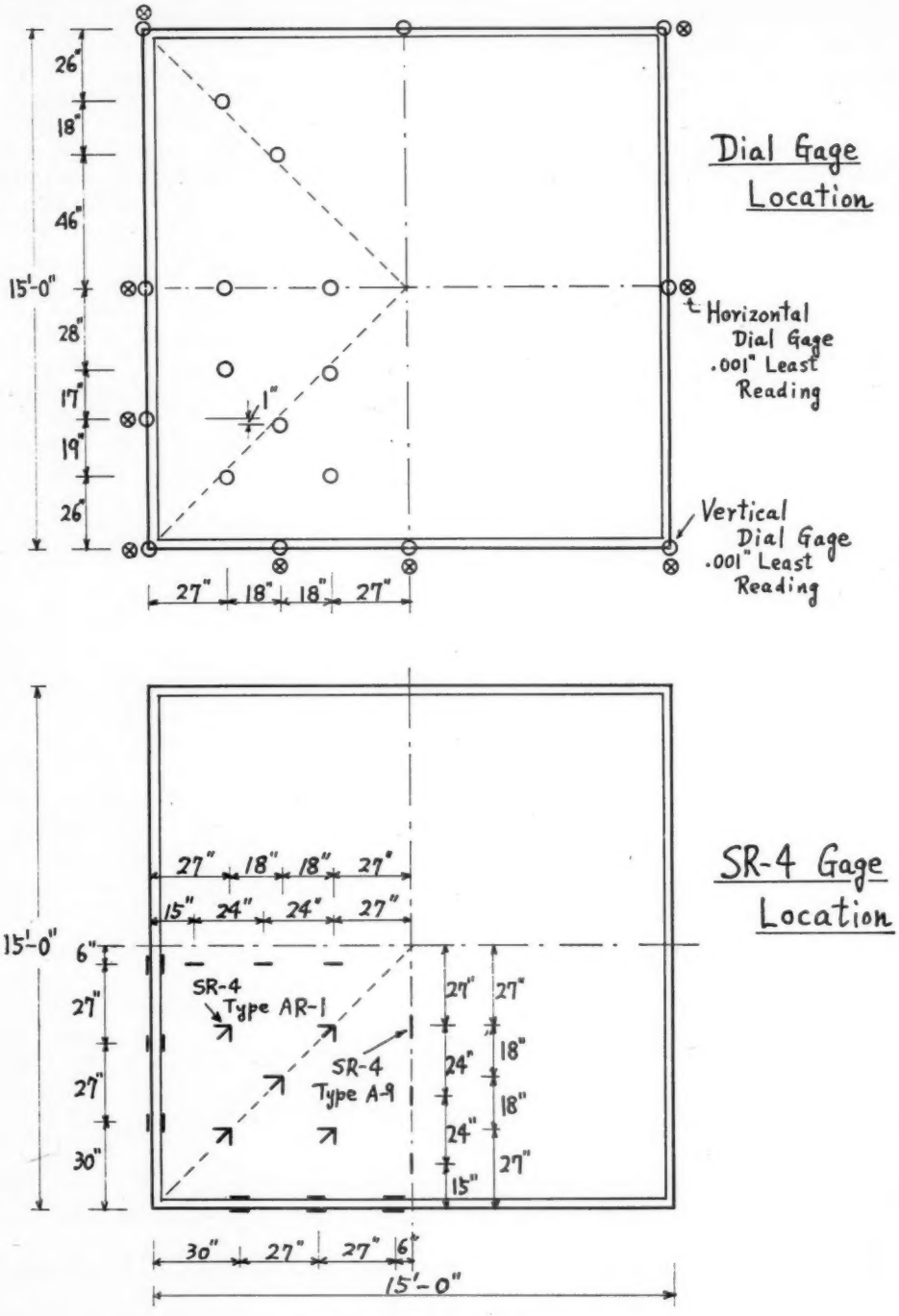

Figure 3— Gage locations

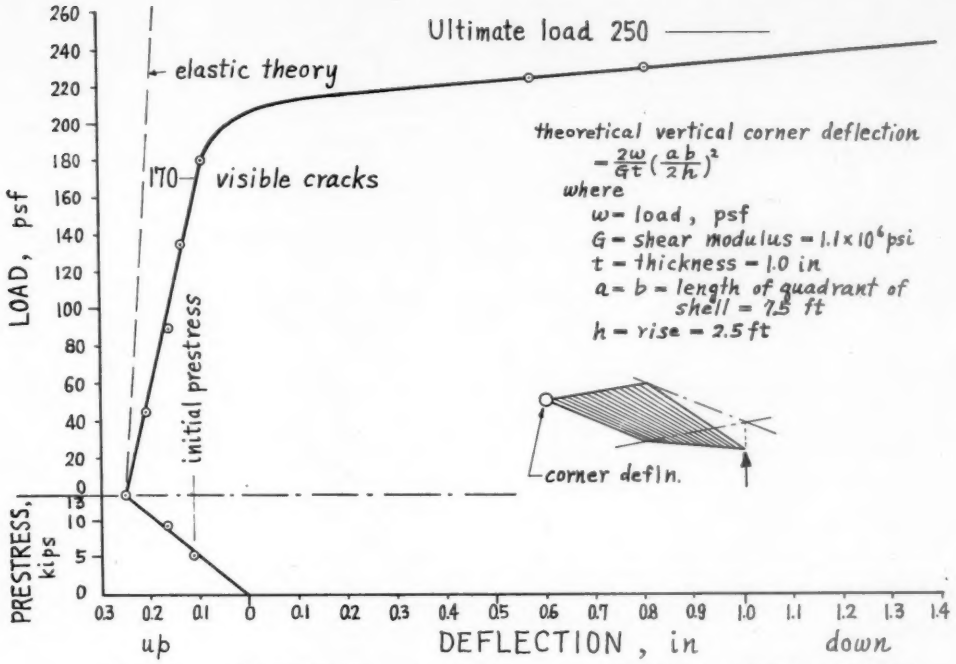

FIG.4 PRESTRESS and LOAD vs CORNER DEFLECTION

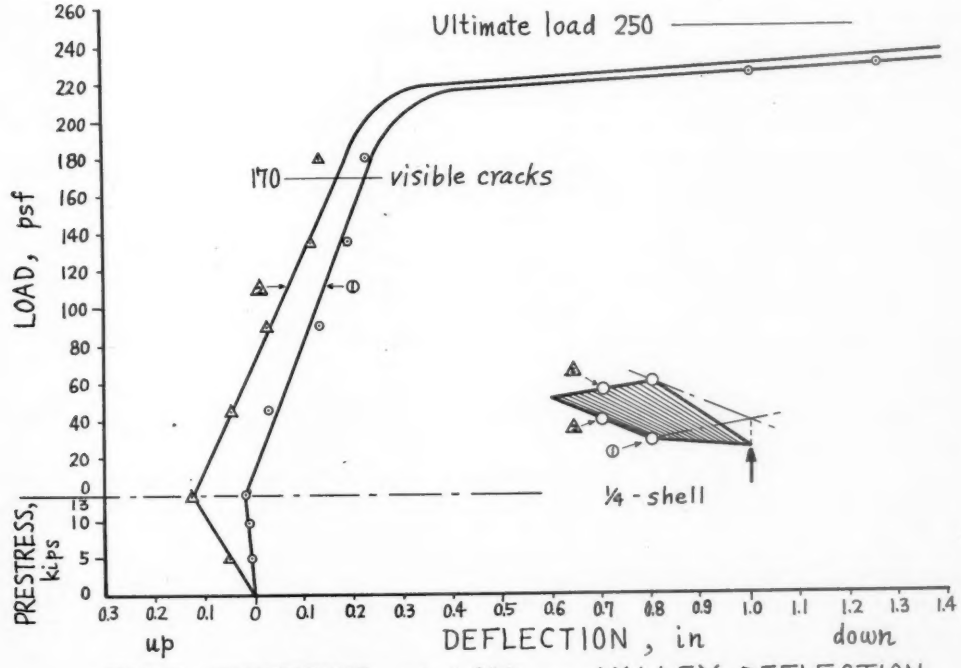

FIG.5 PRESTRESS and LOAD vs VALLEY DEFLECTION

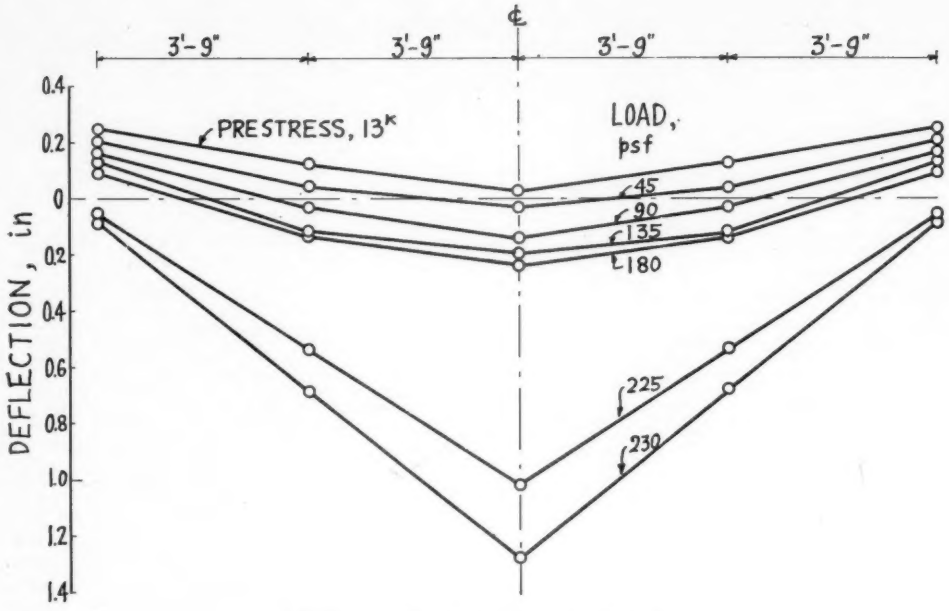

Figure 6—Deflection profile of edge beam

and the observed deflections are plotted on Figure 4. The observed deflections were much greater, largely due to the fact that the membrane theory does not take into account the bending effects of the shell and the edge beams.

B. **Ultimate Theory**

Simple statics can be used to determine the ultimate load if the stress developed in the prestressing steel is known, Figure 9. In the following analysis the stress in the steel is assumed to be at its yield strength (0.2% offset). It may be further assumed that the compression zone is near the column so that the effective lever arm for the steel is about 90% of the full rise of 2.5 ft.

$$T = \tau_y \times A_s = 230{,}000 \times 0.05 \times 2 = 23{,}000 \text{ lbs.}$$

$$\Sigma M_{xx} = 0 \qquad W \times \frac{a}{2} = T \times 0.9h$$

$$w_{ult} = \frac{W}{ab} = \frac{1.8Th}{a^2b} = \frac{1.8 \times 23{,}000 \times 2.5}{7.5^2 \times 7.5} = 246 \text{ psf}$$

$$w_{DL} = 13 \text{ psf}$$

therefore w_{LLult} steel yielding = 233 psf

The ultimate load for shear failure can also be estimated, Figure 10, assuming the ultimate diagonal tension strength of the concrete to be its modulus of rupture, 438 psi. Actually, the principal tension is affected by both the direct shear and radial compressive stresses acting on the perimeter of the shear area. The shear failure perimeter may be assumed to be the perimeter of a circle 30 in. from the center of the column. This is where the thickened portion of the shell ends and can be assumed to be the zone of maximum shear stress.

For the element shown, the principal tension stress, σ_t is given by

$$\sigma_t = \sqrt{\tau^2 + (\frac{\sigma_c}{2})^2} = \frac{\sigma_c}{2}$$

If W is the total ultimate load on one-fourth of the shell, then the total ultimate shearing load, W′, on one-fourth of the shell is

$$W' = \frac{225 = \frac{\pi}{4} 2.5^2}{225} W = 0.978W$$

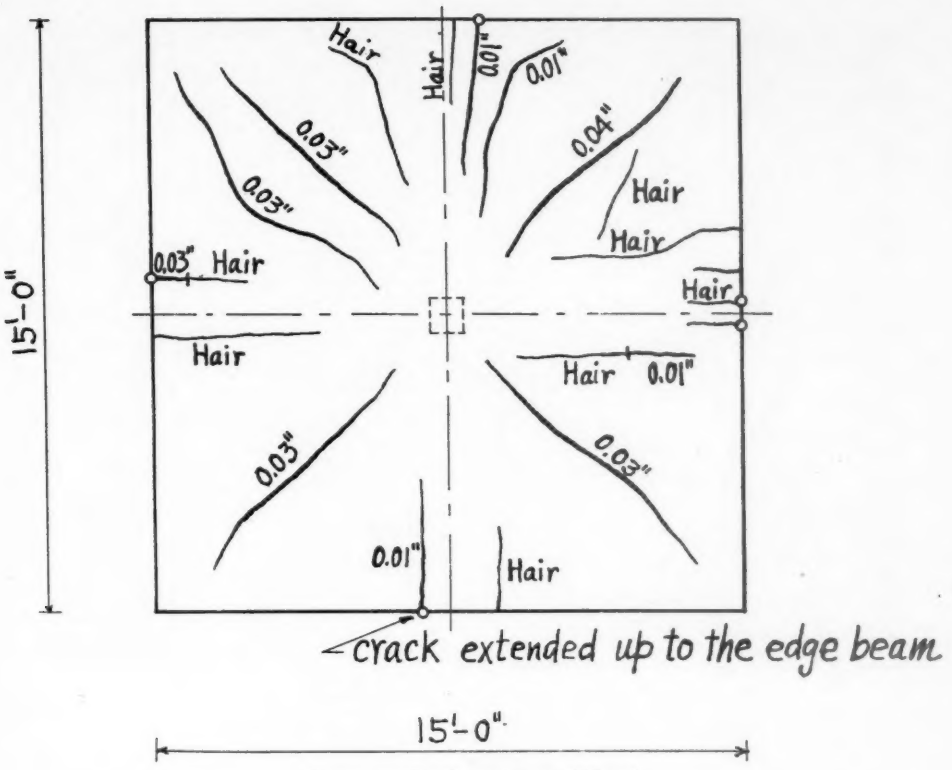

Figure 7—Crack pattern at 180 psf.

then

$$\tau_c = \frac{W'\cos\Theta}{A}$$

and

$$\sigma_c = \frac{W'\sin\Theta}{A}$$

Therefore

$$\sigma_t = \sqrt{\left(\frac{W'\cos\Theta}{A}\right)^2 + \left(\frac{W'\sin\Theta}{2A}\right)^2} - \frac{W'\sin\Theta}{2A}$$

$$= \frac{W'}{2a}\left\{\sqrt{1 + 3\cos^2\Theta} - \sin\Theta\right\}$$

$$= \frac{0.978W}{2x\text{—}x30x1}\left\{\sqrt{1 + 3\,(.9864)^2} - 0.1645\right\}$$

$$= 0.0377\ W$$

Since

$$\sigma_t = 438 \text{ psi}$$

$$W = \frac{438}{.0377} = 11{,}600 \text{ lbs.}$$

Therefore the ultimate load is

$$4 \times W = 46{,}400 \text{ lbs.}$$

The ultimate live load capacity before shear failure takes place is then

$$w_{ult} = \frac{46{,}400}{225} = 211 \text{ psf}$$

$$w_{DL} = 13 \text{ psf}$$

$$w_{LLult} = 198 \text{ psf}$$

The low value of the calculated ultimate shearing load (as compared to the experimental value of 247 psf), may be due to several causes. First, the valleys were thickened so that the average thickness of the shell at the shear perimeter was actually greater than 1 in. Second, the No. 2 reinforcing in the valleys could have contributed some strength. Third, the shearing strength of the concrete was not known exactly.

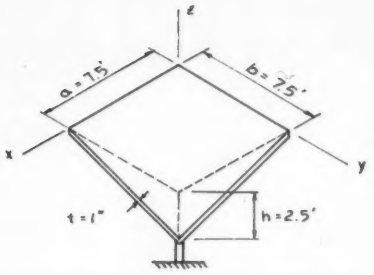

FIG. 8 QUADRANT OF SHELL

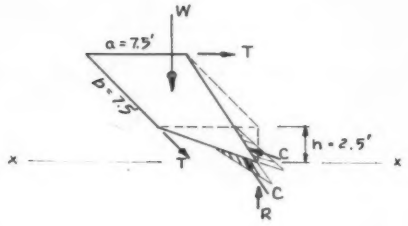

FIG. 9 FREEBODY OF A QUARTER OF SHELL

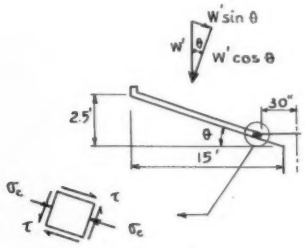

$$\theta = \tan^{-1}\frac{2.5}{15} = 9°\text{-}28'$$

FIG. 10 ULTIMATE SHEAR STRENGTH OF SHELL

X. Conclusions

It is obviously impossible to draw any definite conclusions from this one test. But the test indicated rather clearly the strength and rigidity inherent in this type of construction. By proper prestressing, it is possible to eliminate cracking and to minimize or eliminate deflections under working loads. The amount of prestressing will naturally vary with each design. Whenever possible the prestress should be located to neutralize the tensile stresses in the shells produced by external loads.

It is interesting to note the high live to dead load ratio (247 psf ultimate LL to 13 psf DL), although this ratio will decrease for prototypes with longer spans. The amount of prestress required was also very low, only 0.09 lb. of steel was used per sq. ft. of area for the tested shell.

The strength of doubly-curved surface was also exemplified in this test, the 1-inch shell resisting 247 psf without local failures. However, a great deal of investigation needs to be carried out to determine the real strength in such thin shells.

XI. Acknowledgment

The test was performed with the advice of Professors E. P. Popov and A. C. Scordelis, University of California. The making, testing and analysis of the model was largely the effort of Messrs. Andrew Jean and Amo Ravid, graduate students at the University.

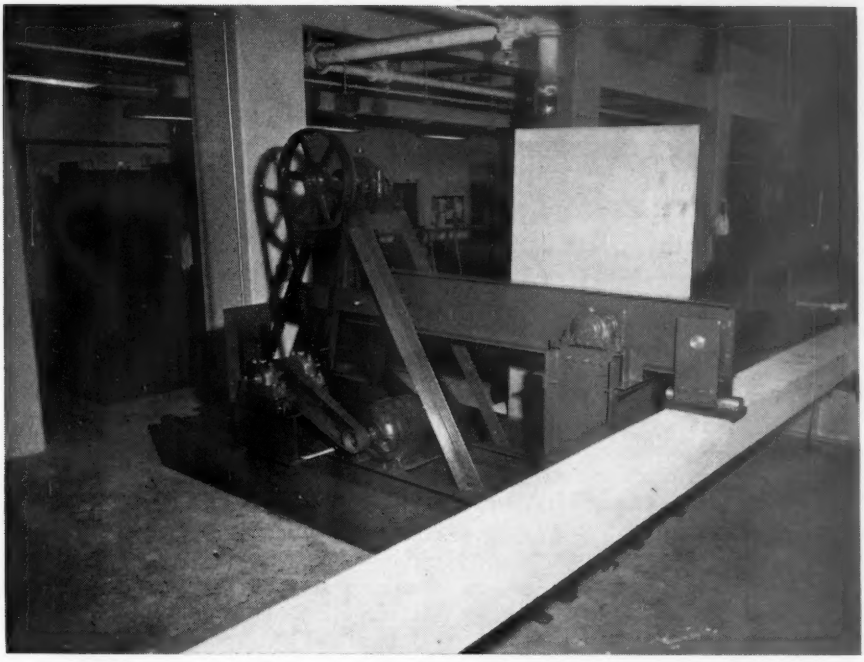

Figure 1—Beam in fatigue machine.

fatigue tests of prestressed concrete beams pretensioned with 1-2 inch strands

A. M. Ozell[1] and J. F. Diniz[2]

[1]Professor of Civil Engineering, University of Florida.

[2]Graduate student, University of Florida

INTRODUCTION

The tests described in this paper are the continuation of fatigue tests of pretensioned prestressed concrete beams under repetitive loads. The previous study[1] was made on beams which were prestressed with 7/16-in. strands and the present tests were conducted on beams prestressed with ½-in. strands.

A fatigue machine of the constant deflection type was used for these tests (Figure 1). The machine consists essentially of a rocker arm connected to an adjustable eccentric driven by an electric motor. The load was applied approximately 80 times per minute and the deflection range was from 0 to 1.75 inches.

DESCRIPTION OF SPECIMENS

The specimens were rectangular beams 8 by 10 inches in cross section and 19 feet center-to-center of supports, prestressed with two ½-inch strands placed 2¾ inches from the bottom of the beam. During testing,

(1) A. M. Ozell and E. Ardaman. "Fatigue Tests of Pre-tensioned Prestressed Beams." Journal A.C.I. Vol. 28, No. 4, Oct. 1956.

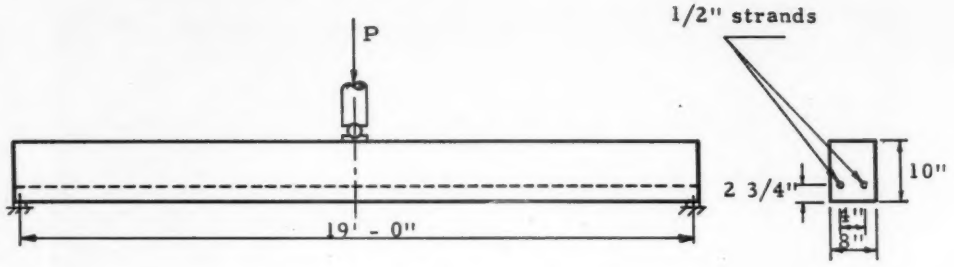

Figure 2. General Details of Specimens and Loading Diagram.

the beams were supported on neoprene pads 1 in. x 4 in. x 8 in. at each end. Figure 2 shows the general details of specimens.

The strands were tensioned initially to 25,200 pounds as recommended by the manufacturer. The design load was taken as 20,160 pounds.

The concrete used in the beams had the following mix design:

8.5 bags type III cement
27 gallons water
8½ quarts Pozzolith.
1094 lb. Tavares sand (fineness modulus: 2.30; specific gravity: 2.63)
1880 lb. Brooksville stone (SRD type 9: specific gravity: 2.52)

Figure 3 shows the compressive strength of cylinders at various curing intervals.

The specimens were cast by Dura-Stress of Leesburg, Florida.

TEST PROCEDURE

Each beam was set in its proper position and a static test was conducted in which the load applied was measured by a dynamometer placed between the loading head of the fatigue machine and the specimen. The deflection of the beam was measured by a dial gage attached to the frame of the fatigue machine. Center loading was used in all cases.

Once the load-deflection characteristics of the specimen were known, the deflection corresponding to the desired load was set in the eccentric so that this load was maintained during the testing of the particular specimen. The specimens were never loaded beyond the required repetitive load.

At regular intervals, or when deemed necessary, the machine was stopped and a static loading through the dynamometer established the new load-deflection characteristics of the specimen at that stage. Thus, the adjustments of the eccentric necessary to keep the repeated load constant (within ± 3 to 5 per cent) could be made whenever they were required.

BEHAVIOR OF SPECIMENS DURING TESTS

A center load of 3,500 lb. was applied to specimen S-1. The load was 1.77 times the design load. Design load is defined as the load which would cause zero tension in the bottom fiber assuming 20 per cent losses. The bottom-fiber stress was 651 psi tension, and the test was discontinued at 2,441,000 cycles without failure of the beam. The pattern of cracks is shown in Figure 4. All cracks appeared at the initial loading and the horizontal portions of cracks 1, 2 and 3 developed during the fatigue loading. The load-deflection diagram and the permanent set versus fatigue cycles are presented in Figures 5 and 6, respectively. The cylinder strength of the concrete in this beam at the beginning of the test was 5,700 psi.

The load applied to specimen S-2 was 4,400 lb., or 2.22 times the design load. The bottom-fiber stress was 1036 psi tension. All cracks appeared when the first load was applied and progressed during the fatigue loading. Failure of the beam occurred at 780,000 cycles. It was subse-

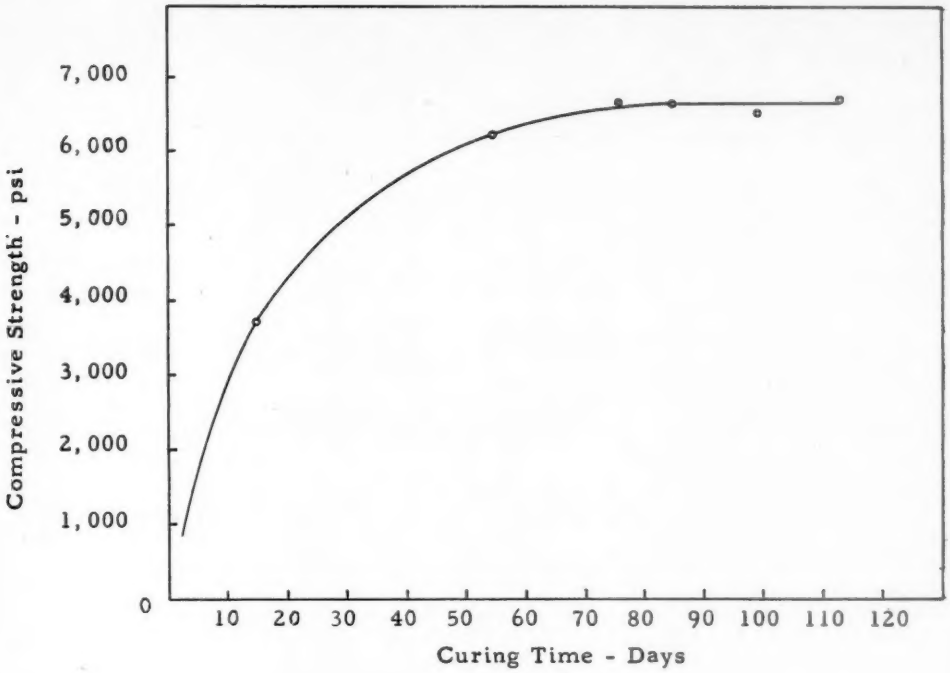

Figure 3. Compressive Strength of Cylinders at Various Curing Intervals

quently found that the strands had failed in bond between the two extreme cracks. Also two wires in one of the strands were broken in two places, at the location of cracks 4 and 7. The cylinder strength of the concrete in specimen S-2 at the beginning of testing was 6,250 psi.

Specimen S-3 was loaded with 5,000 lb. corresponding to 2.52 times the design load, causing a stress of 1291 psi tension in the bottom fiber. All cracks appeared when the initial static load was applied and progressed during the fatigue loading. The test was interrupted at 186,000 cycles and inspection of the beam then revealed that the strands had failed in bond in the region of the cracks. Concrete cylinder strength was 6,680 psi.

The load on specimen S-4 was 4,800 lb. or 2.42 times the design load. The corresponding stress in the bottom fiber was 1,211 psi. Cracks 1 to 8 appeared at the initial loading and cracks 9 and 10 at 10,000 cycles. All cracks progressed during the fatigue loading. After 540,000 repetitions of the load the test was discontinued. One of the wires in one strand and three wires in the other were broken at one location and a fourth wire at another location. Concrete cylinder strength was 6,650 psi.

Specimen S-6 was loaded with 4,000 lb. corresponding to 2.02 times the design load. Cracks 1 to 7 appeared at the first loading, cracks 8 and 9 at 100,000 cycles, and cracks 10, 11 and 12 at 190,000 cycles. The beam failed at 2,273,000 cycles. All wires in one strand were broken at one point, and a single wire at another location; only one wire was broken in the other strand. Concrete cylinder strength was 6,720 psi.

DISCUSSION OF TEST RESULTS

The six beams tested showed the same load deflection characteristics up to the cracking load, which was approximately 3,300 lb. corresponding to a bottom-fiber stress of 560 psi tension. The initial cracks widened and progressed toward the upper half of the beam according to the increase in the number of repetitions of the applied

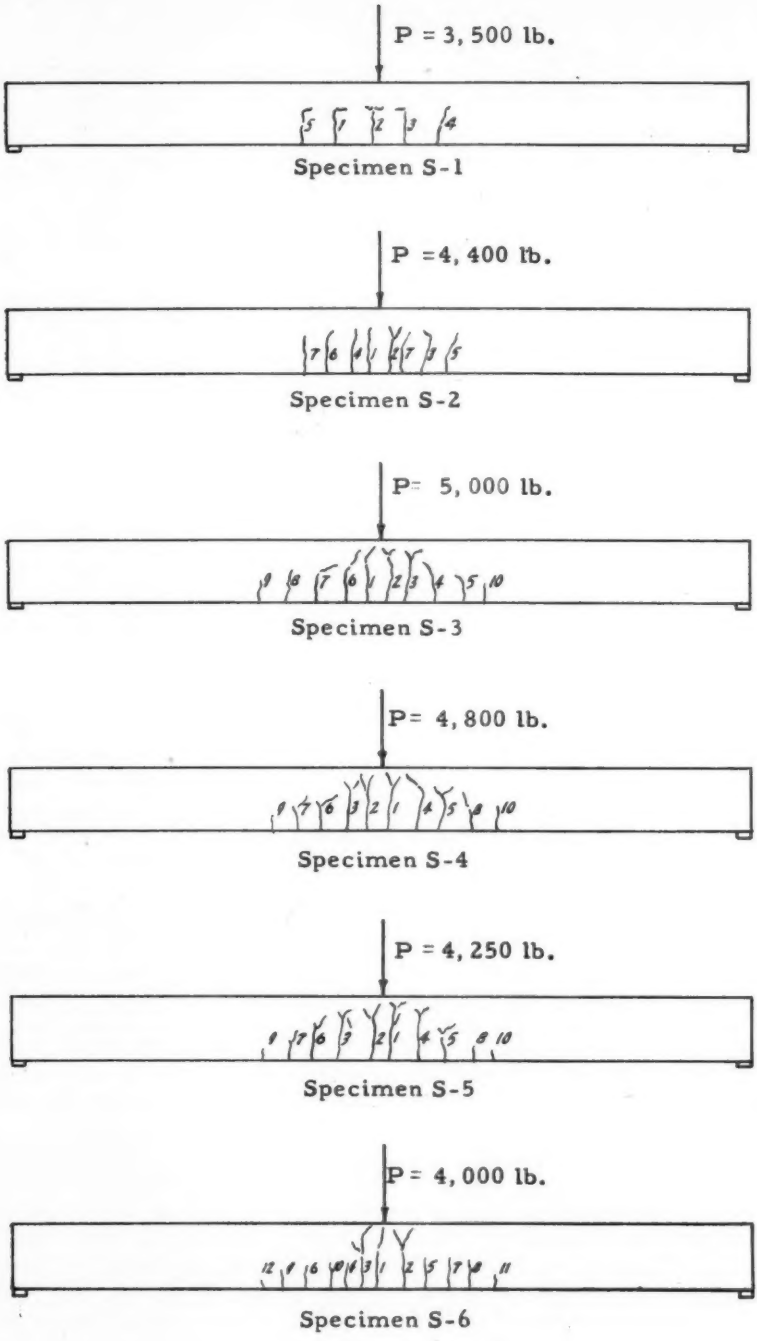

Figure 4. Pattern of Cracks

load. The cumulative effect of the tensile and shear damage to the concrete was shown by the change in the direction of the tensile cracks which finally paralleled horizontal shear planes, as shown in Figure 4.

With the exception of specimen S-1, all beams were broken into after the fatigue test was discontinued for a general inspection.

All failures, except for S-3, occurred by breaking of the wires in the strands. The cracks in the concrete acted as stress raisers and the consequent stress concentrations in the strands contributed to the fatigue failure of the wires at those points. The failure of additional wires in some cases was caused by the increase in stress resulting from the reduction in the number of sound wires in the strand.

The broken strands in specimen S-6 shown in Figure 7 are typical of failure of the wires. In this case, all seven wires of one strand had failed.

Establishing quantitatively the cyclic loading which caused initial failure in the strands was difficult, if not impossible. An obvious change in the load-deflection characteristics of the specimen had to take place before the test could be stopped with assurance of wire failure. This change might have occurred only after several wires had broken.

Following the same criteria of failure established in previous tests[1] the fatigue failure was assumed to occur when the cyclic loading had caused 30 per cent loss in the "spring constant." Spring constant is defined here as the design load divided by the corresponding center deflection. A

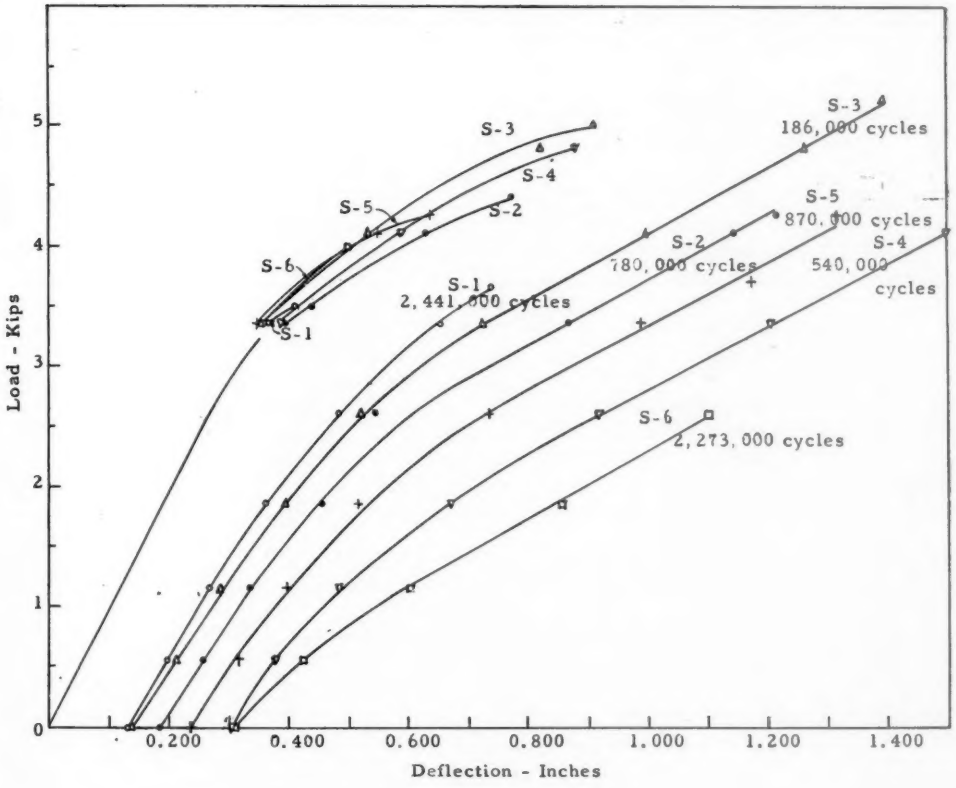

Figure 5. Load Deflection Diagrams

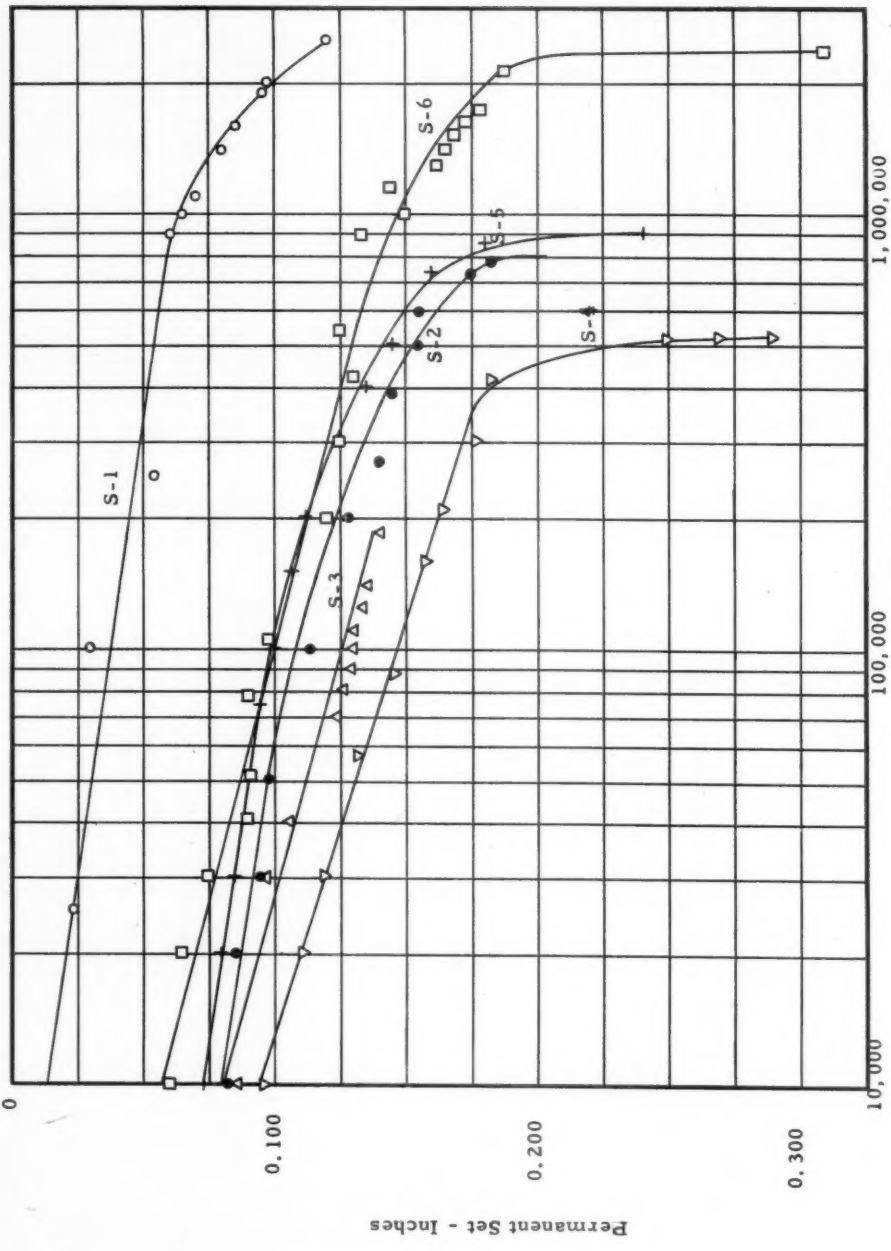

Figure 6. Permanent Set versus Fatigue Cycles Diagram

semilogarithm plot of the number of cycles versus the loss in "spring constant" (Figure 8), shows a sudden drop at the number of cycles corresponding to failure. These curves can then be used to establish the number of applications of the fatigue load which caused failure.

A similar plot (Figure 6) shows that the sudden increase in the permanent set of the beams caused by the repeated loading also provides a good indication of failure.

Figure 9 presents the number of cycles of fatigue loading at failure **versus** applied load in terms of percentage of the design load. For comparison, the results of the previous tests on beams prestressed with 7/16-inch diameter strands are also given in the same graph.

The range of stresses caused by the fatigue loading both in the steel and in the concrete were calculated and are presented in Table II. In these calculations the lever arm of the resisting couple was taken as 4.5 in.

The Goodman diagram for the steel in the strands was drawn and is shown in Figure 10.

Based on a minimum stress of 144,000 psi after losses, the unbonded strands have an allowable maximum stress of 196,000 psi which gives a stress range of 52,000 psi. The calculated minimum stress in the beams tested was 144,000 psi and the calculated maximum stresses are shown in Table II.

Figure 7—Magnified view of wire fracture in specimen S-6.

The severity of the effect of stress concentrations induced in the strands by the cracks in the concrete is illustrated by specimens S-5, and S-6. The stress range in these beams was 16.4 and 37.5 per cent less than the allowable stress range for the unbonded strands and yet the beams failed at 870,000 and 2,273,000 cycles respectively.

TABLE I — SUMMARY OF TEST RESULTS

Beam No.	Center Load Lb.	Test Load ÷ Design Load	Number of Cycles at Failure of Strands	Spring Constant Lb./in.	Loss in Spring Constant Percent	Permanent Set, in.
S-1	3,500	1.77	(*) 0	9,440	0	0.015
			2,441,000	8,080	14.4	0.135
S-2	4,400	2.22	0	9,440	0	0.055
			780,000	7,320	22.5	0.186
S-3	5,000	2.52	0	9,440	0	0.055
			186,000(1)	7,210	23.6	0.140
S-4	4,800	2.42	0	9,440	0	0.062
			514,000	4,770	49.5	0.305
S-5	4,250	2.15	0	9,440	0	0.050
			870,000	6,150	34.9	0.238
S-6	4,000	2.02	0	9,440	0	0.045
			2,273,000	3,290	65.2	0.308

(*) Did not fail
(1) Bond Failure

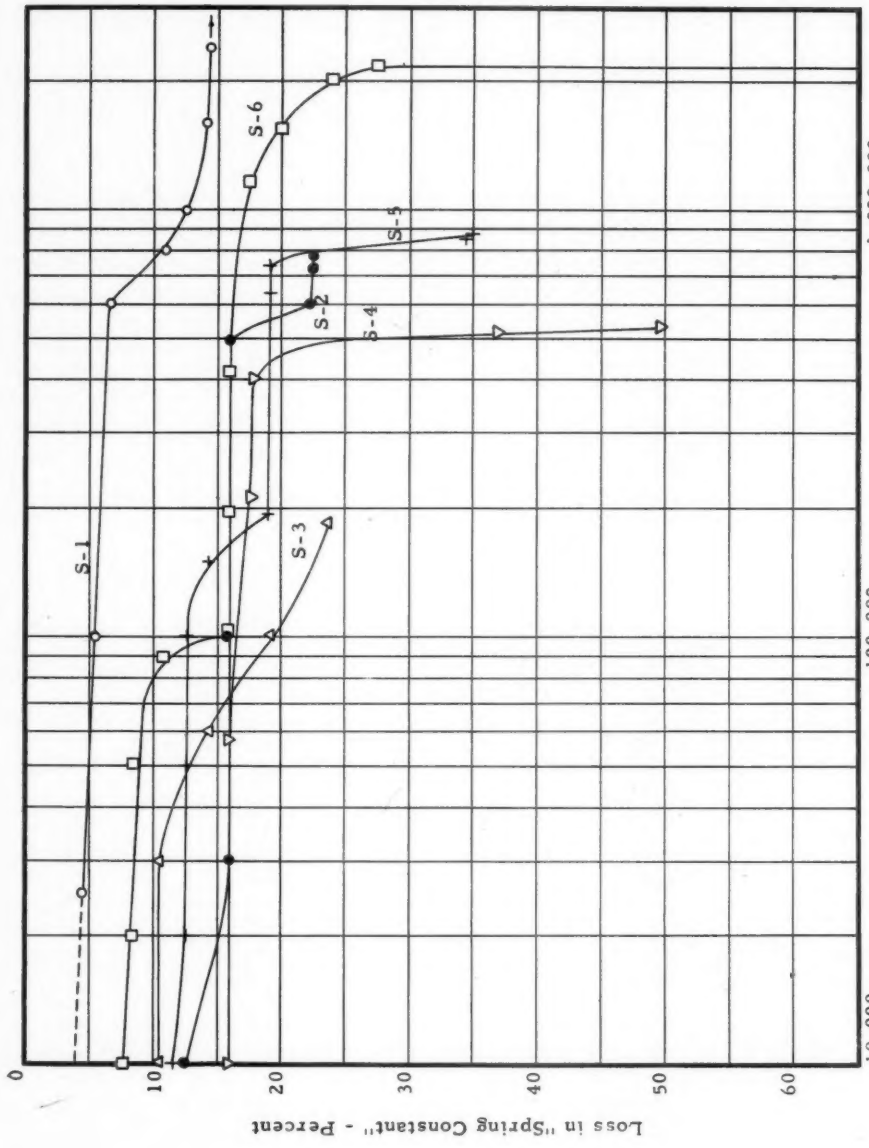

Figure 8. Loss in Spring Constant of Beams Caused by Fatigue

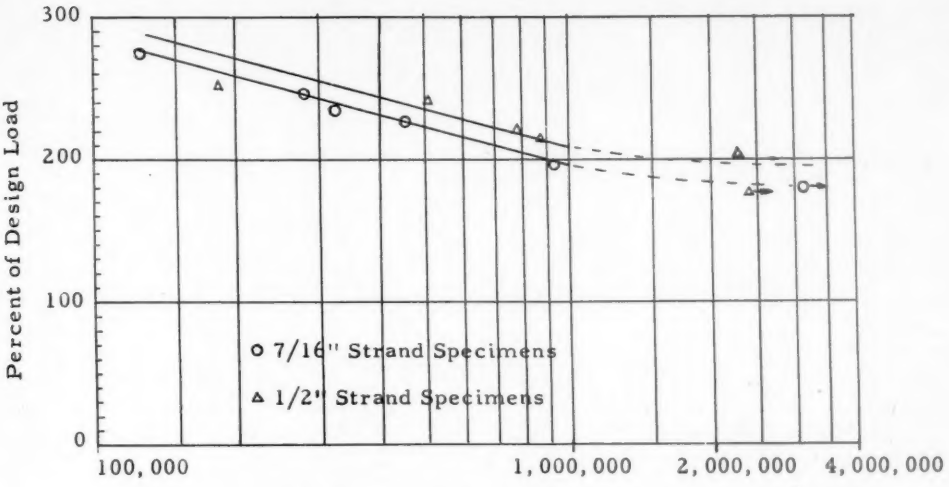

Figure 9. Load versus Adjusted Cycles of Failure Diagram.

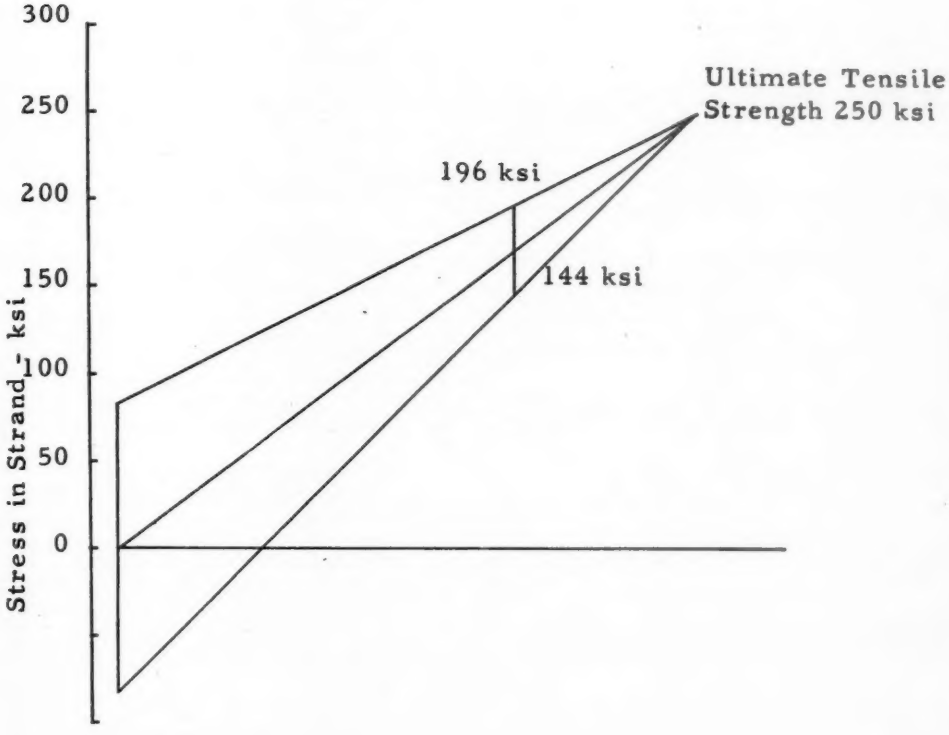

Figure 10. Goodman Diagram for 1/2" Seven Wire Strand

TABLE II — STRESS RANGES IN THE CONCRETE AND IN THE BONDED STRAND

Specimen No.	Test Load lb.	Calculated Bottom Fiber Stress psi Tension	Calculated Strand Stress psi	Stress Range		Cycles At Failure	Stress Range Allowable Range %
				Concrete psi Comp.	Steel psi		
S-1	3,500	651	153,000	1,500	9,000	Did not fail	17.3
S-2	4,400	1036	193,000	1,885	51,500	780,000	99.0
S-3	5,000	1291	220,000	2,140	76,000	186,000	146.0
S-4	4,800	1211	212,000	2,060	68,000	514,000	130.5
S-5	4,250	976	187,500	1,825	43,500	870,000	83.6
S-6	4,000	866	176,500	1,715	32,500	2,273,000	62.5

CONCLUSION

The following conclusions can be drawn from the tests described above:

1. The use of ½ inch strands in pretensioned beams of similar dimensions and under the same fatigue loading conditions seems entirely feasible.
2. The flexural fatigue strength of the beams tested was approximately 2.0 times the design load.
3. Fatigue failures were caused by breaking of the wires in the strands. Only regional bond failure and some evidence of slip close to the cracks were observed. Other conditions of loading causing higher shears may induce bond failure.
4. The load deflection charactertistics and permanent set of the beams were considerably changed as a result of the repeated loading and showed a marked change just before failure.

CORRECTION . . .

On Page 82 of the March (Vol. 2, No. 4) issue of the PCI JOURNAL there is an error of omission in the article by W. J. Jurkovich. The statement "For $\frac{Pi}{A} = 1000$ psi the theoretical loss would be 28,000 psi." Should read "For $\frac{Pi}{A} = 1000$ psi the theoretical loss would be 20,000± psi and for $\frac{Pi}{A} = 1600$ psi the theoretical loss would be 28,000± psi."

PCI PUBLICATIONS

PCI JOURNAL
Published quarterly. Subscriptions: $6.00 per year domestic; $7.20 outside continental limits of U.S.A. Back copies available at $1.00 each.

PCItems
Published monthly. Subscription: $2.50 per year. Special quantity rates available to PCI members.

SPECIFICATIONS—PRETENSIONED
PCI proposed, tentative specification for pretensioned prestressed concrete. Single copy: 35c. For 100 or more — 15c each.

SPECIFICATIONS—POST-TENSIONED
PCI proposed, tentative specification for post-tensioned prestressed concrete. Single copy: 35c. For 100 or more — 15c each.

TYPICAL PRESTRESSED CONCRETE PRODUCTS
A 24-page brochure showing examples of typical prestressed concrete products manufactured throughout the country. Available on request to Executive Secretary.

Subscriptions or orders for back issues of any PCI publication should be addressed to:

PUBLICATION OFFICE
Prestressed Concrete Institute
3132 N. E. Ninth Street
Fort Lauderdale, Florida

425 N. E. FIFTH STREET
BOCA RATON, FLORIDA

MEMBERSHIP QUALIFICATIONS

SCHEDULE OF DUES

Anyone engaged in the production of prestressed concrete, or in the production of materials or equipment allied to the prestressing industry; licensed architects and engineers; engineers and architects in training, and students enrolled in accredited schools of architecture and engineering, are invited to apply for membership in the Prestressed Concrete Institute. Membership classifications have been established as follows:

ACTIVE

Organizations and individuals actively engaged in the production of prestressed concrete products.
Annual Membership Dues **$250.00**

ASSOCIATE

Organizations and individuals engaged in the production of materials and equipment allied to the prestressed concrete industry.
Annual Membership Dues **$250.00**

PROFESSIONAL

Limited to registered architects and engineers.
Annual Membership Dues **$ 25.00**

AFFILIATE

Limited to supervisory and technical employees, non-graduate.
Annual Membership Dues **$ 15.00**

JUNIOR

Limited to architects and engineers in training.
Annual Membership Dues **$ 15.00**

STUDENT

Limited to students of accredited architectural and engineering schools.
Annual membership dues, effective January 1, 1957 **$ 10.00**
(For student members outside continental U. S., Canada included) **$ 12.00**

Members receive the PCI JOURNAL, a quarterly technical publication, and PCItems, a monthly news bulletin, without additional cost, plus research bulletins and other information on prestressing as it becomes available.

PRESTRESSED CONCRETE INSTITUTE

425 N. E. FIFTH STREET

BOCA RATON, FLORIDA

APPLICATION FOR MEMBERSHIP IN PRESTRESSED CONCRETE INSTITUTE
(A non-profit corporation)

1. Name and address of company applying for membership:

_____

_____

_____

2. Name of person to represent company in Institute affairs:

_____

3. Type of membership applied for:

☐ Active (manufacturer)
I have done the following types of prestressing:
- ☐ Post-tensioning
- ☐ Pre-tensioning
- ☐ Combination of both of above
- ☐ Precasting
- ☐ On-the-job post-tensioning
- ☐ On-the-job pre-tensioning
- ☐ Design

☐ Associate (related business)

I am in the business of_____

_____

_____

☐ Professional (registered architect or engineer)
I hold certificate No._____ of the State of_____.

☐ Affiliate (limited to supervisory and technical employees, non-graduate)

☐ Junior (limited to architects and engineers in training)

☐ Student (limited to students of accredited schools of architecture and engineering)
Name of School_____

I understand the financial arrangements and am not to make any payment until approval of this application for membership.

Signed:_____

(cut along this line)

4th ANNUAL

P.C.I. MEETING & CONVENTION

★

September 21-26, 1958
EDGEWATER BEACH HOTEL
Chicago, Illinois

PROFESSIONAL service advertising

This PROFESSIONAL SERVICES *section has been established to enable engineers and architects to list the services they offer to the prestressing industry. Advertising rates are $10.00 per column inch. Copy should conform with ethical standards for advertising as established by the various professional associations which govern advertising of architects and engineers. Copy and inquiries should be directed to the* JOURNAL *Publication Office: 3132 N. E. 9th Street, Fort Lauderdale, Florida.*

CONCRETE TESTERS

The World's Finest Low-Cost Precision Testers

For

CYLINDERS
CUBES
BLOCKS
BEAMS
PIPE

IF IT'S A CONCRETE TESTER YOU NEED-GET IN TOUCH WITH

FORNEY'S, Inc.
TESTER DIVISION
P. O. BOX 310 · NEW CASTLE, PA.

FREDERIC A. NASSAUX ASSOCIATES
Consulting Engineers
Room 226 Trust Building
CHAMBERSBURG, PA.

LEAP ASSOCIATES
Consultants to the Prestressing Industry
P. O. Box 1053 Ph MU 8-5631
Lakeland, Florida

WAYLAN ENGINEERING CO.
Structural Consultants
A. M. OZELL E. ARDAMAN
PAUL M. ZIA, Consultant
Consultants in Prestressed Concrete
Reinforced Concrete — Steel Design
1520 N. W. 13th Street
Gainesville, Florida

Lakeland Engineering Associates, Inc.
Professional Engineers
P. O. Box 495 Phone Mutual 8-3971
Lakeland, Florida
Consultants in Prestressed Concrete Design

New, Lower Cost
Flexible
POST TENSION CASING

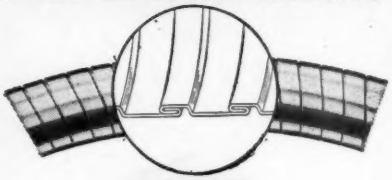

U-100WP
(Wide Profile)
ECONOFLEX
Ask for Bulletin U-100WP

Quality . . . ALL METAL FLEXIBLE HOSE PRODUCTS
UNIVERSAL METAL HOSE CO.
2187 S. Kedzie Ave., Chicago 23, Ill.

P. C Items

Published monthly by

Prestressed Concrete Institute

This lively illustrated news bulletin presents news of Institute activities . . . views of members facilities . . . highlights outstanding prestressed concrete applications, and reports on latest developments in research, production of prestressed concrete.

Subscription $2.50 per year

PCItems
3132 N. E. Ninth Street
Fort Lauderdale, Florida

accurate testing...

ASSURES CONSTRUCTION PERMANENCE . . . SAVES MATERIALS, TIME AND MONEY . . .

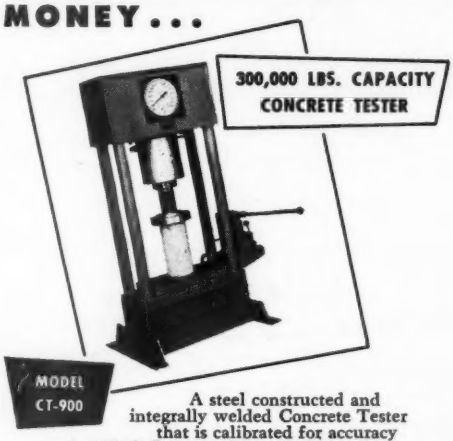

A steel constructed and integrally welded Concrete Tester that is calibrated for accuracy using U. S. Bureau of Standards certified calibration apparatus. The CT-900 meets ASTM and AASHO specifications for hydraulic testing machines and is accurate to within 1% of the indicated load.

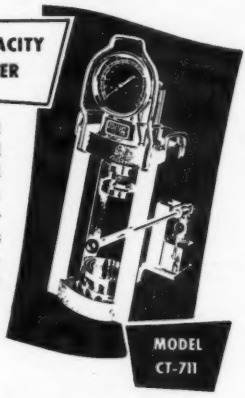

A sturdy, compact and entirely self-contained unit. Easily operated either by hand or by an electrical pump attachment. The CT-711 is also calibrated for accuracy to within 1% of the indicated load.

Many other units of Engineering Test Apparatus for Concrete Testing are available. Our New Catalog covers completely all testing equipment and accessories used in this field. Illustrated Bulletins describe in detail the Apparatus shown above.

SOILTEST *Incorporated*
WRITE TODAY FOR COMPLETE INFORMATION
4711 W. NORTH AVE., CHICAGO 39, ILLINOIS

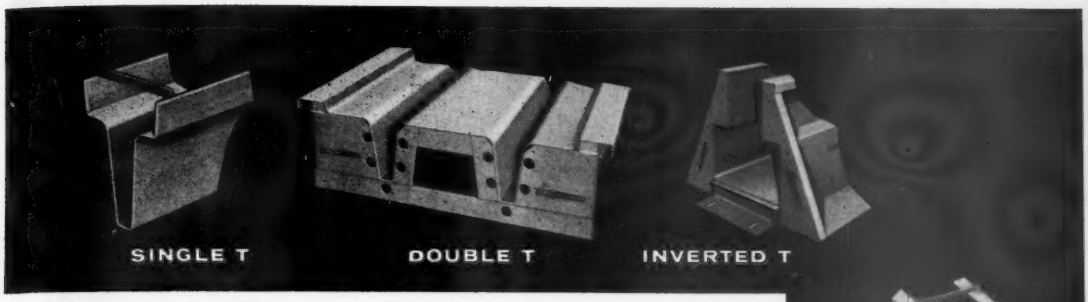

Now! FORM-CRETE

TRADE MARK

OFFERS THE MOST COMPLETE LINE of CASTING FORMS EVER PRODUCED!

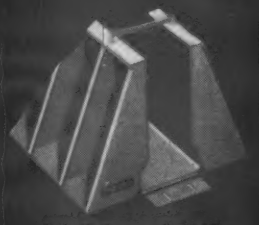

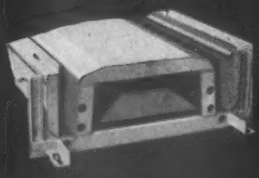

THE FORM-CRETE line of more than 22 basic forms represents the most versatile group of steel forms ever produced for casting prestressed and precast concrete products. Each form has been carefully designed to insure a uniform, smooth edge product. Die-formed product release angles permit easy trouble-free stripping of product. Heavy-gauge steel construction means indefinite form life. What's more, many Form-Crete forms can be quickly adapted to produce a variety of varied finished products. And where special needs call for a custom form, FMC has the know-how and facilities to turn it out quickly and efficiently. That is why we say, call on Form-Crete, rely on Form-Crete for the finest in steel forms delivered on time, when and where you want them.

SEND FOR NEW CATALOG.
Just off the press, this new Catalog illustrates all of the many Form-Crete forms now available including the new PCI and AASHO approved Bridge Beams.

---

fmc®

FOOD MACHINERY AND CHEMICAL CORPORATION
LAKELAND, FLORIDA • RIVERSIDE, CALIFORNIA

Please send me a copy of your new Catalog No. 300.

NAME_____

COMPANY_____

CITY_____ ZONE_____ STATE_____

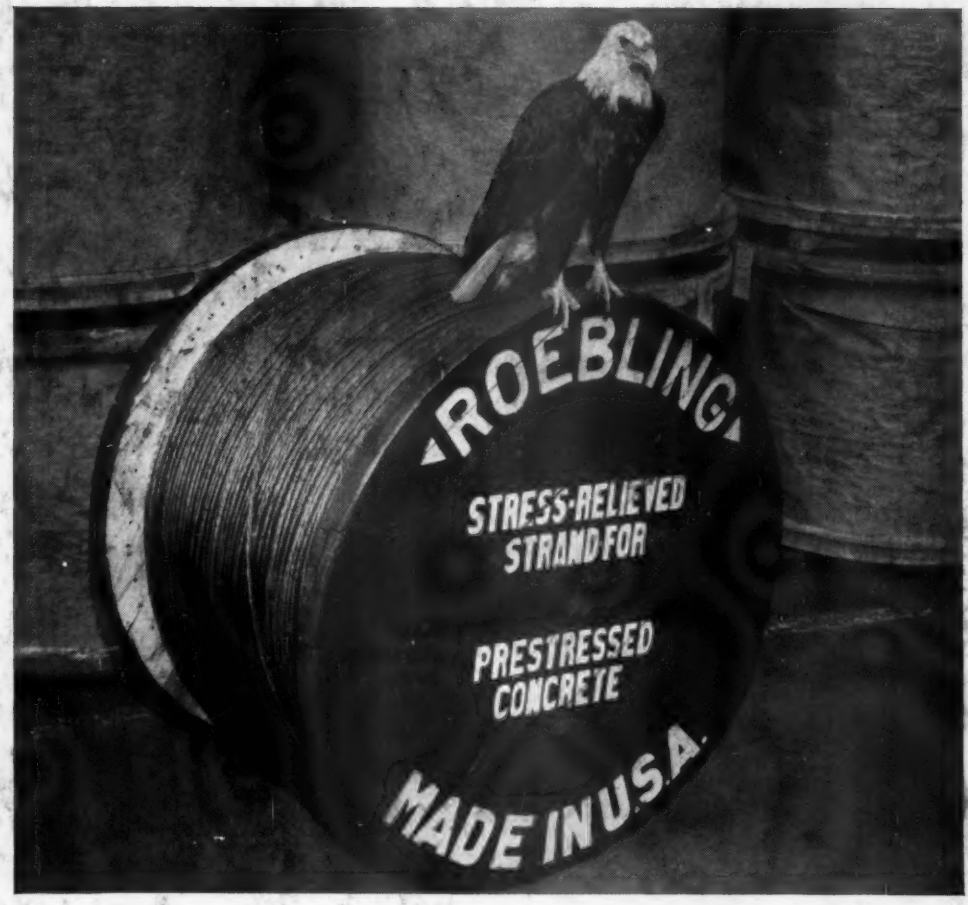

We speak your language

The language of *service* and *engineering assistance* wherever and whenever you need them.

The reel of Roebling Stress-Relieved Strand for prestressed concrete that you see here is but one of many elements of prestressed concrete . . . every one of which Roebling is familiar with and many of which Roebling has instituted and developed.

Fourteen years of experience in every aspect of the prestressed concrete field —tensioning elements, strand development, design procedures, the development and introduction of the stress-relieving process for the uniform behavior of tensioning wires and strands—enable Roebling to *deliver* much more than the strand on the reel.

This from the oldest manufacturer of wire rope in the United States: the highest quality stress-relieved strand delivered in a "package" you cannot get from any other source in the world.

ROEBLING

Branch Offices in Principal Cities
Subsidiary of The Colorado Fuel and Iron Corporation

Consult Roebling...First in the U. S. with Prestressing and Tensioning Elements